CAPITAL UNIVERSITY OF SCIENCE AND TECHNOLOGY, ISLAMABAD

Stabilization of Perturbed Nonholonomic Systems in Chained Form

by

Muhammad Sarfraz

A thesis submitted in partial fulfillment for the
degree of Doctor of Philosophy

in the

Faculty of Engineering

Department of Electrical Engineering

November 2018

Stabilization of Perturbed Nonholonomic Systems in Chained Form

Prof. Dr. Kamran Iqbal

University of Arkansas at Little Rock, Arkansas, USA

(Foreign Evaluator)

Prof. Dr. Cangqi Zhou

Nanjing University of Science and Technology, Nanjing, China

(Foreign Evaluator)

Prof. Dr. Fazal ur Rehman

(Thesis Supervisor)

Prof. Dr. Noor Muhammad Khan

(Head, Department of Electrical Engineering)

Prof. Dr. Imtiaz Ahmed Taj

(Dean, Faculty of Engineering)

DEPARTMENT OF ELECTRICAL ENGINEERING

CAPITAL UNIVERSITY OF SCIENCE AND TECHNOLOGY

ISLAMABAD

Dedicated to my teachers for enlightening my life and soul.

CERTIFICATE OF APPROVAL

This is to certify that the research work presented in the thesis, entitled **"Stabilization of Perturbed Nonholonomic Systems in Chained Form"** was conducted under the supervision of **Dr. Fazal ur Rehman**. No part of this thesis has been submitted anywhere else for any other degree. This thesis is submitted to the **Department of Electrical Engineering, Capital University of Science and Technology** in partial fulfillment of the requirements for the degree of Doctor in Philosophy in the field of **Electrical Engineering**. The open defence of the thesis was conducted on **November 09, 2018.**

Student Name: Mr. Muhammad Sarfraz (PE113001)

The Examining Committee unanimously agrees to award PhD degree in the mentioned field.

Examination Committee :

(a) External Examiner 1: Dr. Zareena Kausar,
Associate Professor
Air University, Islamabad

(b) External Examiner 2: Dr. Mehmood Pervaiz,
Associate Professor
COMSATS University, Islamabad

(c) Internal Examiner : Dr. Aamir Iqbal Bhatti
Professor
CUST, Islamabad

Supervisor Name :   Dr. Fazal ur Rehman
Professor
CUST, Islamabad

Name of HoD :   Dr. Noor Muhammad Khan
Professor
CUST, Islamabad

Name of Dean :   Dr. Imtiaz Ahmad Taj
Professor
CUST, Islamabad

AUTHOR'S DECLARATION

I, **Mr. Muhammad Sarfraz** **(Registration No. PE-113001)**, hereby state that my PhD thesis titled, '**Stabilization of Perturbed Nonholonomic Systems in Chained Form**' is my own work and has not been submitted previously by me for taking any degree from Capital University of Science and Technology, Islamabad or anywhere else in the country/ world.

At any time, if my statement is found to be incorrect even after my graduation, the University has the right to withdraw my PhD Degree.

(Mr. Muhammad Sarfraz)

Dated: 09   November, 2018

Registration No : PE-113001

PLAGIARISM UNDERTAKING

I solemnly declare that research work presented in the thesis titled "**Stabilization of Perturbed Nonholonomic Systems in Chained Form**" is solely my research work with no significant contribution from any other person. Small contribution/ help wherever taken has been duly acknowledged and that complete thesis has been written by me.

I understand the zero tolerance policy of the HEC and Capital University of Science and Technology towards plagiarism. Therefore, I as an author of the above titled thesis declare that no portion of my thesis has been plagiarized and any material used as reference is properly referred/ cited.

I undertake that if I am found guilty of any formal plagiarism in the above titled thesis even after award of PhD Degree, the University reserves the right to withdraw/ revoke my PhD degree and that HEC and the University have the right to publish my name on the HEC/ University Website on which names of students are placed who submitted plagiarized thesis.

(**Mr. Muhammad Sarfraz**)

Dated: 09 November, 2018

Registration No. PE-113001

List of Publications

1. M. Sarfraz, F. Rehman, and I. Shah, "Robust stabilizing control of non-holonomic systems with uncertainties via adaptive integral sliding mode: An underwater vehicle example," *International Journal of Advanced Robotic Systems*, vol. 14, 2017.

2. M. Sarfraz, and F. Rehman, "Feedback stabilization of nonholonomic drift-free systems using adaptive integral sliding mode control," *Arabian Journal for Science and Engineering*, vol. 42, pp. 2787-2797, 2017.

3. M. Sarfraz, and F. Rehman, "Stabilization of 2nd order nonholonomic systems in canonical chained form using adaptive integral sliding mode," *Submitted to Journal of Applied Research and Technology*.

4. M. Sarfraz, and F. Rehman, "Robust stabilizing control of a class of systems with higher-order nonholonomic constraints using adaptive integral sliding mode control," *Submitted to Advanced Robotics*.

5. M. Sarfraz, and F. Rehman, "Adaptive sliding mode control for a second order nonholonomic planar four-link UMS," *13th International Conference on Emerging Technologies ICET2017*, 27-28 Dec.

Acknowledgements

All praise to the Almighty Lord, the Creator of the universe and the mankind. First of all, I am thankful to Allah (SWT) who blessed me with the knowledge and the will to complete this work. Also, I want to pay tribute to the greatest, the perfect human and the last prophet Muhammad (PBUH) for enlightening our conscience and soul.

I would like to acknowledge my supervisor, Dr Fazal ur Rehman, for his valuable guidance throughout my studies at the university. I am extremely grateful for his patience and continuous encouragement during the various courses he taught on signal processing and nonlinear control theory. He has been a constant source of motivation and a ray of hope during the challenging times. His advice and knowledgeable inputs during the research activities and meetings will always be cherished.

I am also indebted to my colleague Mr Ibrahim Shah for his valuable support during various phases of my PhD. He always offered candid and practical advice during the research interactions and informal sessions. Also, I want to pay my appreciation to my nonlinear group mates Mr Waseem Abbasi and Mr Sami Uddin for their valuable inputs during the research meetings.

At the same time, I also want to acknowledge the National Engineering and Scientific Commission (NESCOM) for offering me the opportunity to pursue my higher studies.

Last but not the least I owe my regards and respect to my parents, brothers, sister, parents-in-law and brother-in-law for their patience and support during the course of my studies. My family including my wife and kids have been a constant source of motivation during the entire study period.

Abstract

Many real-world systems exhibit velocity-dependent and/or acceleration-dependent constraints in their mathematical models. If these constraints are non-integrable then these systems are known as nonholonomic systems. Examples of such non-holonomic systems include hopping robots, unmanned aerial vehicles (UAVs), car-like robots, autonomous underwater vehicles (AUVs), surface vessels, vertical take-off and landing systems and many more. These systems are special as, in general, the stabilization problem of these systems cannot be solved by smooth (or continuous) static state-feedback and, thus, requires time-varying or discontinuous state-feedback control. In this research, we are considering first-, second- and higher-order nonholonomic systems that can be transformed into chained or power form which are canonical representations of these mechanical systems. The importance of stabilization problem of perturbed nonholonomic systems is further magnified by the variety of real-world day-to-day applications.

This research presents the solution to the stabilization problems for a selected class of perturbed first-, second- and higher-order nonholonomic mechanical systems. The methodologies are based on adaptive integral sliding mode control (AISMC). For the perturbed nonholonomic system, the original system is transformed into perturbed chained form. Then this perturbed chained form system is further transformed into a special structure containing nominal part and some unknown terms through input transformation. The unknown terms are computed adaptively. Later the transformed system is stabilized using integral sliding mode control (ISMC). The stabilizing controller for the transformed system is constructed which consists of the nominal control plus some compensator control. The compensator controller and the adaptive laws are derived in such a way that derivative of a Lyapunov function becomes strictly negative. A similar approach is applied to the third-order nonholonomic system with a jerk constraint. The validity of the proposed controllers is ascertained by simulating the perturbed first-, second- and higher-order nonholonomic systems in MATLAB / SIMULINK. The proposed control algorithms globally steer the whole system to the origin.

Contents

List of Figures

List of Tables

Abbreviations

AUV	Autonomous Underwater Vehicle
FONHS	First Order Non-Holonomic System
ISMC	Integral Sliding Mode Control
LARC	Lie Algebra Rank Condition
NN	Neural Network
PVTOL	Planar Vertical Take-Off and Landing
SMC	Sliding Mode Control
SONHS	Second Order Non-Holonomic System
TONHS	Third Order Non-Holonomic System
UAV	Unmanned Aerial Vehicle
UMS	Underactuated Mechanical System
VSC	Variable Structure Control

Symbols

$\parallel x \parallel$	2-Norm of a vector
$\mathbb{R}^n$	n-Dimensional Euclidean space
$\mathbb{R}^{n \times m}$	Set of $n \times m$ matrices with elements in $\mathbb{R}$
$\mathbb{R}^+$	Non-negative real number set
$\in$	is a member of
A^T	Transpose of A
$diag$	Diagonal Matrix

Chapter 1

Introduction

This chapter begins with a brief overview of nonholonomic systems. The introduction is followed by research motivation for stabilizing perturbed and higher-order nonholonomic systems in a canonical form. A summary of major accomplishments and contributions of the thesis is provided afterwards. The chapter concludes with an overall layout of the thesis.

1.1   Background

There has been a growing curiosity in designing robust stabilizing control algorithms for nonholonomic systems during the last couple of decades. Based on the type of constraints on motion, general mechanical systems can be categorized into holonomic and nonholonomic systems. The word "holonomic" originates from two Greek words, *holos* and *nomos*, that mean "whole" and "law" [1]. In mechanics, holonomic systems are mechanical systems working under constraints, which limit the overall configuration of the mechanical system. The basic difference between a holonomic and nonholonomic constraint (usually provided in form of velocity, acceleration or higher-order time derivative of acceleration) is that the holonomic constraint is integrable, whereas the nonholonomic constraint is non-integrable. A typical example of a holonomic constraint is the fixed length of a simple pendulum;

whereas, the rolling ball and rolling disk without sideslip are classic examples of systems having nonholonomic constraints [2].

The presence of non-integrable constraints in nonholonomic systems makes the control problem of these systems much more challenging. Because of the broad range of applications of nonholonomic systems, much attention has been granted to designing feedback controllers for such systems. These systems are prevalent in various industries including transportation, robotics, space exploration, security and inspection [3], [4], [5] and [6]. Although this class of nonlinear systems is controllable; however, this class is not generally stabilizable by continuous/smooth static state feedback as these fail to satisfy Brockett's necessary condition [7] for smooth stabilization. As a result, the well-developed methods of smooth nonlinear control theory are not directly applicable to the control problem of these mechanical systems. Also, real-world systems often operate alongside input/model uncertainties and noise disturbances. The effects of these disturbances on the overall system dynamics must be considered during the controller design phase since these uncertainties or disturbances can degrade system performance or may even cause system instability. Thus, the problem of stabilizing nonholonomic systems while catering for the input/model uncertainties has become an important area of research.

Nonholonomic systems can further be classified as first-, second- and higher-order systems. The first-order systems have position and velocity constraints $\varphi\left(q, \dot{q}\right) = 0$ that cannot be written as $\psi\left(q\right) = 0$ and thus are non-integrable. Wheeled vehicles and robots are models of first-order nonholonomic systems. The second-order systems have position, velocity and acceleration constraints $\varphi\left(q, \dot{q}, \ddot{q}\right) = 0$ that cannot be written as $\psi\left(q, \dot{q}\right) = 0$, i.e., these are non-integrable constraints. Space robots, spacecrafts, underwater vehicles, surface vessels and under-actuated manipulators are real-world examples of nonholonomic models subject to second-order constraints [8]. Similarly, the higher-order nonholonomic systems specifically the third-order systems have constraints on positions, velocities, accelerations and jerk $\varphi\left(q, \dot{q}, \ddot{q}, \dddot{q}\right) = 0$ that cannot be written as $\psi\left(q, \dot{q}, \ddot{q}\right) = 0$ thereby meaning that their constraints are non-integrable. Dynamics represented by the movement

of a PPR (Prismatic-Prismatic-Revolute) manipulator under a jerk constraint is an model of a third-order nonholonomic system [9].

In designing control systems, it is always advantageous to first transform the system under consideration into some canonical form using input and/or state transformations. Chained form is one of the canonical form introduced in [10]. In [3], it is shown that nonholonomic systems can be (locally / globally) transformed into chained form under a suitable coordinate transformation. Many nonholonomic systems having first-order constraints can be globally or locally transformed into first-order canonical form. Similarly, the second-order canonical form plays the same role for the second-order systems as the simple canonical form system [11]. By conversion into the canonical form, the dynamics of the system are substantially simplified and, therefore, it becomes easier to design the control laws.

1.2 Research Motivation and Objectives

Various schemes have been proposed by the researchers to mitigate the stabilization problem of low-order nonholonomic systems. The applied methodologies for low-order nonholonomic systems include open-loop control, time-varying feedback control, discontinuous control and hybrid control, whereas control problem concerning higher-order nonholonomic systems is yet to be explored. The control of nonholonomic systems containing disturbances and / or uncertainties pose a special problem while considering real-world systems. The effect of these disturbances on the dynamics should be meticulously studied during the design phase as these perturbations can degrade the system performance and / or make the system unstable. For these reasons, the problem of designing control for nonholonomic systems in the presence of input and modelling uncertainties has become a principal area of research.

The open-loop control methodologies are based on sinusoidal inputs [12], polynomial inputs [13] and piece-wise constant inputs. Although the open-loop approach

is simple and useful in specific low-order nonholonomic systems, however, it does not provide a general solution for second- and higher-order nonholonomic systems.

The advantages of periodic and aperiodic time-varying continuous controls are that the input and state response are smooth and asymptotically converging without any oscillations. Nonetheless, the major drawback is that the control depends heavily on tuning the controller parameters specifically relating to initial conditions of the system. Thus, these time-varying approaches are less favourable as these do not qualify to be purely state feedback. Furthermore, it was shown in experimental work in [14] that smooth time-periodic feedback control fails to move mobile-robots towards a small neighbourhood region of wanted configuration in an acceptable duration.

In hybrid control, both discrete-time and continuous-time features are used. The methodology of hybrid control system relies on switching between different continuous time controllers at discrete-time instants. The controller switching instants may be altered online during the controller operation or may be defined a priori. Neural networks, fuzzy logic control and probabilistic reasoning based genetic algorithms are being used in the hybrid controllers. The neural networks have some drawbacks including the difficulty in selecting appropriate networks and slow convergence to the equilibrium point. Similarly, the major drawback of fuzzy logic control is the difficulty in getting fuzzy rules and membership functions.

Sliding mode control (SMC), proposed in [15], can be utilized to develop discontinuous time-invariant feedback laws. These discontinuous time-invariant laws enforce the system trajectory to slide along a well-designed stable manifold towards the equilibrium. SMC construction has been utilized for a certain class of higher-dimensional classical and dynamic models of nonholonomic systems [16]. However, the main drawback of SMC that hinders its widespread use is chattering phenomenon. Another disadvantage of using SMC is that the controller is sensitive to parameter and modelling variations and may cause instability during the reaching phase.

In this research, we propose robust stabilizing control algorithms for systems with first, second and higher-order nonholonomic constraints. Integral sliding mode control (ISMC) is used to eliminate the reaching phase of SMC. As a consequence, the robustness of the nonholonomic systems against parameter and modelling uncertainties can be achieved from initial instant. The main idea of disturbance rejection through sliding mode is achieved by the discontinuous term in the controller. A low pass filter may also be used to average the discontinuous part so that the proposed methodology can be easily implemented in real-world mechanical systems without long-term damage to the actuators. ISMC on its own does not solve the chattering problem; however, it eliminates the reaching phase of SMC. Thus, the advantage of robustness against parameter and modelling uncertainties is achieved from the beginning. Also, adaptive control methodology is utilized along with integral sliding mode (AISMC) to estimate the unknown terms in the proposed algorithms.

Additionally, to the best of our knowledge, stabilization problem concerning third-order nonholonomic systems has not been addressed yet. In this research, a third-order nonholonomic system having a jerk constraint is considered as a prototype model for higher-order nonholonomic systems. We propose novel stabilizing control algorithms for third-order nonholonomic systems based on adaptive ISMC.

1.3 Thesis Contributions

The main contributions of this research work include:

1. Feedback stabilization of drift-free systems with nonholonomic constraints is proposed using two different methodologies. Both the approaches are based on adaptive integral sliding mode control. The first approach uses Lie bracket extended system as the nominal system, whereas, the second approach is based on function approximation technique. Both approaches are applied to drift-free nonholonomic systems to prove the correctness. Afterwards, the methodologies are proposed for first-order nonholonomic systems

in chained form. The robust stabilizing control algorithm is implemented on a bench-mark underwater vehicle example of first-order nonholonomic systems containing uncertainties. Perturbations (both in input and the system model in matched form) are added to the original underwater vehicle system and the results obtained through simulations prove the correctness of the algorithm.

2. Novel stabilizing algorithms for second-order mechanical nonholonomic systems in chained form are proposed. The presented methodologies are general and may be applied to various second-order mechanical systems with nonholonomic constraints. The first approach uses Lie bracket extended system and the second approach is based on function approximation technique. The robustness of the methodologies is proved by applying the algorithms to the perturbed cases of second-order nonholonomic systems.

3. Stabilizing control is proposed for a higher-order nonholonomic system, specifically the third-order systems with jerk constraint. The algorithm is based on adaptive ISMC and the results are provided for both unperturbed and perturbed third-order nonholonomic systems in chained form.

1.4 Thesis Outline

The organization of the thesis is given below:

- Chapter 2 provides an detailed literature review of stabilization problem of nonholonomic systems.

- Preliminary concepts regarding the nonholonomic systems, various canonical form representations, some notions of differential geometry, controllability and stabilizability of nonholonomic systems, perturbation theory and SMC are presented briefly in chapter 3.

- Chapter 4 presents feedback stabilization algorithms for drift-free nonholonomic mechanical systems, chained form first-order nonholonomic systems and perturbed first-order nonholonomic systems.

- Chapter 5 provides a novel approach for the control of chained form second-order nonholonomic systems (both perturbed and unperturbed cases).

- AISMC based algorithm for chained form higher-order nonholonomic systems is provided in chapter 6.

- Finally, Chapter 7 contains conclusions of the thesis and some directions for probable topics of future research and applications.

Chapter 2

Literature Review

The chapter presents an in-depth literature review of control problems for systems with nonholonomic constraints. Review of applied control strategies for the stabilization of various nonholonomic systems is also presented in depth.

2.1 Control Problem of Nonholonomic Systems

The problem of controlling systems subject to non-integrable constraints has attracted the attention of the control community since the 80's. Initial research activities were focused on systems with non-integrable kinematic relations..Examples of these classical or first-order nonholonomic systems include systems with rolling constraints and systems involving symmetries which result in non-integrable conserved angular momentum. The studied examples were regarding mobile robots, wheeled vehicles, robot manipulation and space robots. These studies covered the areas of controllability, motion planning, feedback stabilization and tracking control. The motion planning problem was initially investigated in [17] achieving controllability of car-like robot with a single nonholonomic constraint. In [18], nonholonomic systems as a class of inherently nonlinear control system were identified and a general procedure for constructing a piece-wise analytic state feedback was presented. Controllability proof for a multibody mobile robot using tools from

differential geometry was given in [19]. A nonholonomic motion planning approach using geometrical phases was illustrated in [20]. In [21], it was suggested to stabilize the system about a trajectory instead of a point. Using a nonsmooth and time-varying feedback controller, global asymptotic stability for any desired configuration was achieved in [22] . Other notable developments include the study of controllability [23], motion planning ([12], [24]), stabilization ([25], [26],[27], [28]) and tracking control([8], [29], [30]) of classical first-order nonholonomic systems.

In [31], the ideas presented in [18] were extended to systems satisfying the second-order nonholonomic constraints. These second-order nonholonomic systems emerge by imposing specific design constraints on the allowable motion of redundant robotic manipulators. Similarly, some underactuated systems also qualify as second-order nonholonomic systems based on their configuration. The underactuated mechanical systems (UMS) are systems with fewer actuators than total degrees of freedom. The underactuated robot manipulators ([32], [33]), autonomous underwater vehicles, underactuated surface vessels, the planar vertical take-Off and landing aircraft and underactuated space vehicles [34] are examples of UMS belonging to this class. The main difference is that the second-order nonholonomic systems include drift terms that make control of these much more difficult. Whereas, in general, the second-order nonholonomic systems also do not satisfy Brocketts necessary condition [7] similar to the first-order nonholonomic systems. Various approaches have been identified for resolving this problem [3] which can be categorized into time-varying continuous feedback control ([35], [36]), discontinuous control ([37], [38], [39]) and hybrid control [40].

In recent times, substantial effort on the dynamics formulation for higher-order nonholonomic systems has been witnessed. Representative work in this area of higher-order nonholonomic systems include the research by Nielsen, Mangeron, Tzenoff, Appell, Deleanu and Gibbs (see [41] and the references therein). Subsequently, modern forms of differential equations of nonholonomic systems with higher-order constraints were derived. A special constraint known as program constraint is a demand imposed on a system by design. These program and material constraints are then included in a unified formulation providing a theoretical

framework for the study of robot performance under constrained environments [41]. Example of a higher-order nonholonomic system is a planar Prismatic-Prismatic-Revolute robotic manipulator exposed to a jerk constraint [42]. Jerk is a novel example of third-order constraint and is identified with fast changing actuator forces in the domain of robot manipulators. Furthermore, jerk is characterized as the triple time derivative of distance. Excessive amount of jerk leads to early wear and tear of the actuators. It produces resonant vibrations in the robotic body and thus makes accurate tracking even more challenging. Specific studies on humans reveal that human brain also realizes a variant of minimum-jerk while grasping actions are being planned for our arms [43].

2.2 Control Strategies for Stabilization of Non-holonomic Systems

Control of nonholonomic and canonical form systems has been an agile area of research in recent times. The topics of controllability, tracking, stabilization and motion planning have gained significant attention from the research community. In early 1980's feedback linearization technique was in vogue. Exact feedback linearizations of affine nonlinear systems were explicitly obtained by using differential geometric methods. Later on, Lyapunov methods received renewed interest with the introduction of recursive design technique such as backstepping and the notion of control Lyapunov function [44]. These methods were used to control large classes of nonlinear systems having matched and unmatched uncertainties [45]. Apart from these nonlinear classes, there exist a class of inherently nonlinear systems for which the linearization becomes uncontrollable. This class of inherently nonlinear systems does not permit any smooth (continuous) pure state feedback controls. Thus, making Lyapunov direct method and the standard feedback linearization technique no longer applicable to these systems. This specific class is known as the nonholonomic systems. As these nonholonomic systems fail to meet

the Brockett's necessary condition [7], the feedback stabilization problem of these systems is a challenging task.

In order to better analyze complex nonlinear systems, it is convenient to utilize canonical representations. Chained forms [12] are the canonical representations of many nonholonomic mechanical and electrical systems like AUVs, mobile/hopping robots and UAVs. These nonholonomic systems can be transformed to chained form systems by input and state transformations. As smooth feedback stabilization is not possible for these systems, therefore time-varying, discontinuous and hybrid control methods are used to resolve the stabilization problem [3]. In general, discontinuous controls can achieve exponential stability ([18], [46], [38]), whereas time-varying feedback control renders asymptotic stability ([47], [48]). While the existing strategies offer suitable answers, there is still a wish to explore global singularity-free solutions that may map the chained forms into controllable linear systems.

2.2.1 Open Loop Controls

The control action is not dependent on system output in an open loop control system. These open loop methodologies are based on polynomial, sinusoidal inputs and piecewise constants. The framework behind the sinusoidal inputs is to steer all the states one at a time using the sinusoids [12]. Open loop motion planning for low-dimensional mobile robots was proposed in [49]. Sinusoidal inputs were proposed in [12] in order to steer the open loop configuration of nonholonomic system in canonical form. Later on, this method was generalized in [50] by utilizing Lie-brackets of the input vectors.

Consider a drift-free n-dimensional system with nonholonomic constraints that can be stated as:

$$\dot{x} = g_1(x)\, u_1 + \cdots + g_m(x)\, u_m, \quad u \in \mathbb{R}^m, \quad x \in \mathbb{R}^n \qquad (2.1)$$

where $g_i(x)$ are vector fields (linearly-independent) and u is the control input, $m < n$. The steps for sinusoidal control are:

1. Find control input u_1 so that x_1 tends towards $x_1(t_f)$.

2. Find control input u_2 so that x_2 goes to $x_2(t_f)$.

3. Choosing $u_1 = A_1 \sin \theta$ and $u_2 = B_1 \cos \theta$ to stabilize x_3 from $x_3(t_0) \to x_3(t_f)$.

4. Again, choosing $u_1 = A_2 \sin \theta$ and $u_2 = B_2 \cos 2\theta$ to stabilize x_4 from $x_4(t_0) \to x_4(t_f)$.

   $\vdots$

   Step (n)

Whereas, the total steering time T is equally distributed into sub-intervals in the piecewise constants approach. Each sub-interval is δ in length in which a constant input is applied. Also, the open-loop control based on polynomials is similar to the piece-wise constant approach, but with improved smoothness properties [13].

2.2.2 Closed Loop Controls

The closed-loop approaches have received wider acknowledgement owing to the fact that these provide stabilization of second- and higher-order nonholonomic systems [3]. These include time-varying continuous control, discontinuous control and the hybrid control.

2.2.2.1 Time-Varying Continuous Controls

The two approaches for crafting time-varying continuous control suggested in the literature are periodic and aperiodic feedback control. The periodic method was proposed by [47] and [51] and is based on the power form. Whereas, the aperiodic time-varying feedback control was investigated in [35]. The Pomet's method [47] relies on Lyapunov's direct method which is similar to the technique of [52]. The

practical use of time-varying control introduced in the mobile robot by [48]. In [53], it is shown that classical nonholonomic systems can be asymptotically stabilized by using smooth periodic static state feedback. The saturation type functions and averaging method were used to design smooth time-periodic control to achieve global asymptotic stabilization ([12], [51], [54]). Whereas [48] and [21] provide stabilization established on constructing a nominal motion that moves towards the equilibrium asymptotically. The approach requires selection of a nominal trajectory a priori and can be used for designing time-varying control laws for nonholonomic problems.

The advantages of periodic and aperiodic time-varying continuous methodologies are that the input controls and states are all smooth, asymptotically converging without any oscillations. However, their disadvantage is that the input relies on suitable tuning of parameters dependent on the system's initial states. Thus, these are less favourable as these fail to be pure state feedback control. Furthermore, [14] showed in experimental work that these time-periodic controls do not stabilize moving robots to a small neighbourhood of the desired configuration in an acceptable time.

2.2.2.2 Discontinuous Feedback Controls

The discontinuous feedback control avoids the difficulty to construct a single continuous control as in the time-varying counterpart. The main idea in discontinuous control is to alter the control law when system states try to move away from the stable manifold. These feedback controllers for stabilizing nonholonomic systems can further be categorized into piecewise continuous and the sliding mode controllers.

The σ-process [27] is a prevalent methodology of the discontinuous control system design. After state transformation, a stabilizable linear system is obtained and one can choose linear control laws to assign stable eigenvalues. Hence, the system (in transformed coordinates) is globally exponentially stable. At the same time, the drawback is that the linear control is not defined for the whole state space.

In order to overcome this challenge, it is suggested to first move the system away from the singularity by applying open-loop controls for an a-priori calculated time t_s and afterwards change to the linear feedback control law [27]. In [50] a formula is acquired from a piecewise control Lyapunov function for global stabilization. While no general method exists for designing control Lyapunov functions that satisfy conditions of [50], piecewise continuous stabilization of some specific models have been mentioned.

In [55] a discontinuous controller has been designed for the higher-order canonical form system involving two inputs. The discontinuous controller does not stabilize the system, but only achieves exponential convergence towards the point to be stabilized meaning that the system trajectories converge exponentially towards the point to be stabilized. However, since the controller and therefore the closed-loop system is discontinuous at the point to be stabilized, no stability property in the sense of Lyapunov can be shown to hold.

Sliding mode control (SMC), proposed in [15], can also be utilized to develop discontinuous time-invariant feedback laws. This discontinuous control enforces the system to move along a well-defined stable manifold in the direction of equilibrium. SMC construction has been utilized for a certain class of higher-dimensional classical and dynamic models of nonholonomic systems [16]. However, the main drawback of SMC that hinders its widespread use is chattering phenomenon. [15] suggested to apply smoothing between gradients on both sides of the sliding surface in order to overcome chattering. Other methods to alleviate the chattering have also been reported in the literature. Another disadvantage of SMC is that it is not immune to measurement noise as the input signal relies on the sign of a measured variable which is close to zero.

2.2.2.3   Hybrid Control

In hybrid control, both discrete-time and continuous-time features are used. The working of hybrid control system relies on changing between different continuous-time controllers at discrete-time instants. The controller switching instants can

be either specified a priori or be altered online during the operation of the controller. Soft computing methodolies include the fuzzy logic control (FL), artificial neural networks (ANN) and probabilistic reasoning (PR) methods are used with continuous time controllers in order to achieve the desired results. Also, there is an increasing enthusiasm in using soft-computing algorithms alongside SMC.

In [22] hybrid controllers were developed for stabilizing classical nonholonomic systems in canonical form. The proposed method in [56] was applicable to large class of systems with classical nonholonomic constraints. It used a family of periodic inputs that result in periodic trajectories. In [57] a neural network-based adaptive SMC was constructed to ensure trajectory tracking by a robotic manipulator. Similarly, in [58] a self-tuning fuzzy inference SMC method for single inverted pendulum position tracking control was presented. Fuzzy logic is basically concerned with approximate reasoning and imprecision, whereas neural networks are chiefly curve fitting and learning tools. The neural networks have some drawbacks including the difficulty in selecting appropriate networks and the slow convergence to the equilibrium point. Similarly, the major drawback of fuzzy logic control is the difficulty in getting membership functions and fuzzy rules.

2.3   Research Gap

Owing to the famous Brockett's necessary condition for smooth static state-feedback for nonholonomic systems [7], the problem of controlling nonholonomic systems becomes non-trivial. Also, real-world applications offer a daunting task of addressing parameter variations and modelling uncertainties. Various methods have been suggested by the research community to address the stabilization problem of systems with first- and second-order nonholonomic constraints. However, to the best of our knowledge, control problem concerning higher-order nonholonomic systems has not been solved yet. Although the open-loop approach is simple and useful in specific low-order nonholonomic systems, however, it does not provide

a general solution for the second- and higher-order nonholonomic systems. Similarly, the main drawback of using time-varying approach is that the control law relies heavily on tuning of parameters that relate to initial conditions of the system. Thus, the time-varying techniques are less favourable as these are not pure state feedback control. Also, hybrid techniques involving the neural networks and fuzzy logic control have drawbacks including the difficulty in selecting appropriate networks and slow convergence to the equilibrium point.

In this research, we propose robust stabilizing control algorithms based on adaptive integral SMC to resolve the problem of stabilization in general first-, second- and higher-order perturbed nonholonomic systems in chained form. The integral SMC is used to eliminate the reaching phase of SMC. As a result, robustness of nonholonomic systems against parameter and modelling uncertainties can be achieved from the initial time instant. Additionally, stabilization problem concerning third-order nonholonomic systems having a jerk constraint has not been addressed yet. In this research, we also propose novel stabilizing control algorithms for third-order nonholonomic systems based on adaptive ISMC.

2.4 Summary

This chapter presented a detailed literature review of control problem and various control methodologies applied to kinematic and dynamic nonholonomic systems. The application of these control methodologies to higher-order nonholonomic systems is still an open problem. Furthermore, the research gap highlights the drawbacks and limitations of existing methodologies.

Chapter 3

Preliminaries

This chapter presents some preliminary notions regarding nonholonomic systems (nonholonomic systems), types/orders of nonholonomic systems, controllability and stabilization of these systems. Some detail about different canonical forms of nonlinear systems is also presented in this chapter. This is followed by a brief review of perturbation theory. Sliding mode control (SMC) theory, its advantages and integral SMC are presented towards the end of this chapter.

3.1 Nonholonomic Systems

Generally, drift-free systems with nonholonomic constraints are given as:

$$\dot{x} = \sum_{i=1}^{m} g_i(x)\, u_i \qquad (3.1)$$

where $g_i(x)$ are linearly-independent vector fields and $u = \begin{bmatrix} u_1 & \cdots & u_m \end{bmatrix}^T$ is the control input. Here x is specified in local coordinates and is an element of n-dimensional smooth manifold M which is locally diffeomorphic to the Euclidean space $\mathbb{R}^n$. Some basic terminologies of differential geometry along with their definitions are presented in Appendix-1 for developing general understanding.

While many drift-free systems with nonholonomic constraints can be specified in the control-affine form (3.1), our research is oriented towards the first-, second- and higher-order nonholonomic systems that can be converted into a suitable canonical form. For first-order kinematic systems, the position x is equivalent to the configuration $q \in Q$ and $g_i(x)$ are vector fields representing velocity directions. In case of second-order dynamic systems, the state space becomes $x = (q, \dot{q})$, controls u are generalized forces and the linearly independent vector fields represent acceleration directions. Similarly, for the third-order nonholonomic systems, $x = (q, \dot{q}, \ddot{q})$ and the linearly independent vector fields represent applied jerk directions. In the subsequent section, we will describe the difference between holonomic and nonholonomic constraints.

3.1.1   Holonomic vs Nonholonomic Constraints

Consider a general kinematic system and assume that $q = \begin{bmatrix} q_1 & q_2 & \cdots & q_n \end{bmatrix}^T \in Q$ defines configuration of the system. Assume also that the configuration space Q is locally diffeomorphic to the Euclidean space $\mathbb{R}^n$ and is an n-dimensional smooth manifold. At any point $q(t) \in Q$ along system trajectory, the generalized velocity is given by the tangent vector $\dot{q} = \begin{bmatrix} \dot{q}_1 & \dot{q}_2 & \cdots & \dot{q}_n \end{bmatrix}^T \in T_q(Q)$.

Broadly speaking, there are two types of velocity or kinematic constraints that may be applied to the system. These are known as holonomic and nonholonomic constraints based on integrability condition of the kinematic constraints. When the velocity constraint is integrable, the constraint is called *holonomic*; whereas, in case the applied velocity constraint is non-integrable, the constraint is said to be *nonholonomic*. The holonomic constraint is also known as a pure geometric constraint and is described as:

$$h_i(q) = 0, \quad i = 1, 2, \cdots, k < n \tag{3.2}$$

where $h_i(q)$ are independent and smooth functions. The result of geometric or holonomic constraint is to restrict the achievable configuration to an $(n - k)$-dimensional sub-manifold of Q.

The second type of velocity-dependent constraint i.e. the nonholonomic constraint involves generalized coordinates and their respective derivatives. This constraint cannot be integrated to form a geometric constraint. The nonholonomic constraint is described as:

$$a_i(q, \dot{q}) = 0, \quad i = 1, 2, \cdots, k < n \tag{3.3}$$

Mostly the kinematic constraints are linear in terms of velocities and are known as affine in velocity or Pfaffian constraints. Thus, owing to the linear property, these can be described as:

$$a_i^T(q)\dot{q} = 0, \quad i = 1, 2, \cdots, k < n \tag{3.4}$$

or in compact form as:

$$A^T(q)\dot{q} = 0$$

3.1.1.1   Example of a Linear Kinematic Constraint

Take a simple model of a four-wheel car as portrayed in Figure 3.1. The rear wheels of the car are fixed, whereas, the front wheels can rotate about the vertical axis. Constraints on the car emerge when the wheels are permitted to spin and roll, however, slipping motion of the wheels is not allowed.

Let us take the configuration of the four-wheel system as (x, y, θ, ϕ), identified by xy location of the rear wheel. Let θ be the angle relative to the horizontal axis and ϕ be the steering angle. Now, constraints for both rear and front wheels are formed by setting the perpendicular velocity of the car to zero. This makes the velocity of the rear wheels perpendicular to their direction as $\dot{x} \sin \theta - \dot{y} \cos \theta$ and the front wheels as $\dot{x} \sin(\theta + \phi) - \dot{y} \cos(\theta + \phi) - l\dot{\theta} \cos \phi$. The Pfaffian constraints
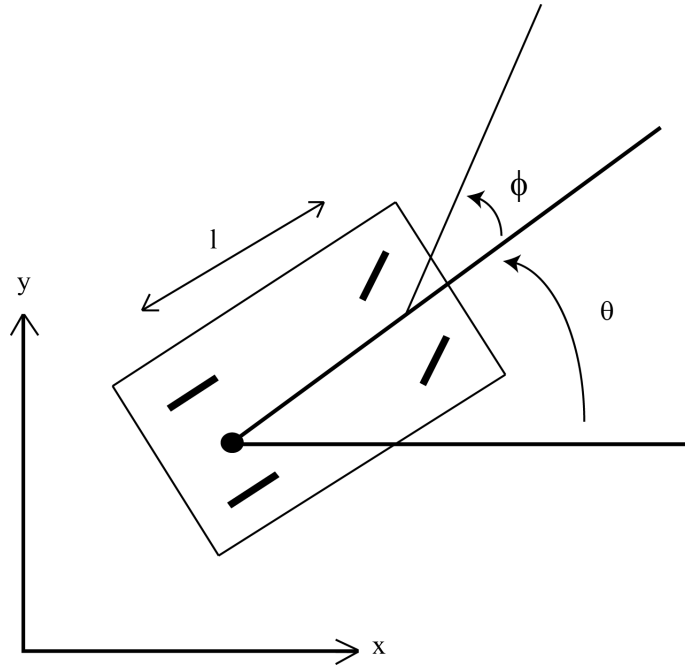
FIGURE 3.1: Kinematic Model of a Four-wheel Car.

on the car are:

$$\dot{x}\sin\theta - \dot{y}\cos\theta = 0$$

$$\dot{x}\sin(\theta + \phi) - \dot{y}\cos(\theta + \phi) - l\dot{\theta}\cos\phi = 0$$

or

$$A^T(q)\dot{q} = 0$$

where $A^T(q) = \begin{bmatrix} \sin\theta & -\cos\theta & 0 & 0 \\ \sin(\theta + \phi) & -\cos(\theta + \phi) & 0 & -l\cos\phi \end{bmatrix}$

3.1.2   Integrability of Kinematic Constraints

The kinematic constraints are labeled as integrable if there exists k scalar functions h_i so that the following equation is satisfied:

$$\frac{\partial h_i(q(t))}{\partial q} = a_i^T(q), \quad i = 1, 2, \cdots, k \tag{3.5}$$

By replacing (3.5) in (3.4), we obtain:

$$\frac{\partial h_i(q(t))}{\partial q}\dot{q} = 0, \quad i = 1, 2, \cdots, k \tag{3.6}$$

thus, resulting in the following geometric constraint,

$$h_i(q) = c_i, \quad i = 1, 2, \cdots, k \tag{3.7}$$

Equations (3.5) to (3.7) show that when the kinematic constraints are integrable and can be reduced to pure geometric constraints, these are said to be holonomic constraints. In this case, the integrable constraints can be substituted by algebraic constraints which do not involve velocities. The effect of a holonomic constraint on the system dynamics is that it reduces the overall dimension of the configuration space.

If the solution of (3.5) does not exist, then the constraints cannot be integrated and are known as nonholonomic. In such nonholonomic systems, there is no reduction in the dimension of the reachable space, rather the effect is the only reduction in the dimension of the feasible velocities. Specific discussion on the reachable configuration of nonholonomic systems will be discussed in the controllability of nonholonomic systems.

3.1.3 Test for Integrability of Constraints

A simple method to quickly verify whether the constraint is nonholonomic is as follows:

Suppose $h(q) = 0$ function exists, then we have $\dfrac{\partial h}{\partial q}\dot{q} = 0$. Now, denote $\left(\dfrac{\partial h}{\partial q}\right)_{ij} = \dfrac{\partial h_i}{\partial q_j}$, then we get the following:

$$
\begin{aligned}
\frac{\partial \left(\dfrac{\partial h}{\partial q}\right)_{ij}}{\partial q_k} &= \frac{\partial^2 h_i}{\partial q_j \partial q_k} \\
&= \frac{\partial^2 h_i}{\partial q_k \partial q_j} \\
&= \frac{\partial \left(\dfrac{\partial h}{\partial q}\right)_{ik}}{\partial q_j}
\end{aligned}
\tag{3.8}
$$

Thus, for $A^T(q)$ in (3.4), if the following equality does not hold, the system is nonholonomic,

$$
\frac{\partial A_{ij}}{\partial q_k} = \frac{\partial A_{ik}}{\partial q_j}
\tag{3.9}
$$

3.2 Types / Orders of Nonholonomic Systems

The nonholonomy in a system can arise because of the following two factors:

- A rolling body moves over another body or plane without any slippage.

- In a multi-body system, conservation of momentum is maintained with under-actuated control.

Nonholonomic systems can further be classified as first-, second- and higher-order systems. Systems with constraints of first-, second- or even third-order have been mathematically modelled and reported in the literature. The First Order Non-Holonomic Systems (FONHS) have position and velocity constraints $\varphi\left(q, \dot{q}\right) = 0$ that cannot be written as $\psi\left(q\right) = 0$) and thus are non-integrable. Wheeled vehicles and robots are examples of FONHS. The Second Order Non-Holonomic Systems (SONHS) have position, velocity and acceleration constraints $\varphi\left(q, \dot{q}, \ddot{q}\right) = 0$ that cannot be written as $\psi\left(q, \dot{q}\right) = 0$ i.e. these are non-integrable constraints. The main cause of acceleration constraints in SONHS systems is because of the fact

that the system under consideration is mainly underactuated, i.e. fewer controls are available in the mechanical system than the overall system configuration. Similar to the FONHS systems, the acceleration constraints cannot be integrated in SONHS case. Space robots, spacecrafts, underwater vehicles, surface vessels and under-actuated manipulators are real-world examples of SONHS [8]. Similarly, the higher-order nonholonomic systems specifically the Third Order Non-Holonomic Systems (TONHS) have constraints on positions, velocities, accelerations and jerk $\varphi\left(q, \dot{q}, \ddot{q}, \dddot{q}\right) = 0$ that cannot be written as $\psi\left(q, \dot{q}, \ddot{q}\right) = 0$ thereby meaning that their constraints are non-integrable. Dynamics represented by the movement of a PPR (Prismatic-Prismatic-Revolute) manipulator under a jerk constraint is a model of a TONHS [9]. This third-order nonholonomic constraint occurs by imposing torsion and curvature constraints on trajectories of the robot.

3.2.1 First-Order Nonholonomic Systems

For the kinematic systems, the state x is equal to the configuration q and the number of velocity constraints is given by $k = n - m \geq 1$, i.e. the overall dimension of configuration space excluding the control space.

3.2.1.1 Four-Wheel Car

Again taking the simple first-order model of a four-wheel car presented in Section 3.1.1.1 and shown in Figure 3.1. Now, choosing u_1 and u_2 as the driving and steering velocities respectively, the control system can be given as:

$$
\begin{bmatrix} \dot{x} \\ \dot{y} \\ \dot{\theta} \\ \dot{\phi} \end{bmatrix} = \begin{bmatrix} \cos\theta \\ \sin\theta \\ \dfrac{1}{l}\tan\phi \\ 0 \end{bmatrix} u_1 + \begin{bmatrix} 0 \\ 0 \\ 0 \\ 1 \end{bmatrix} u_2 \tag{3.10}
$$

For the above-mentioned four-wheel car, the null-space representing two kinematic constraints is of 2-dimensional. It is easy to verify that the constraints are nonholonomic by nature by using (3.9). Similarly, in case of front-driven four-wheel car, the nonholonomic system is same except that the term $\frac{1}{l}\sin\phi$ replaces $\frac{1}{l}\tan\phi$.

3.2.2 Second-Order Nonholonomic Systems

As mentioned earlier, Under-actuated Mechanical Systems (UMS) lead towards second-order constraints. Consider a UMS with q as the set of generalized coordinates. Partition the set of generalized coordinates as $q = (q_a, , q_b)$, where $q_a \in \mathbb{R}^m$ denotes the directly actuated part and $q_b \in \mathbb{R}^{n-m}$ denotes the unactuated part. The equation of motion of the UMS becomes:

$$M_{11}(q)\ddot{q}_a + M_{12}(q)\ddot{q}_b + F_1(q, \dot{q}) = B(q)u \tag{3.11}$$

$$M_{21}(q)\ddot{q}_a + M_{22}(q)\ddot{q}_b + F_2(q, \dot{q}) = 0 \tag{3.12}$$

Equation (3.12) defines $n-m$ relations involving the generalized coordinates, first-order and second-order derivatives. If these $n-m$ equations are not integrable, then these can be interpreted as nonholonomic constraints of second order.

3.2.2.1 Underactuated Surface Vessel

The vessel, shown in Figure 3.2, is a nonholonomic system with zero velocity constraints and added damping factor. The objective is to control the bearings as well as position of the vessel with two independent propellers.
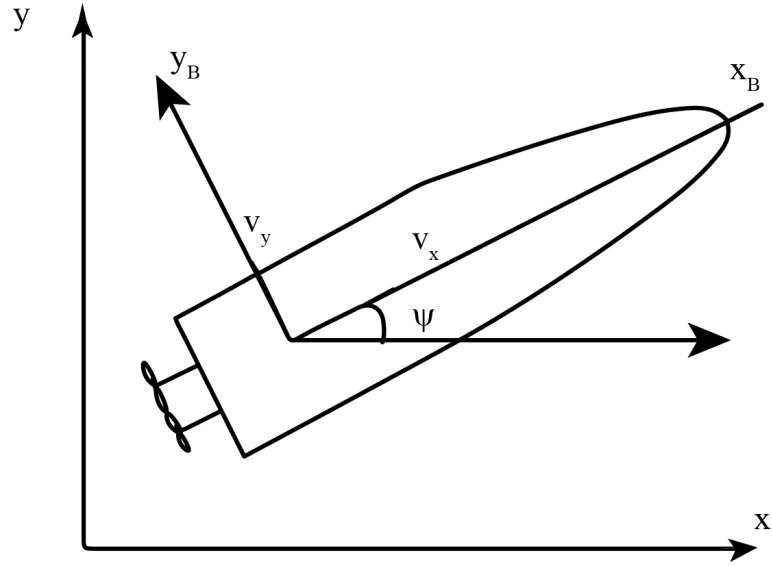
FIGURE 3.2: Underactuated Surface Vessel.

The relationship between the earth-fixed (inertial frame) and the body fame is specified by the following kinematic model:

$$\dot{x} = v_x \cos\psi - v_y \sin\psi$$
$$\dot{y} = v_x \sin\psi + v_y \cos\psi \qquad (3.13)$$
$$\dot{\psi} = \omega_z$$

where (x, y) represents the inertial location of the center of mass, ψ represents orientation of vessel, (v_x, v_y) are the linear velocities and ω_z is angular velocity of the vessel in body axis. The motion equations in the body axis are given as:

$$M\dot{v} + C(v)v + D(v)v = \tau \qquad (3.14)$$

where v represents the velocity vector, $\tau = \begin{bmatrix} F_x & 0 & T_z \end{bmatrix}^T$ is the force and torque generated by independent propellers, $M \in \mathbb{R}^{3\times3}$ is the inertia matrix, $C(v) \in \mathbb{R}^{3\times3}$ represents the Coriolis/Centrifugal matrix and $D(v) \in \mathbb{R}^{3\times3}$ denotes the damping matrix. Assuming that both M and D are constant and diagonal, we obtain the

following simplified model:

$$m_{11}\dot{v}_x - m_{22}v_y\omega_z + d_{11}v_x = F_x$$

$$m_{22}\dot{v}_y + m_{11}v_x\omega_z + d_{22}v_y = 0 \tag{3.15}$$

$$m_{33}\dot{\omega}_z + (m_{22} - m_{11})v_xv_y + d_{33}\omega_z = T_z$$

and $m_{ii}, d_{ii}, i = 1, 2, 3$ are constants and positive.

The vessel under consideration has no side thruster. Assume (ξ, η) represent the center of mass in the body axis:

$$(\xi, \eta) = (x\cos\psi + y\sin\psi, -x\sin\psi + y\cos\psi)$$

The configuration space parameterized by $q = \begin{bmatrix} \psi & \xi & \eta \end{bmatrix}^T$ is denoted as $Q = \mathbb{S}^1 \times \mathbb{R}^2$. Therefore, by defining input transformations from (F_x, T_z) to new control inputs (u_1, u_2), the motion equations can be rewritten as:

$$\ddot{\psi} = u_1 \tag{3.16}$$

$$\ddot{\xi} = u_2 \tag{3.17}$$

$$\ddot{\eta} = -\xi\ddot{\psi} - \alpha(\dot{\eta} + \dot{\psi}\xi) - (1 + \beta)\dot{\psi}\dot{\xi} + \beta\dot{\psi}^2\eta \tag{3.18}$$

where $\alpha = d_{22}/m_{22}$ and $\beta = m_{11}/m_{22}$.

The above (3.18) represents a nonintegrable constraint and involves generalized coordinates, velocities and accelerations. Thus, the underactuated vessel is a non-holonomic system having second-order constraint.

3.2.3 Third-Order Nonholonomic Systems

Since the beginning of the last century, considerable effort has been put in to formulate theory with respect to higher-order nonholonomic constraints [59]. The constraints, defined as program constraints, occur by imposing specific conditions on the allowable trajectories. For example, second- and third-order nonholonomic

constraints occur by imposing torsion and curvature constraints on robot trajectories. By following ([60], [59]), systems with higher-order non-holonomic constraints can be given by the following models after suitable state and input transformations [42]:

$$q_1^{(p)} = u \tag{3.19}$$

$$q_2^{(p)} = J(q, \dot{q}, ..., q^{(p-1)})u + R(q, \dot{q}, ..., q^{(p-1)}) \tag{3.20}$$

where $q_1 \in \mathbb{R}^m$, $m \geq 2$ denotes the directly actuated configuration variables, $u \in \mathbb{R}^m$ represents the modified control for the directly actuated variables and $q_2 \in \mathbb{R}^{n-m}$ represents the configuration variables where control is achieved through system coupling.

3.2.3.1 PPR Manipulator

Let us take a planar prismatic-prismatic-revolute (PPR) robot manipulator moving on a horizontal plane such that the gravity term could be avoided, as shown in Figure 3.3.
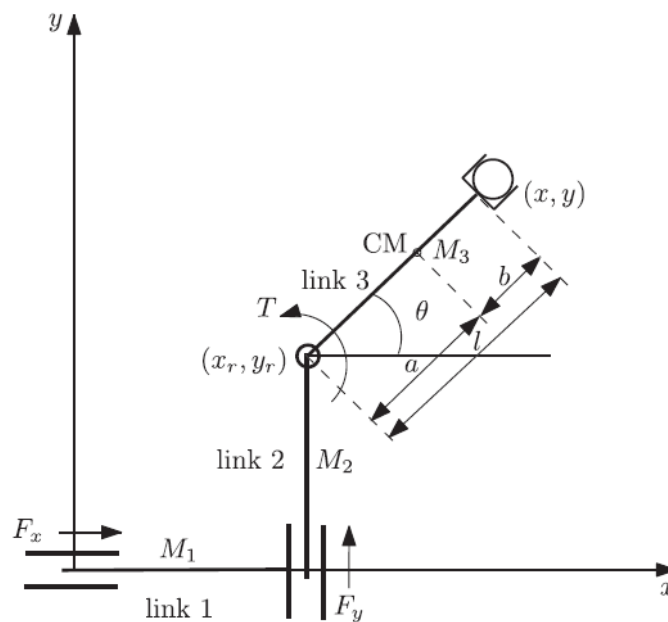
FIGURE 3.3: Planar PPR Manipulator.

Here, the objective is to maneuver the PPR manipulator between two position configurations, (x_0, y_0, θ_0) and (x_f, y_f, θ_f) so that the transverse jerk is zero at the end-effector, that is,

$$\dddot{x} \sin \theta - \dddot{y} \cos \theta = 0 \qquad (3.21)$$

or

$$A^T(q, \dot{q}, \ddot{q}) \dddot{q} = 0$$

where $A^T(q, \dot{q}, \ddot{q}) = \begin{bmatrix} \sin \theta & -\cos \theta & 0 \end{bmatrix}$

The above constraint can be thought of as a design constraint. Also, $p = n = 3$ and $m = 2$ in this particular example. Above equation presents a nonintegrable relationship and involves the generalized distances, velocities, accelerations and jerk. Thus, the PPR manipulator is a nonholonomic system with third-order constraint. Jerk is envisioned as rapidly changing actuator force in the robot manipulators which leads to vibrations in the robotic structure, premature wear and tear of the actuators and is difficult to track accurately by the controller.

3.3 Chained Form Systems

In order to proceed with a systematic development of either open-loop or closed-loop control systems, it is convenient to represent the nonholonomic systems in some canonical form. The chained form is one of the most useful canonical representation in various cases [12]. Many practical systems, both electrical and mechanical, can be transformed into the following drift-free model through diffeomorphic control/state transformations:

$$\dot{x}_1 = u_1$$
$$\dot{x}_2 = u_2$$
$$\dot{x}_3 = x_2 u_1 \qquad (3.22)$$
$$\vdots$$
$$\dot{x}_n = x_{n-1} u_1$$

General studies may involve multiple chains, which is an extension of the above-mentioned $(2, n)$ form.

$$\dot{x}_1 = u_1$$
$$\dot{x}_2 = x_1 u_1$$
$$\dot{x}_3 = x_2 u_1 \tag{3.23}$$
$$\dot{x}_4 = u_2$$
$$\dot{x}_5 = x_4 u_2$$
$$\vdots$$
$$\dot{x}_n = x_{n-1} u_2$$

Now, considering the chained form and by applying another transformation:

$$\xi_1 = x_1$$
$$\xi_2 = x_2$$
$$\xi_3 = -x_3 + x_1 x_2$$
$$\xi_4 = x_4 - x_1 x_3 + \frac{1}{2} x_1^2 x_2 \tag{3.24}$$
$$\vdots$$
$$\xi_n = (-1)^n x_n + \sum_{i=2}^{n-1} (-1)^i \frac{1}{(n-i)!} \xi_1^{n-i} \xi_i$$

we get the following power form which is yet another canonical form:

$$\dot{\xi}_1 = u_1$$
$$\dot{\xi}_3 = \xi_1 u_2$$
$$\dot{\xi}_4 = \frac{1}{2}\xi_1^2 u_2 \qquad (3.25)$$
$$\vdots$$
$$\dot{\xi}_n = \frac{1}{(n-2)!}\xi_1^{n-2} u_2$$
$$\dot{\xi}_2 = u_2$$

In essence, the control design of nonholonomic mechanical system usually begins from the canonical representation instead of the specific mechanical model of the system.

3.3.1   First-Order Chained Form

Equation (3.22) represents first-order chained form. As an example, consider a car-like robot model given below:

$$\begin{bmatrix} \dot{x} \\ \dot{y} \\ \dot{\theta} \\ \dot{\phi} \end{bmatrix} = \begin{bmatrix} \cos\theta \\ \sin\theta \\ \frac{1}{l}\tan\phi \\ 0 \end{bmatrix} v_1 + \begin{bmatrix} 0 \\ 0 \\ 0 \\ 1 \end{bmatrix} v_2 \qquad (3.26)$$

This robotic model can be modified into:

$$\dot{\zeta}_1 = u_1$$
$$\dot{\zeta}_2 = u_2 \qquad (3.27)$$
$$\dot{\zeta}_3 = \zeta_2 u_1$$
$$\dot{\zeta}_4 = \zeta_3 u_1$$

through the transformations:

$$\zeta_1 = x, \quad \zeta_2 = \frac{\tan\phi}{l\cos^3\theta}, \quad \zeta_3 = \tan\theta, \quad \zeta_4 = y$$

$$v_1 = \frac{u_1}{\cos\theta}, \quad v_2 = -\frac{3\sin\theta}{l\cos^2\theta}\sin^2\phi u_1 + l\cos^3\theta\cos^2\phi u_2$$

3.3.2 Second-Order Chained Form

A special canonical form called second-order chained form system is defined as:

$$\ddot{y}_1 = v_1$$
$$\ddot{y}_2 = v_2$$
$$\ddot{y}_3 = y_2 v_1 \qquad\qquad (3.28)$$
$$\vdots$$
$$\ddot{y}_n = y_{n-1} v_1$$

This second-order chained form plays the same role for the SONHS as the simple chained form system for the FONHS. It is well known that a class of UMS having two inputs and three degrees of freedom (3-DOF) can be converted to chained form (3.28) by formulating input and coordinate transformations [11]. Through this conversion, system dynamics are significantly reduced and it becomes easier to design the control law.

Consider a 3-DOF manipulator having a passive joint. Let $\ddot{x} = u_1$, $\ddot{y} = u_2$. Then, system dynamics can be written as:

$$\ddot{x} = u_1$$
$$\ddot{y} = u_2 \qquad\qquad (3.29)$$
$$\ddot{\theta} = \frac{1}{\lambda}\sin\theta\, u_1 - \frac{1}{\lambda}\cos\theta\, u_2$$

With the following input transformation

$$u_1 = \xi_1$$
$$u_2 = \tan\theta\,\xi_1 - \lambda\sec\theta\,\xi_2 \tag{3.30}$$

the system (3.29) can be transformed as:

$$\ddot{x} = \xi_1$$
$$\ddot{\theta} = \xi_2 \tag{3.31}$$
$$\ddot{y} = \tan\theta\,\xi_1 - \lambda\sec\theta\,\xi_2$$

Using another transformation

$$y_1 = x + \lambda\cos\theta$$
$$y_2 = \tan\theta$$
$$y_3 = y + \lambda\sin\theta \tag{3.32}$$
$$v_1 = \xi_1 - \lambda\sin\theta\,\xi_2 - \lambda\cos\theta\,\dot{\theta}^2$$
$$v_2 = \sec^2\theta\,\xi_2 + 2\sec^2\theta\,\tan\theta\,\dot{\theta}^2$$

where v_1, v_2 are modified inputs and $y_i, i = 1, 2, 3$ are new coordinate variables. Thus, we get the following chained form system:

$$\ddot{y}_1 = v_1$$
$$\ddot{y}_2 = v_2 \tag{3.33}$$
$$\ddot{y}_3 = y_2 v_1$$

Second-order systems that can be modified into the chained form include: an underactuated planar horizontal 3-link serial-drive PPR manipulator (PPR means two prismatic and one revolute joint), an underactuated planar horizontal PPR manipulator with a spring-coupled 3rd link, an underactuated planar horizontal 3-link serial-drive RRR manipulator, a manipulator driven by end-effector forces,

an underactuated planar horizontal parallel drive RRR manipulator with any two joints unactuated, a planar rigid body with an unactuated DOF, an underactuated surface vessel [8].

Similarly, third-order or even higher-order chained form systems may be defined as:

$$
\begin{aligned}
\dddot{z}_1 &= w_1 \\
\dddot{z}_3 &= z_2 w_1 \\
&\vdots \\
\dddot{z}_n &= z_{n-1} w_1 \\
\dddot{z}_2 &= w_2
\end{aligned}
\tag{3.34}
$$

Next, controllability of nonholonomic systems is explained as if the system is uncontrollable, then it is useless and there is no point in investigating the stabilization of such uncontrollable system.

3.4 Controllability and Stabilizability

For the kinematic constraints mentioned in (3.4), the effect of constraints can be easily studied using an alternate approach i.e. to study the directions where motion of the system is permitted instead of where the motion is restrained. Equation (3.4) implies that system motion is permitted in the null space of constraints $a_i(q)$. That is, vector fields $g_j(q)$ can be defined in a way that the following equation holds:

$$
a_i^T(q)g_j(q) = 0, \quad j = 1, \cdots, n-k \quad i = 1, \cdots, k,
$$

or in compact form as:

$$
A^T(q)G(q) = 0
$$

The solutions $q(t)$ of the following equation give feasible trajectories of the system:

$$\dot{q}(t) = \sum_{j=1}^{m} g_j(q)u_j = G(q)u \tag{3.35}$$

with input $u(t) \in \mathbb{R}^m, m = n - k$. System (3.35) is also called driftless in the sense that the states stay at any configuration when there is no control input.

3.4.1   Contollability of Nonholonomic Systems

The definition of controllability with regards to the driftless nonholonomic system (3.35) is given below.

Definition 3.1. *The driftless system is known as controllable if there exists control input $u(t) \in \mathbb{R}^m, m = n - k$ and time $T > 0$ for any initial and final conditions in $\mathbb{R}^n$, so that $q(0) = q_0$ and $q(T) = q_f$.*

The controllability of driftless system (3.35) is governed by the properties of the vector fields $g_j(q), j = 1, 2, \cdots, m$. It is beneficial to go through some basic concepts from differential geometry mentioned in Appendix-1 in order to fully appreciate these properties.

Obviously, when the system (3.35) is allowed to move in all directions of the configuration space, it is said to be controllable. Nevertheless, owing to the presence of nonholonomic constraints, the system's movement is restricted in the null space of the constraints. Therefore, the tangent space is of reduced dimension than the overall configuration space $(m < n)$. Now, the controllability of the system is dependent upon whether it is possible to generate new linearly independent control directions by manoeuvering control inputs along the permitted directions. The famous Chow's theorem provides guidance regarding generation of new linearly independent control directions and controllability. It states that:

Theorem 3.1. *If there exists involutive distribution $\bar{\Delta} = \mathbb{R}^n$ for all $q \in Q$, then the system (3.35) is controllable on Q.*

For vector fields $g_1, ..., g_m$ as mentioned in system (3.35), Chow's theorem can be interpreted as: *if the union of distribution represented by the vector fields and the subspace consisting of the Lie Brackets has equivalent dimension as the configuration space of the system at all points, the system is said to be controllable.*

It means that the Lie Bracket of vector fields contributes movement in restricted directions and in this way controllability can be obtained. Thus, the operation of Lie Bracket is tantamount in determining controllability of driftless systems.

3.4.2   Feedback Stabilization

Brockett's theorem provides necessary conditions for feedback stabilization of nonlinear systems and was proposed in [7].

Theorem 3.2. *Taking a nonlinear system $\dot{x} = f(x, u)$ with $f(.,.)$ as continuously differentiable in a neighborhood of $(x_0, 0)$ and $f(x_0, 0) = 0$. There exists a continuously differentiable controller for asymptotically stabilization of $(x_0, 0)$ if following necessary conditions are fulfilled:*

1. *There are no uncontrollable modes in the linearized system having positive real eigenvalues.*

2. *A small neighborhood N exists around $(x_0, 0)$ so that control $u_\xi(t)$ drives the solution for each $\xi \in N$ and for all $t > 0$ from $x = \xi$ at $t = 0$ to $x = x_0$ at $t = \infty$.*

3. *The mapping $\gamma : N \times \mathbb{R}^m \to \mathbb{R}^n$ given by $\gamma : (x, u) \to f(x, u)$, where N is a neighborhood of the origin, should be onto an open set of the origin.*

By extending the above conditions to the continuous feedback, we get the main result for kinematic systems which is as follows:

Proposition 3.1. *Take the system*

$$\dot{x} = \sum_{k=1}^{m} g_k u_k,$$

where $x \in \mathbb{R}^n, m < n$ and $rank\{g_1(0), \cdots, g_m(0)\} = m$. No continuous feedback control law exists that locally asymptotically stabilizes the origin.

In order to overcome this condition, time-varying smooth or continuous feedback control is used. Another approach is by using non-smooth or discontinuous static state feedback.

3.5 Perturbation Theory

Consider the following perturbed system:

$$\dot{x} = f(t, x) + g(t, x) \tag{3.36}$$

where the functions $f : \mathbb{R}_+ \times D \to \mathbb{R}^n$ and $g : \mathbb{R}_+ \times D \to \mathbb{R}^n$ are piecewise continuous functions in time t. Both the functions are locally Lipschitz in x on $\mathbb{R}_+ \times D$ and domain $D \subset \mathbb{R}^n$ encompasses the origin. Moreover, assume that f is continuously differentiable function and its Jacobian $[\partial f / \partial x]$ is bounded on D. System (3.36) can be considered as a perturbed form of:

$$\dot{x} = f(t, x) \tag{3.37}$$

Now, suppose that the nominal system (3.37) has a uniformly exponentially stable eq. at the origin and we want to assess the stability behaviour of the perturbed equation (3.36). Since the nominal system has exponentially stable equilibrium, therefore, the converse theorem states that a Lyapunov function exists for this nominal system. A common approach to probe the stability of the overall perturbed case is to utilize a Lyapunov function candidate for the perturbed system. Thereafter one distinguishes between vanishing perturbations, i.e. $g(t, 0) = 0, \forall t > t_0$ and nonvanishing perturbations, i.e. $\exists t > t_0 : g(t, 0) \neq 0$.

3.5.1   Vanishing Perturbations

In case when the perturbation term is disappearing at the origin $x = 0$, the origin is said to be an eq. point of the perturbed system. When the origin is uniformly exponentially stable eq. point of the nominal system, then existence of a Lyapunov function $V(t, x)$ for the nominal system is guaranteed [44]. By analysis of the derivative of the Lyapunov function along solutions of the perturbed system, we obtain the following conclusion that could be utilized to investigate the stability of the perturbed system.

Theorem 3.5.1 [44] [P-341] *Suppose $V(t, x)$ represents Lyapunov function of the nominal system (3.37) and let the origin be a uniformly exponentially stable eq. point of the nominal system. Also consider that the perturbation $g(t, x)$ satisfies a linear growth bound, i.e.*

$$\| g(t, x) \| \leq \gamma \| x \|, \ \forall t \geq t_0, \ \forall x \in D \tag{3.38}$$

Then $x = 0$ is a uniformly exponentially stable eq. point of the perturbed system (3.36) if

$$\gamma < \frac{c_3}{c_4} \tag{3.39}$$

Furthermore, $x = 0$ is known to be globally exponentially stable when all the assumptions hold globally.

The theorem reveals that uniform exponential stability of $x = 0$ is robust for a class of perturbation that satisfies a linear growth condition (3.38) - (3.39). When $V(t, x)$ is explicitly known, then the bound (3.39) can be calculated. When $V(t, x)$ is not explicitly known, then conclusion regarding the robustness becomes a qualitative one where one says that $x = 0$ is uniformly exponentially stable for uncertainties satisfying (3.38) with sufficient small γ. It should be noted that the bound (3.38) could be conservative for a given $g(t, x)$. This results from the worst-case analysis performed in the analysis of the derivative of the Lyapunov function for the nominal system along solutions of the perturbed system. If the bound is

required for all $g(t, x)$ satisfying (3.38), including dynamic mappings, then this bound is not conservative.

3.5.2 Non-vanishing Perturbations

In the case when the perturbation is not disappearing at the origin, then this origin may not be an eq. point of system (3.36) anymore. It is no longer possible to investigate the stability properties of $x = 0$ as an equilibrium point, nor should one hope that the solution of the perturbed system approaches $x = 0$ as $t \to \infty$. The most favorable possibility is that if $g(t, x)$ is small in some sense, then the solution $x(t)$ becomes ultimately bounded by a small bound. Or in other words, $\| x(t) \|$ becomes small for sufficiently large t.

Definition 3.5.1. The solutions of $\dot{x} = f(t, x)$ are known as uniformly ultimately bounded if positive constants b and c exist, and for every $\alpha \in (0, c)$ positive constant $T = T(\alpha)$ exists so that

$$\| x(t_0) \| \implies \| x(t) \| \leq b, \ \forall t \geq t_0 + T, \ \forall t_0 > 0 \tag{3.40}$$

When (3.40) holds for arbitrary large α, the result of the system is globally uniformly ultimately bounded.

Uniform ultimate boundedness of the solution is usually called as practical stability and the constant b in (3.40) is known as the ultimate bound. If the equilibrium $x = 0$ of the nominal system is uniformly exponentially stable, the analysis of the perturbed system can be performed with the following theorem.

Theorem 3.5.2. [44] [P-348] *Suppose $x = 0$ is a uniformly exponentially stable eq. point of (3.37) and assume Lyapunov function to be $V(t, x)$ that satisfies the converse theorem on $\mathbb{R}_+ \times D$, where $D = \{x \in \mathbb{R}^n, \| x \| < r\}$. Also, suppose that $g(t, x)$ satisfies*

$$\| g(t, x) \| \leq \delta < \frac{c_3}{c_4} \sqrt{\frac{c_1}{c_2}} \theta r, \ \forall t \geq t_0, \ \forall x \in D \tag{3.41}$$

for some positive constant $\theta < 1$. Then for all initial conditions $\| x(t_0) \| \leq \sqrt{c_1} c_2 r$, $x(t)$ of the perturbed system (3.36) *satisfies*

$$\| x(t) \| \leq k \| x(t_0) \| \exp(-\gamma(t - t_0)), \ \forall t_0 \leq t \leq t_1,$$

and

$$\| x(t) \| \leq b, \ \forall t \geq t_1,$$

for a finite time t_1, where

$$k = \sqrt{\frac{c_2}{c_1}}, \ \gamma = \frac{(1 - \theta)c_3}{2c_2}, \ b = \frac{c_4 \delta}{c_3 \theta} \sqrt{\frac{c_2}{c_1}}$$

Furthermore, one can allow the arbitrary large δ by choosing r large enough.

The previous result states that when the nominal system is globally uniformly exponentially stable, the solution of the perturbed system will be uniformly bounded for any uniformly bounded perturbation. If the system is only uniformly asymptotically stable, then a bounded perturbation could drive the solutions of the perturbed system to infinity. This explains why uniform exponential stability is a desirable property. It should be noted that exponential stability by itself is not sufficient to achieve the robustness result in Theorem 3.5.2; one needs uniformity.

3.6 Sliding Mode Control

Sliding Mode Control (SMC) has a unique importance in robust control theory. SMC came into existence early in the 60's by Emelyanov and his co-researchers ([61], [62]) while carrying out analysis on a second-order linear system. As a result, a discontinuous switching law was proposed showing significant improvement against feedback control. Since its inception, it became a general design method for various systems including discrete time models, MIMO systems, uncertain or perturbed systems, large-scale and infinite dimensional system etc.

Essentially, SMC uses discontinuous feedback control to enforce system states to reach and thereafter remain on a stable sliding manifold. When the system dynamics are confined to this stable sliding manifold, the system behaviour is represented in a controlled fashion. The advantage of obtaining this kind of motion is two-fold: firstly the movement on the sliding manifold is invariant to model uncertainties and perturbations of a particular kind, and secondly, the system order is reduced on the sliding manifold. The invaraince property to the matched uncertainties is the distinguished feature of SMC and makes this method particularly ideal for perturbed/uncertain nonholonomic systems.

During the reaching phase, the SMC attracts the states towards a stable manifold. These surfaces are designed traditionally as some hypersurface in the state-space. The feedback structure is adaptively altered during the sliding phase when the states reach the stable manifold. Now, during the sliding phase the system states are allowed to slide along the switching manifold [63]. After entering the sliding phase, the system remains insensitive to internal parametric variations, unmodelled dynamics and external disturbances and just depends on the gradient of the switching manifold. This constrained motion is called Sliding Mode. However, the only drawback to this approach is the imperfections in switching devices resulting in an undesired chattering phenomenon. Because of the chattering, the system states cross the sliding manifold instead of staying on it [64].

3.6.1 Mathematical Foundations

Let us take a nonlinear system affine in control:

$$\dot{x} = f(x,t) + g(x,t)v(t) \tag{3.42}$$

where $x(t) \in \mathbb{R}^n$, $v(t) \in \mathbb{R}^m$, $f \in \mathbb{R}^{n \times n}$ and $g \in \mathbb{R}^{n \times m}$. The discontinuous feedback is specified as:

$$v_i = \begin{cases} v_i^+(x,t), & if \ \sigma_i(x) > 0 \\ v_i^-(x,t), & if \ \sigma_i(x) < 0 \end{cases} \quad i = 1, \cdots, m \qquad (3.43)$$

where i^{th} sliding surface is given as $\sigma_i(x) = 0$, and

$$\sigma(x) = \begin{bmatrix} \sigma_1 & \sigma_2 & \cdots & \sigma_m \end{bmatrix}^T = 0 \qquad (3.44)$$

is the $(n-m)$-dimensional sliding manifold.

The control problem comprises designing the sliding surface $\sigma(x) = 0$ and continuous function v_i^+, v_i^- such that the closed-loop system (3.42) - (3.43) exhibit a sliding mode.

The construction of SMC can be broken down into the following two phases:

1. First phase comprises construction of a suitable sliding surface in order to produce the desired stable behaviour of the system when confined to the sliding manifold.

2. Second phase consists of construction of a discontinuous law which moves system trajectories towards the sliding surface and then keeps it there.

Mostly linear switching surfaces are prevalent in design([64], [65]), though general nonlinear switching surfaces (3.44) are also possible. In this research, our focus is on linear sliding manifold of the form for simplicity:

$$\sigma(x) = Sx(t) \qquad (3.45)$$

where $S \in \mathbb{R}^{m \times n}$.

Existence of a sliding mode is the next decisive feature of SMC after designing the switching surface. A sliding mode in the vicinity of the switching surface $\sigma(x) = 0$ exists if the velocities are always directed toward the sliding manifold. As can be seen in Fig. 3.4, a sliding mode on $\sigma(x) = 0$ can appear even when it does not separately exist on surfaces $\sigma_i(x) = 0$. An ideal sliding mode exists only if
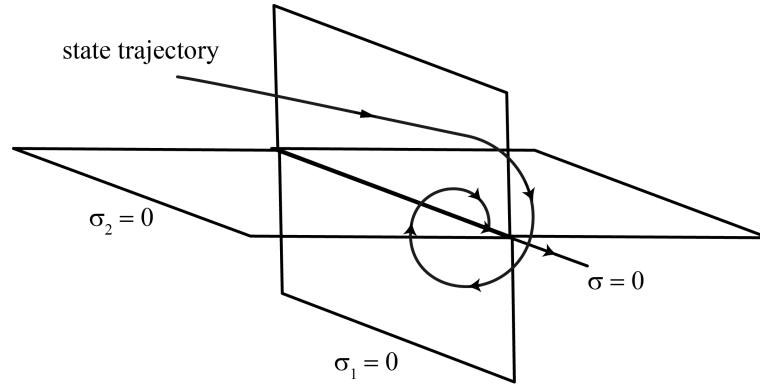
FIGURE 3.4: Sliding Mode in the interaction of discontinuity.

the trajectory of the controlled system satisfies $\sigma[x(t)] = 0$ at every time instant $t \geq t_0$. This requires fast switching at an infinite rate. However in real-world systems, abnormalities such as hysteresis, delay, etc. are present that compel occurrence of switching at some finite frequency. During this, the system states oscillate within the neighborhood of the switching surface. This finite oscillation is called chattering and mostly it is undesired in mechanical systems.

3.6.2 Chattering

In real applications, the control signal cannot operate/switch at infinite frequency. Thus, it is realistic to assume that the control works at a finite frequency owing to the inertias of the sensors/actuators. The main consequence of this understanding is that the sliding mode exhibits in a small region around switching surface [66], [65] and [67].

The notion of real and ideal sliding mode is borrowed to differentiate between the sliding motion that occurs exactly on the switching surface and the one that takes place in a boundary layer around the switching surface due to imperfections of the control law implementation (see Fig. 3.5). These imperfections because of the finite switching frequency are known as chattering in the literature ([68], [69]). Fundamentally, the high-frequency control components excite the undesired oscillations and unmodeled fast dynamics while propagating through the system. These can be harmful to the overall system performance and may even cause
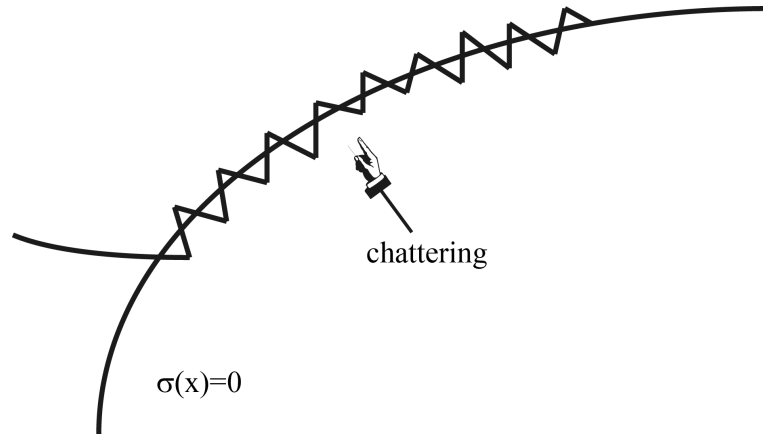
FIGURE 3.5: Chattering Problem.

system instability([70], [71] and [69]). The trade-off problem among robustness, performance and chattering has engaged the attention of control research community. Reduction in switching control amplitude against the manifold can be achieved at the expense of robustness and performance degradation. Whereas, improved robustness and performance result in higher control amplitude. Subsequently, different variants of SMC technique including integral SMC, higher-order SMC and adaptive SMC techniques have been proposed in order to achieve better results.

3.7 Integral Sliding Mode Control

Chattering phenomenon, inherently prevalent in SMC technique, makes it unsuitable to the real-world mechanical applications. Also, the robustness of SMC against variations in external disturbances and system parameters can only be obtained after the sliding mode is established. Thus, there is no guarantee of this robustness property during the reaching phase of SMC. By invoking sliding mode during the entire system response, integral SMC attempts to eliminate the reaching phase ([72],[73],[74]). Consequently, system order in ISMC becomes equal to that of the original system. As a result, the robustness property can be achieved from the very initial time.

Consider a nonlinear system given as:

$$\dot{x} = f(x) + Bu + h(t, x) \tag{3.46}$$

where $x(t) \in \mathbb{R}^n$, $u(t) \in \mathbb{R}^m$, $m < n$, $f(x)$ is a nonlinear function, $B \in \mathbb{R}^n$ denotes input gain with $rank(B) = m$ and $h(t, x)$ represents the bounded matched uncertainty such that $h(t, x) \in span(B)$ and $h(t, x) \leq h_{max}$. The control law for the ISMC can be given as:

$$u = u_0 + u_1 \tag{3.47}$$

where $u_0 \in \mathbb{R}^m$ is the ideal control and $u_1 \in \mathbb{R}^m$ is constructed to reject the disturbances. By using (3.46) and (3.47), the system dynamics can be given as:

$$\dot{x} = f(x) + B(u_0 + u_1) + h(t, x) \tag{3.48}$$

Now define the sliding surface as:

$$s = s_0(x) + z \tag{3.49}$$

where $s_0(x)$ is the switching surface and can be constructed through standard SMC technique. The z term incorporates the integral term in the switching surface. By taking derivative of the above equation, we get,

$$\dot{s} = \frac{\partial s_0}{\partial x}[f + B(u_0 + u_1) + h] + \dot{z} \tag{3.50}$$

In order to achieve the ISMC, the nominal trajectory should be equal to the ISMC trajectory. For this, $u_{1eq}(t)$ which is equivalent control of u_1, should satisfy:

$$Bu_{1eq}(t) = -h(t, x) \tag{3.51}$$

Equivalent control is the average value of the discontinuous control and can be achieved by using a suitable low-pass filter before the control input. It provides more accurate description of the trajectories along the sliding surface when

$s(x) = 0$. The concept of ISMC can be broadened to design a new type of perturbation estimator which resolves the chattering problem without any loss of control accuracy and robustness [63]. z can be computed by substituting (3.51) in (3.49):

$$\dot{s} = \frac{\partial s_0}{\partial x}[f(x) + B(u_0 + u_1) + h(t, x)] + \dot{z}$$
$$0 = \frac{\partial s_0}{\partial x}[f(x) + Bu_0] + \dot{z}$$
$$\dot{z} = -\frac{\partial s_0}{\partial x}[f(x) + Bu_0]$$

where $z(0) = -s_0(x(0)$. $z(0)$, the initial condition, ensures $s = 0$ meaning that the sliding mode will exist from the initial time instant. The system dynamics in ISMC may be given as:

$$\dot{x} = f(x) + Bu_0 \tag{3.52}$$

As $h(t, x)$ is completely canceled out, therefore, the system has no disturbance.

3.8 Adaptive ISMC

The basic idea of the adaptive control comprises design of systems clearly showing same dynamic response under parameter varying conditions by utilizing current information. The controller is modified considering the fact that the system parameters being controlled are uncertain or slowly time-varying. Furthermore, adaptive control entails improvement in dynamic characteristics while plant properties are varying ([70], [5]). Adaptive SMC methods allow dynamical adjustment of the control gains without knowledge of uncertainty bounds ([75],[76],[77]). Particularly, several adaptive fuzzy SMC algorithms have been proposed in literature but these fail to provide the desired tracking performance [58]. Without using adaptive idea, the original ISMC demonstrates robustness with respect to disturbances and parameter variations. In this research work, Adaptive control methodology is utilized along with integral sliding mode (AISMC) to estimate the unknown terms.

3.9 Summary

In this chapter, some basic terminologies and concepts regarding nonholonomic systems and controllability of such systems are presented. Some details regarding different canonical forms, a brief review of perturbation theory and basics of SMC are also briefly presented.

Chapter 4

Stabilization of First-Order Perturbed Nonholonomic Systems in Chained Form

This chapter presents two novel robust stabilizing control algorithms for first-order nonholonomic systems (FONHS). The control algorithms are based on adaptive integral sliding mode control (AISMC) technique. Extended Lie bracket system which can easily be asymptotically stabilized is used as a nominal system in the first method. The proposed method is applied to two general nonholonomic drift-free systems including a hopping robot which is in flying phase and fire-truck model. The second method utilizes function approximation technique and is applied on FONHS in chained form. The simulations are carried out on two FONHS in chained form including a four-wheel car and the fire-truck model.

Later on, first-order underwater vehicle model, a nonholonomic system which is affected by uncertainties is taken as a benchmark system and AISMC technique is applied to it. Firstly, the original underwater system is transformed in a way that the new system has uncertainties in matched form. A change of coordinates is carried out for this purpose and the nonholonomic system is transformed into chained form with matched uncertainties. Secondly, the chained form system with

uncertainties is converted into a special structure comprising nominal portion and some unknowns through input transformation. Adaptive method is used to compute these unknown terms. Afterwards, the transformed system is stabilized via ISMC. The stabilizing control for the transformed system is established comprising of the nominal and compensator control. The compensator and adaptive control laws are derived in such a way that the derivative of a suitable Lyapunov function becomes strictly negative. Two different cases of perturbation are considered including the bounded uncertainty present in any single control input and the uncertainties present in the overall system model of the underwater vehicle. Finally, simulation results show the validity and correctness of the proposed controllers for both cases of the nonholonomic underwater system affected by uncertainties.

4.1 Nonholonomic Drift-Free Systems

FONHS arise frequently in real-world applications and normally represent mechanical systems that have non-integrable velocity constraints. Generally, these systems have restricted mobility because of the presence of non-integrable constraints. The importance of these systems is highlighted by the fact that these are used in many diverse applications in robotics, security, transportation, inspection and exploration. Because of the existence of nonholonomic constraints, the kinematic nonholonomic systems [78] are given by:

$$\dot{x} = \sum_{i=1}^{m} Y_i(x)\, u_i, \qquad x \in \mathbb{R}^n \tag{4.1}$$

where $Y_i, \quad i = 1, \cdots, m, \ m < n$ are vector fields which are linearly independent on $\mathbb{R}^n$ and u_i are locally bounded, piece-wise continuous control functions characterized on the interval $[0, \infty)$.

4.2   Problem Formulation : Unchained FONHS

We begin this section by stating the importance of extended system as this will be used in the proposed first method.

4.2.1   Extended System

The proposed first methodology for stabilizing control uses Lie bracket extension of system (4.1). Lie-bracket extension of a general FONHS model is a mathematical technique; however, it provides useful information regarding controllability of system under consideration. This extended system is virtually a new system whose components are a linear combination of vector fields spanning the entire state space locally [2]. The first m components are the vector fields of the original system; whereas, the last $n - m$ components are the vector fields that are obtained using the Lie brackets. Thus, after adding the missing Lie brackets, the original system in extended-form can be written as:

$$\dot{x} = \sum_{i=1}^{m} Y_i(x)u_i(x) + \sum_{i=m+1}^{n} Y_i(x)u_i(x), \qquad x \in \mathbb{R}^n \qquad (4.2)$$

where $Y_i, \quad i = m+1, \cdots, n$ are the Lie brackets obtained from $L(Y_1, Y_2, \cdots, Y_m)$. The benefit of the extended system from control perspective lies in the fact that it allows motion in the missing Lie bracket direction i.e. $Y_k = [Y_i, Y_j]$.

4.2.2   Stabilization Problem

Given a desired set point $x_{des} \in \mathbb{R}^n$, design control laws so that the desired point x_{des} is an attractive set for system (4.1) and there exists an $\varepsilon > 0$, so that $x(t;\ t_0,\ x_0) \to x_{des}$ as $t \to \infty$ for any $(t_0,\ x_0) \in \mathbb{R}^+ \times B(x_{des}; \varepsilon)$.

For stabilization problem, we can take $x_{des} = 0$ which is obtained through a suitable translation of the coordinate system.

Assumption 4.1: *The vector fields $Y_1(x) \cdots , Y_m(x)$ of the original system* (4.1) *are linearly independent.*

Assumption 4.2: *System* (4.1) *satisfies the Lie Algebra Rank Condition (LARC) for accessibility, i.e. the Lie algebra $L(Y_1, \cdots , Y_m)(x)$ spans $\mathbb{R}^n$ at each point $x \in \mathbb{R}^n$.*

$$span\{Y_i, \ [Y_i, Y_j], \cdots , \ [Y_k, [Y_i, Y_j]], \cdots , i, \ j, \ k = 1, \cdots , m\}(x) = \mathbb{R}^n \qquad (4.3)$$

4.2.3   Control of the Extended System

By defining the following control inputs, the extended system of (4.2) can be made globally asymptotically stable:

$$u(x) = -G^{-1}(x)x \qquad (4.4)$$

where $G(x) = \begin{bmatrix} Y_1(x) & Y_2(x) & \dots & Y_n(x) \end{bmatrix}$ and $u(x) = \begin{bmatrix} u_1(x) & u_2(x) & \dots & u_n(x) \end{bmatrix}^T$. The existence of $G^{-1}(x)$ is guaranteed by the LARC condition (4.3).

Lemma 4.1: *The feedback control given in* (4.4) *makes the extended system* (4.2) *asymptotically stable.*

Proof. Consider a Lyapunov function $V = \frac{1}{2}x^T M \, x$, here M is any positive definite and symmetric matrix. Along the controlled extended system trajectories, we have,

$$
\begin{aligned}
\frac{d}{dt}V(x) &= x^T M \, \dot{x} \\
&= x^T M (G(x) \, u(x)) \\
&= x^T M (G(x) \, (-G(x)^{-1} x)) \\
&= -x^T M \, x = -2 \, V(x) < 0, \quad \forall \, x \in \, \mathbb{R}^n \backslash \{0\}
\end{aligned}
$$

endorsing asymptotic stability of (4.2) *with feedback controls* (4.4). $\qquad\square$

4.2.4 Adaptive Integral Sliding Mode Controller Design

In SMC, there is no guarantee for robustness during the reaching phase; whereas, ISMC ensures elimination of the reaching phase by enforcing sliding mode for the entire response duration [66]. In this research, we have used an adaptive technique with ISMC to solve the stabilization problem in drift-free FONHS. First of all, a stabilizing control is constructed for a nominal system by choosing a Hurwitz sliding surface (nominal sliding surface). Afterwards, the nominal sliding surface with an added integral term is chosen as sliding surface for the original system. Then, the stabilizing controller is designed comprising of nominal and compensator controllers. The compensator and adaptive control laws are derived in a way that the time derivative of a suitable Lyapunov function becomes strictly negative and the closed-loop system stability can be guaranteed as system behaviour on the sliding surface is similar to that of the nominal system. Following algorithm is proposed for general nonholonomic drift-free systems that satisfy the assumptions mentioned in Section 4.2.2.

4.2.5 The Proposed Algorithm : Method-1

Here, the first algorithm is proposed which is based on Lie bracket extended system. The second method is presented later in Section 4.3.4.

Step 1: First of all, consider the nonholonomic drift-free system (4.1) and compute its Lie brackets in order to get the extended system (4.2). Now, augment the system (4.1) as:

$$\dot{x} = \sum_{i=1}^{m} Y_i(x)\,u_i = \sum_{i=1}^{m} Y_i(x)\,u_i + \sum_{i=m+1}^{n} Y_i(x)\,u_i - v \qquad (4.5)$$

where $v = \sum\limits_{i=m+1}^{n} Y_i(x)\,u_i$, i.e., adding and subtracting the missing Lie brackets in order to get the same original system (4.1). Here, assume that v is unknown that can be computed adaptively. Let $\hat{v}$ be the estimated value of v and $\tilde{v} = v - \hat{v}$ be the error in estimation of v.

Step 2: After replacing $v = \hat{v} + \tilde{v}$, system (4.5) can be stated in vector form as:

$$\dot{x} = G(x)\, w - \hat{v} - \tilde{v} \tag{4.6}$$

where $G(x) = [Y_1 \quad Y_2 \quad \cdots \quad Y_n](x)$ and $w = [u_1 \quad u_2 \quad \cdots \quad u_n]^T$.

Step 3: Taking first part of system (4.6) as the nominal system and using subscript form w_0 for the nominal input, we get:

$$\dot{x} = G(x)\, w_0 \tag{4.7}$$

Now, select the sliding surface for the nominal system (4.7) as $S_0 = x$. Then, $\dot{S}_0 = G(x)\, w_0$ and the choice of

$$w_0 = -G(x)^{-1} S_0 \tag{4.8}$$

gives $\dot{S}_0 = -S_0$.

Take $V(x) = \frac{1}{2} S_0^{\,T} S_0$ as a Lyapunov function for (4.7), which makes $\dot{V}(x) = S_0^{\,T} \dot{S}_0 = -S_0^{\,T} S_0 < 0$. Thus, the nominal system (4.7) is asymptotically stable.

Step 4: Now, consider complete system (4.6) and choose $w = w_0 + w_s$, where w_0 is the nominal control given at (4.8) and w_s is the switching control designated as compensator control that is determined during step 5. Also, define the sliding surface as $S = S_0 + Z$ where Z is the integral term. Then,

$$\dot{S} = \dot{S}_0 + \dot{Z} = \dot{x} + \dot{Z} = G(x)w_0 + G(x)w_s - \hat{v} - \tilde{v} + \dot{Z} \tag{4.9}$$

Step 5: At the end, design adaptive laws for $\tilde{v}$, $\hat{v}$ and compute w_s such that $\dot{V} < 0$.

Theorem 4.1: *The following choices of adaptation laws for $\tilde{v}$, $\hat{v}$ and w_s:*

$$w_s = G(x)^{-1}(\hat{v} - K \text{ sgn}(S)), \text{ where } K = diag\{k_1, \cdots, k_n\}, k_i > 0, i = 1, \cdots, n$$

$$\dot{Z} = -G(x)w_o$$

$$\dot{\tilde{v}} = \Gamma^{-1}(S - \Gamma\tilde{v})$$

$$\dot{\hat{v}} = -\dot{\tilde{v}}$$

give $\dot{V} < 0$ for the Lyapunov function $V = \frac{1}{2}S^T S + \frac{1}{2}\tilde{v}^T \Gamma \tilde{v}$, where Γ is an $n \times n$ positive definite diagonal matrix.

Proof. Since

$$\dot{V} = S^T \dot{S} + \tilde{v}^T \Gamma \dot{\tilde{v}}$$

$$= S^T(G(x)w - \hat{v} - \tilde{v} + \dot{Z}) + \tilde{v}^T \Gamma \dot{\tilde{v}}$$

$$= S^T(G(x)w_0 + G(x)w_s - \hat{v} + \dot{Z}) + \tilde{v}^T(\Gamma\dot{\tilde{v}} - S)$$

Therefore, the following adaptation laws:

$$w_s = G(x)^{-1}(\hat{v} - K \text{ sgn}(S)), \text{ where, } K = diag\{k_1, \cdots, k_n\}, k_i > 0, i = 1, \cdots, n$$

$$\dot{Z} = -G(x)w_o$$

$$\dot{\tilde{v}} = \Gamma^{-1}(S - \Gamma\tilde{v})$$

$$\dot{\hat{v}} = -\dot{\tilde{v}}$$

give $\dot{V} = -S^T K \text{ sgn}(S) - \tilde{v}^T \Gamma \tilde{v} < 0$. $\qquad\square$

Thus, we conclude that since S and $\tilde{v} \to 0$, hence, vector x (all states) goes to zero and stabilization of FONHS is achieved.

4.2.6 Application Examples

4.2.6.1 Hopping Robot

Considering an example of a hopping robot as shown in Figure 4.1. The three different phases of the hopping robotic system include compression phase, thrusting phase and flight phase. During the compression phase, the leg touches the ground and the spring in the leg compresses. In the thrusting phase, the leg spring extends while injecting additional energy into the system. Whereas, during the flight phase the system takes off, undergoes a parabolic trajectory and finally touches down again [79].
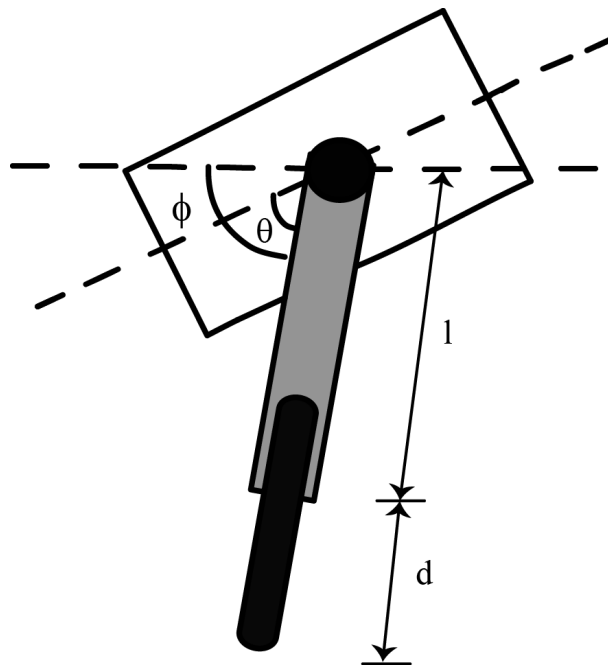
FIGURE 4.1: The Hopping Robot.

The angular momentum of the system in flight phase is conserved as the robot is not furnished with external gas jets. The kinematic model for the hopping robot

in flight phase is given by the following state-space equation [12]:

$$\dot{\psi} = u_1$$
$$\dot{l} = u_2 \tag{4.10}$$
$$\dot{\theta} = -\frac{m\,(l+d)^2}{I + m\,(l+d)^2} u_1$$

The configuration variable ψ denotes hip angle of the robot during flying, l is length of the leg elongation and θ is the angle as shown in Figure 4.1. Also m is the mass of leg concentrating at the foot, I is the moment of inertia and d is the lenght of upper leg. For simplicity, let us assume that $d = m = I = 1$ and introduce a new set of variables $x \triangleq (x_1, x_2, x_3) = (\psi, l+1, \theta)$, the kinematic model of (4.10) can be stated as:

$$\dot{x}_1 = u_1$$
$$\dot{x}_2 = u_2$$
$$\dot{x}_3 = -\frac{x_2^2}{1 + x_2^2} u_1$$

or in compact vector form as:

$$\dot{x} = Y_1(x)\,u_1 + Y_2(x)\,u_2, \qquad x \in \mathbb{R}^3 \tag{4.11}$$

where $Y_1(x) = \begin{bmatrix} 1 \\ 0 \\ -\dfrac{x_2^2}{1+x_2^2} \end{bmatrix}$ and $Y_2(x) = \begin{bmatrix} 0 \\ 1 \\ 0 \end{bmatrix}$.

The kinematic model (4.11) has the two properties mentioned in Sec 4.2.2. In order to verify the second assumption, it is sufficient to calculate the following Lie brackets of $Y_1(x)$ and $Y_2(x)$:

$$[Y_1, Y_2](x) = \begin{bmatrix} 0 \\ 0 \\ \dfrac{2x_2}{(1+x_2^2)^2} \end{bmatrix}$$

$$Y_3(x) \triangleq [Y_2, [Y_1, Y_2]](x) = \begin{bmatrix} 0 \\ 0 \\ \dfrac{2 - 6x_2^2}{(1 + x_2^2)^3} \end{bmatrix}$$

which satisfy the LARC condition, i.e.

$$span\{Y_1, Y_2, Y_3\}(x) = \mathbb{R}^3 \qquad \forall x \in \mathbb{R}^3$$

The extended system for (4.11) is given as:

$$\dot{x} = Y_1(x)u_1 + Y_2(x)u_2 + Y_3(x)u_3 = G(x)u \tag{4.12}$$

where

$$G(x) = \begin{bmatrix} Y_1(x) & Y_2(x) & Y_3(x) \end{bmatrix} = \begin{bmatrix} 1 & 0 & 0 \\ 0 & 1 & 0 \\ -\dfrac{x_2^2}{1 + x_2^2} & 0 & \dfrac{2 - 6x_2^2}{(1 + x_2^2)^3} \end{bmatrix}$$

and $u = \begin{bmatrix} u_1 & u_2 & u_3 \end{bmatrix}^T$ The extended system can be asymptotically stabilized by choosing $u = G(x)^{-1}(-x)$. After applying the steps 1 - 5 on the hopping robot, we achieve the desired results given in the following subsection.

Simulation Results

Figure 4.2 shows simulation results of the applied algorithm on the model of hopping robot in actuator failure mode. Verification has been carried out for various initial conditions and time response of states (original and the extended system) is shown here for the initial condition (-1,3,4,1,-3,-4). x_i are the time trajectories of the original system, whereas, x_{i_e} are the trajectories of the extended system. The time trajectories show that all states are going towards zero for the initial condition. Also, it can be seen that the unknown variable v, estimated $\hat{v}$ and the error signal $\tilde{v} = v - \hat{v}$, all are also converging towards zero, thus validating the correctness of the proposed algorithm.

Note: Metric convention is used throughout in this thesis. Time is expressed in seconds, whereas, distance is expressed in meters.

4.2.6.2   Firetruck Model

The fire truck model is a nonholonomic system having three control inputs and overall six configuration variables. The controllability Lie algebra of this model has two Lie brackets of depth one and one of depth two. By defining the states as $(x_1, x_2, x_3, x_4, x_5, x_6)^T \overset{def}{=} (x, \varphi_0, \varphi_1, \theta_0, \theta_1, y)^T$ in the kinematic model of fire truck [80] and keeping $l_0 = l_1 = 1$, we get the following model:

$$\dot{x} = Y_1(x)u_1 + Y_2(x)u_2 + Y_3(x)u_3 \qquad (4.13)$$

where

$$Y_1(x) = \begin{bmatrix} 1 \\ 0 \\ 0 \\ \tan x_2 \sec x_4 \\ -\sin(x_3 - x_4 + x_5)\sec x_3 \sec x_4 \\ \tan x_4 \end{bmatrix}, \quad Y_2(x) = \begin{bmatrix} 0 \\ 1 \\ 0 \\ 0 \\ 0 \\ 0 \end{bmatrix}, \quad Y_3(x) = \begin{bmatrix} 0 \\ 0 \\ 1 \\ 0 \\ 0 \\ 0 \end{bmatrix}$$

In order to verify the second proposition given in Sec 4.2.2., it is sufficient to calculate the following Lie brackets:

$$Y_4(x) \overset{def}{=} [Y_1, Y_2](x) = \begin{bmatrix} 0 \\ 0 \\ 0 \\ -(\sec x_2)^2 \sec x_4 \\ 0 \\ 0 \end{bmatrix},$$
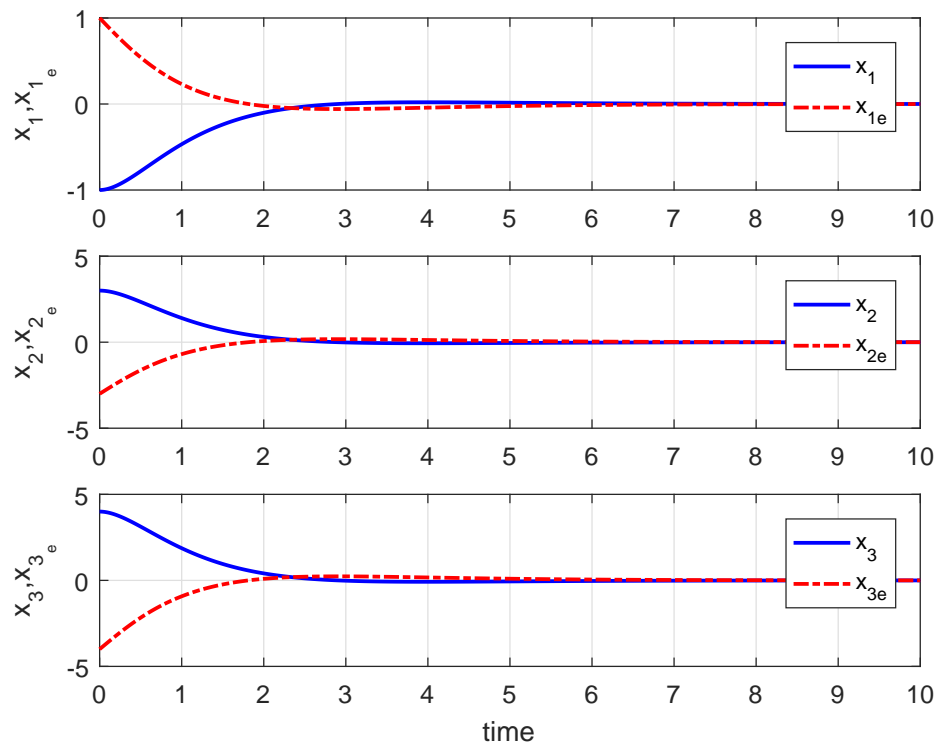
(a)
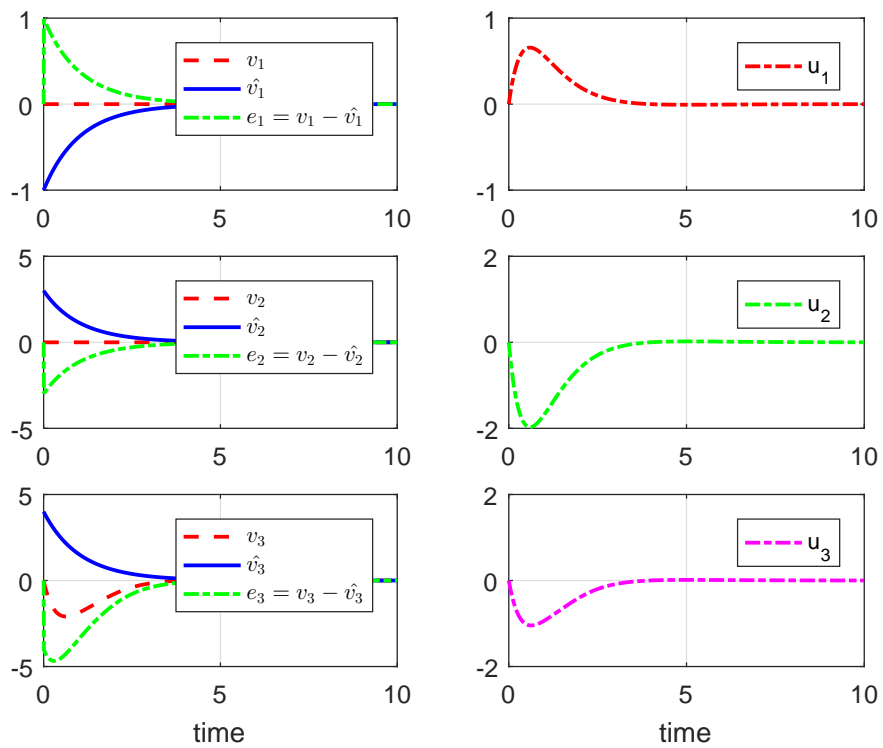
(b)

FIGURE 4.2: (a) Time response of the Hopping Robot in Actuator Failure Mode corresponding to initial condition (-1,3,4,1,-3,-4) (b) Time response of v, $\hat{v}$, $e = v - \hat{v}$ and the control effort

$$Y_5(x) \overset{def}{=} [Y_1, Y_3](x) = \begin{bmatrix} 0 \\ 0 \\ 0 \\ 0 \\ \sec x_3 \sec x_4 \cos(x_3 - x_4 + x_5) + \sin(x_3 - x_4 + x_5) \tan x_3 \\ 0 \end{bmatrix}$$

$$Y_6(x) \overset{def}{=} [Y_1, [Y_1, Y_2]](x)$$

$$= \begin{bmatrix} 0 \\ 0 \\ 0 \\ 0 \\ (\sec x_2 \sec x_4)^2 \sec x_3 \cos(x_3 - x_4 + x_5) - \sin(x_3 - x_4 + x_5) \tan x_4 \\ (\sec x_2)^2 (\sec x_5)^3 \end{bmatrix}$$

The LARC condition namely,

$$span\{Y_1(x), Y_2(x), \cdots, Y_6(x)\} = \mathbb{R}^6, \qquad \forall \, x \in M$$

is satisfied if the motion of firetruck is restricted to the manifold

$$M \overset{def}{=} \{x \in \mathbb{R}^6 : |x_i| < \frac{\pi}{2}, i = 2, \, 3, \, 4\}$$

Therefore, ensuring that the system (4.13) satisfies the conditions for LARC.

The extended system for (4.13) is given as:

$$\dot{x} = Y_1(x)\bar{u}_1 + Y_2(x)\bar{u}_2 + Y_3(x)\bar{u}_3 + Y_4(x)\bar{u}_4 + Y_5(x)\bar{u}_5 + Y_6(x)\bar{u}_6 = G(x)\bar{u} \qquad (4.14)$$

where

$$G(x) = \begin{bmatrix} Y_1(x) & Y_2(x) & Y_3(x) & Y_4(x) & Y_5(x) & Y_6(x) \end{bmatrix}$$

$$= \begin{bmatrix} 1 & 0 & 0 & 0 & 0 & 0 \\ 0 & 1 & 0 & 0 & 0 & 0 \\ 0 & 0 & 1 & 0 & 0 & 0 \\ \tan x_2 \sec x_4 & 0 & 0 & -(\sec x_2)^2 \sec x_4 & 0 & 0 \\ b_1 & 0 & 0 & 0 & b_2 & b_3 \\ \tan x_4 & 0 & 0 & 0 & 0 & (\sec x_2)^2 (\sec x_4)^3 \end{bmatrix}$$

with $b_1 = -\sin(x_3 - x_4 + x_5) \sec x_3 \sec x_4$,

$b_2 = \sec x_3 \sec x_4 \cos(x_3 - x_4 + x_5) + \sin(x_3 - x_4 + x_5) \tan x_3$,

$b_3 = (\sec x_2 \sec x_4)^2 \sec x_3 \cos(x_3 - x_4 + x_5) - \sin(x_3 - x_4 + x_5) \tan x_4$

and $\bar{u} = \begin{bmatrix} \bar{u}_1 & \bar{u}_2 & \bar{u}_3 & \bar{u}_4 & \bar{u}_5 & \bar{u}_6 \end{bmatrix}^T$

The extended system can be asymptotically stabilized by choosing $\bar{u} = G(x)^{-1}(-x)$. After applying the steps 1 - 5 on the firetruck system, we achieve the desired results given in the following subsection.

Simulation Results

Figure 4.3 shows simulation results of the applied algorithm on the model of firetruck. Again the verification has been carried out for various initial conditions and the results are shown for the initial condition (0.9,-0.7,0.8,-0.6,0.5,-0.4,-0.9,0.7,-0.8,0.6,-0.5,0.4). x_i are the time trajectories of the original system, whereas, x_{i_e} are the trajectories of the extended system. Time trajectories show that all the states are converging towards zero for the initial condition. Also, it can be seen that the unknown variable v, estimated $\hat{v}$ and the error signal $\tilde{v} = v - \hat{v}$, all are also going towards zero, thus validating the correctness of the proposed algorithm.
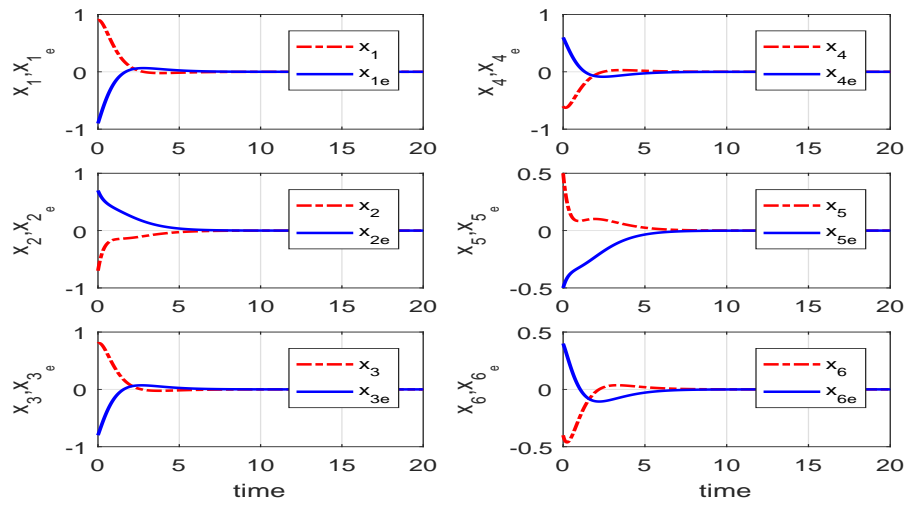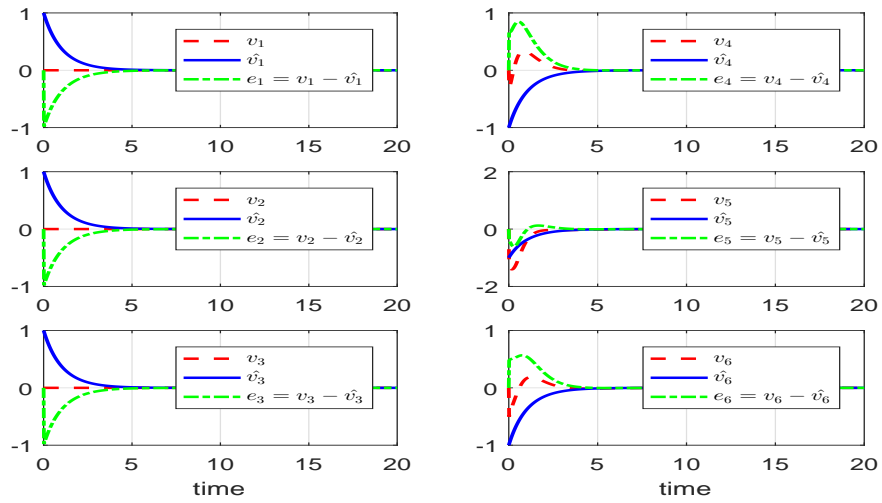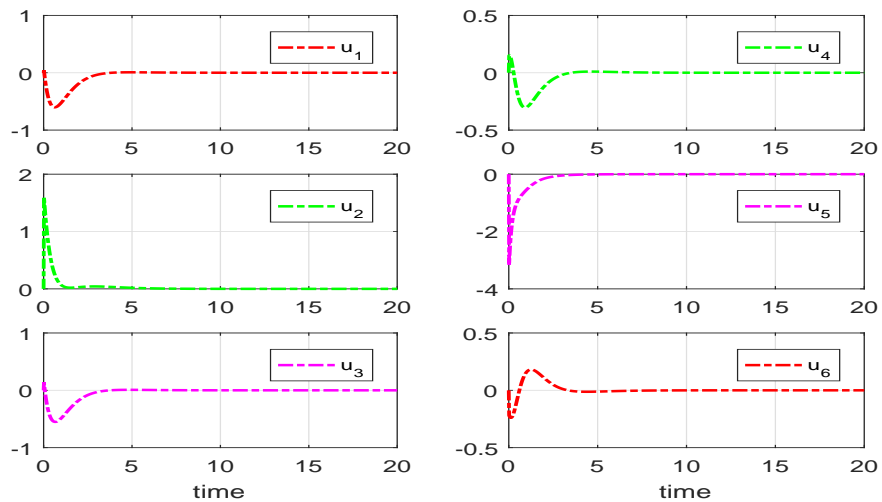
FIGURE 4.3: (a) Time response of the fire truck corresponding to initial condition (b) Time response of $v, \hat{v}$ and $e = v - \hat{v}$. (c) The control effort

Next, we consider the unperturbed FONHS in chained form.

4.3 Problem Formulation : FONHS in Chained Form

Here, we will first convert the FONHS in chained form. Then a slightly different methodology (Method-2) is proposed for the problem of stabilizing FONHS in chained form; though, the proposed Method-1 of Section 4.2.5 is equally applicable.

4.3.1 First-Order Chained Form Systems

It has been shown in [47] that FONHS described by (4.1) can be globally/locally modified to the chained form under a control mapping and a coordinate transformation. As a consequence, the chained form has been adopted as a canonical form in control design and analysis of nonholonomic systems. This modified form is also similar to skew-symmetric chained form [4] and the power canonical form [26] and their dynamic extension has been investigated in [12]. The simplest chained system obtained from (4.1) is a nonlinear system which has two control inputs (v_1, v_2) and n outputs $x_1, x_2, \cdots, x_n$, where $n > 2$. The general form is:

$$
\begin{aligned}
\dot{x}_1 &= v_1 \\
\dot{x}_2 &= v_2 \\
\dot{x}_3 &= x_2 v_1 \\
&\vdots \\
\dot{x}_n &= x_{n-1} v_1
\end{aligned}
\tag{4.15}
$$

In [12], it has been proved that any FONHS model can be transformed into chained form as in the case of cars with trailers or unicycles.

4.3.2 Stabilization Problem

Given a desired set point $x_{des} \in \mathbb{R}^n$, design feedback control laws so that the desired point x_{des} is an attractive set for system (4.1) and there exists an $\varepsilon > 0$, such that $x(t;\ t_0,\ x_0) \to x_{des}$ as $t \to \infty$ for any $(t_0,\ x_0) \in \mathbb{R}^+ \times B(x_{des}; \varepsilon)$.

For stabilization problem, we can take $x_{des} = 0$ which is achieved by a suitable translation of the coordinate system. Also, both assumptions mentioned in Section 4.2.2 are applicable to the control problem.

4.3.3 Adaptive Integral Sliding Mode Control

We propose a simple yet elegant method for designing the stabilizing control laws for nonholonomic chained form systems. The method depends on adaptive ISMC. First, the chained form system is converted into a special construction that comprises nominal portion and unknowns. Adaptive method is used to compute these unknown terms. A stabilizing control called nominal control is constructed for the nominal system by choosing a Hurwitz sliding surface called the nominal surface. Then for the original system, the sliding surface is chosen as the nominal sliding surface plus an integral term. The stabilizing control for chained form is designed comprising of the nominal control and compensator control. A suitable Lyapunov function is used to verify that the closed-loop systems stability is guaranteed and the systems behaviour on the sliding surface is similar to the nominal system.

4.3.4 The Proposed Algorithm : Method-2

Step 1: Transform the system (4.15) by choosing $v_1 = x_3$ and $v_2 = v$, where v is the new input:

$$
\begin{aligned}
\dot{x}_1 &= x_3 \\
\dot{x}_2 &= v \\
\dot{x}_3 &= x_2 x_3 \\
\dot{x}_4 &= x_3^2 \\
&\vdots \\
\dot{x}_{n-1} &= x_{n-2} x_3 \\
\dot{x}_n &= x_{n-1} x_3
\end{aligned}
\tag{4.16}
$$

Step 2: Write the above system (4.16) as:

$$
\begin{aligned}
\dot{x}_1 &= x_3 \\
\dot{x}_3 &= x_2 x_3 \\
\dot{x}_4 &= x_3^2 \\
&\vdots \\
\dot{x}_{n-1} &= x_{n-2} x_3 \\
\dot{x}_n &= x_{n-1} x_3 \\
\dot{x}_2 &= v
\end{aligned}
\tag{4.17}
$$

After some manipulation, system (4.17) can be written as:

$$\dot{x}_1 = x_3$$
$$\dot{x}_3 = x_4 + F_3$$
$$\dot{x}_4 = x_5 + F_4 \qquad\qquad (4.18)$$
$$\vdots$$
$$\dot{x}_{n-1} = x_n + F_{n-1}$$
$$\dot{x}_n = x_2 + F_n$$
$$\dot{x}_2 = v$$

where $F_i = -x_{i+1} + x_{n-1}x_3$, $i = 3, \cdots, n-1$ and $F_n = -x_2 + x_{n-1}x_3$

Step 3: Now, assume that F_i are unknowns and can be computed adaptively. Let $\hat{F}_i$ be an estimate of F_i and $\tilde{F}_i = F_i - \hat{F}_i$ be the errors in estimation of F_i, $i = 3, \cdots, n-1$ respectively. Then, system (4.18) can be written as:

$$\dot{x}_1 = x_3$$
$$\dot{x}_3 = x_4 + \hat{F}_3 + \tilde{F}_3$$
$$\dot{x}_4 = x_5 + \hat{F}_4 + \tilde{F}_4 \qquad\qquad (4.19)$$
$$\vdots$$
$$\dot{x}_{n-1} = x_n + \hat{F}_{n-1} + \tilde{F}_{n-1}$$
$$\dot{x}_n = x_2 + \hat{F}_n + \tilde{F}_n$$
$$\dot{x}_2 = v$$

Step 4: The nominal system for (4.19) becomes:

$$\dot{x}_1 = x_3$$
$$\dot{x}_3 = x_4$$
$$\dot{x}_4 = x_5 \qquad (4.20)$$
$$\vdots$$
$$\dot{x}_{n-1} = x_n$$
$$\dot{x}_n = x_2$$
$$\dot{x}_2 = v_0$$

Now, choose a sliding surface for (4.20) as $s_0 = x_1 + \sum\limits_{i=3}^{n} c_i x_i + x_2$, where $c_i > 0$ are selected in a way that s_0 becomes Hurwitz polynomial. Then

$$\dot{s}_0 = \dot{x}_1 + \sum_{i=3}^{n} c_i \dot{x}_i + \dot{x}_2 = x_3 + \sum_{i=3}^{n} c_i x_{i+1} + v_0$$

Then, by taking

$$v_0 = -x_3 - \sum_{i=3}^{n} c_i x_{i+1} - k s_0, \quad k > 0$$

we get $\dot{s}_0 = -k s_0$. Thus, the nominal system (4.20) is asymptotically stable.

Step 5: Define the sliding surface for (4.19) as $s = s_0 + z$, where z is the integral part that is computed afterwards. Select $z(0)$ such that $s(0) = 0$ to avoid the reaching phase,. Take $v = v_0 + v_s$, where v_0 is the nominal part and v_s is compensator part that is computed afterwards. Then,

$$\dot{s} = \dot{s}_0 + \dot{z} = \dot{x}_1 + \sum_{i=3}^{n} c_i \dot{x}_i + \dot{x}_2 + \dot{z} = x_3 + \sum_{i=3}^{n} c_i x_{i+1} + v_0 + v_s + \dot{z}$$

Step 6: Now, by choosing a Lyapunov function $V = \frac{1}{2}s^2 + \frac{1}{2}\sum\limits_{i=1}^{n-1} \tilde{F}_i^2$, design the adaptive laws for $\tilde{F}_i$ and $\hat{F}_i$, $i = 1, \cdots, n-1$ and compute v_s such that $\dot{V} < 0$.

Since,

$$\dot{V} = s\dot{s} + \sum_{i=1}^{n-1} \tilde{F}_i \, \dot{\tilde{F}}_i$$

$$= s\left(x_3 + \sum_{i=3}^{n} c_i x_{i+1} + \hat{F}_i + \tilde{F}_i + v_0 + v_s + \dot{z}\right) + \sum_{i=3}^{n} \tilde{F}_i \dot{\tilde{F}}_i$$

$$= s\left(x_3 + \sum_{i=3}^{n} c_i x_{i+1} + \hat{F}_i + v_0 + v_s + \dot{z}\right) + \sum_{i=3}^{n} \tilde{F}_i(\dot{\tilde{F}}_i + c_i s)$$

Therefore, by using

$$\dot{z} = -x_3 - \sum_{i=3}^{n} c_i x_{i+1} - v_0$$

$$v_s = -\sum_{i=3}^{n} c_i \hat{F}_i - k \, \text{sgn}(s)$$

$$\dot{\tilde{F}}_i = -c_i s - k_i \, \tilde{F}_i, \ \ k, k_i > 0, \ i = 3, \cdots, n$$

$$\dot{\hat{F}}_i = -\dot{\tilde{F}}_i$$

we have $\dot{V} = -k\,s\,\text{sgn}(s) - \sum_{i=3}^{n} k_i \tilde{F}_i^2 < 0$. From this we conclude that s, $\tilde{F}_i \to 0$. Since $s \to 0$, therefore $x \to 0$.

4.3.5 Application Examples

4.3.5.1 Four-Wheel Car

The front-wheel car, as shown in Figure 4.4, represents four-dimensional system having control deficiency of second order. Its Lie algebra contains Lie brackets of depth one and two. The front wheels of the car are allowed to spin about the vertical axes, while the rear wheels are aligned with the car. The constraints on the system appear when the wheels are allowed to spin and roll, however slipping is not allowed.

Let the configuration of car is denoted by (x, y, θ, ϕ), parameterized by xy location of the rear wheel. Let θ denote the angle of the car relative to the horizontal axis
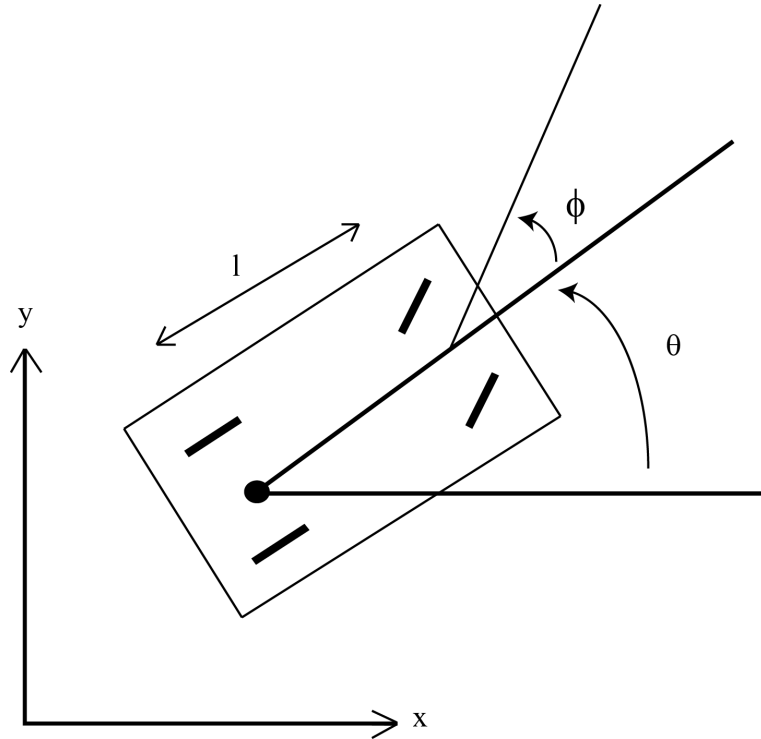
FIGURE 4.4: Kinematic Model of a Four-wheel Car.

and ϕ be the steering angle relative to the car. By setting the sideways velocity of the car to zero, the constraints for the front and rear wheels are established. Thus, the velocity of the rear wheels perpendicular to their direction is $\sin\theta\dot{x} - \cos\theta\dot{y}$ and the velocity of the front wheels is $\sin(\theta+\phi)\dot{x} - \cos(\theta+\phi)\dot{y} - l\dot{\theta}\cos\phi$. The Pfaffian constraints on the car are:

$$\sin\theta\dot{x} - \cos\theta\dot{y} = 0$$

$$\sin(\theta+\phi)\dot{x} - \cos(\theta+\phi)\dot{y} - l\dot{\theta}\cos\phi = 0$$

Now, choosing u_1 as the driving velocity and u_2 as the steering velocity, the control system can be given as:

$$\begin{bmatrix} \dot{x} \\ \dot{y} \\ \dot{\theta} \\ \dot{\phi} \end{bmatrix} = \begin{bmatrix} \cos\theta \\ \sin\theta \\ \frac{1}{l}\tan\phi \\ 0 \end{bmatrix} u_1 + \begin{bmatrix} 0 \\ 0 \\ 0 \\ 1 \end{bmatrix} u_2 \tag{4.21}$$

The following transformation

$$x_1 = x$$

$$x_2 = \frac{1}{l}\sec^3\theta\tan\phi$$

$$x_3 = \tan\theta$$

$$x_4 = y$$

$$v_1 = \cos\theta\, u_1$$

$$v_2 = -\frac{3}{l}\tan\theta\sin^2\phi\, u_1 + l\cos^3\theta\cos^2\phi\, u_2$$

converts the system (4.21) into the following chained form system:

$$\dot{x}_1 = v_1$$

$$\dot{x}_2 = v_2$$

$$\dot{x}_3 = x_2 v_1 \tag{4.22}$$

$$\dot{x}_4 = x_3 v_1$$

or

$$\dot{x} = Y_1(x)u_1 + Y_2(x)u_2, \ \ x \in \mathbb{R}^4$$

$$\text{where } Y_1(x) = \begin{bmatrix} 1 \\ 0 \\ x_2 \\ x_3 \end{bmatrix} \quad \text{and } Y_2(x) = \begin{bmatrix} 0 \\ 1 \\ 0 \\ 0 \end{bmatrix}.$$

The kinematic model (4.22) has the two properties mentioned in Sec 4.2.2. In order to verify the second assumption, it is sufficient to calculate the following Lie brackets of $Y_1(x)$ and $Y_2(x)$:

$$Y_3(x) \triangleq [Y_1, Y_2](x) = \begin{bmatrix} 0 \\ 0 \\ -1 \\ 0 \end{bmatrix}, \ Y_4(x) \triangleq [Y_1, Y_3](x) = \begin{bmatrix} 0 \\ 0 \\ 0 \\ 1 \end{bmatrix}$$

which satisfy the LARC condition, i.e.

$$span\{Y_1, Y_2, Y_3, Y_4\}(x) = \mathbb{R}^4 \qquad \forall x \in \mathbb{R}^4$$

After applying the steps 1 - 6 as mentioned in Section 4.3.4 on the front wheel car model in chained form, we achieve the desired results given in the following subsection.

Simulation Results

Figure 4.5 shows simulation results of the applied algorithm on the model of four-wheel car. Here, the verification has been carried out for various initial conditions of state including (1,-2,pi/6,-pi/4). Time trajectories show that all the states are going towards zero for the initial condition, thus validating the correctness of the proposed algorithm.

4.3.5.2 Firetruck Model

The fire truck model is a nonholonomic system having three control inputs and overall six configuration variables. The controllability Lie algebra of this model has two Lie brackets of depth one and one Lie bracket of depth two. By defining the states as $(x_1, x_2, x_3, x_4, x_5, x_6)^{T} \overset{def}{=} (x, \varphi_0, \varphi_1, \theta_0, \theta_1, y)^{T}$ in the kinematic model of fire truck [80] and keeping $l_0 = l_1 = 1$, we get the following model:

$$\dot{x} = Y_1(x)u_1 + Y_2(x)u_2 + Y_3(x)u_3 \tag{4.23}$$
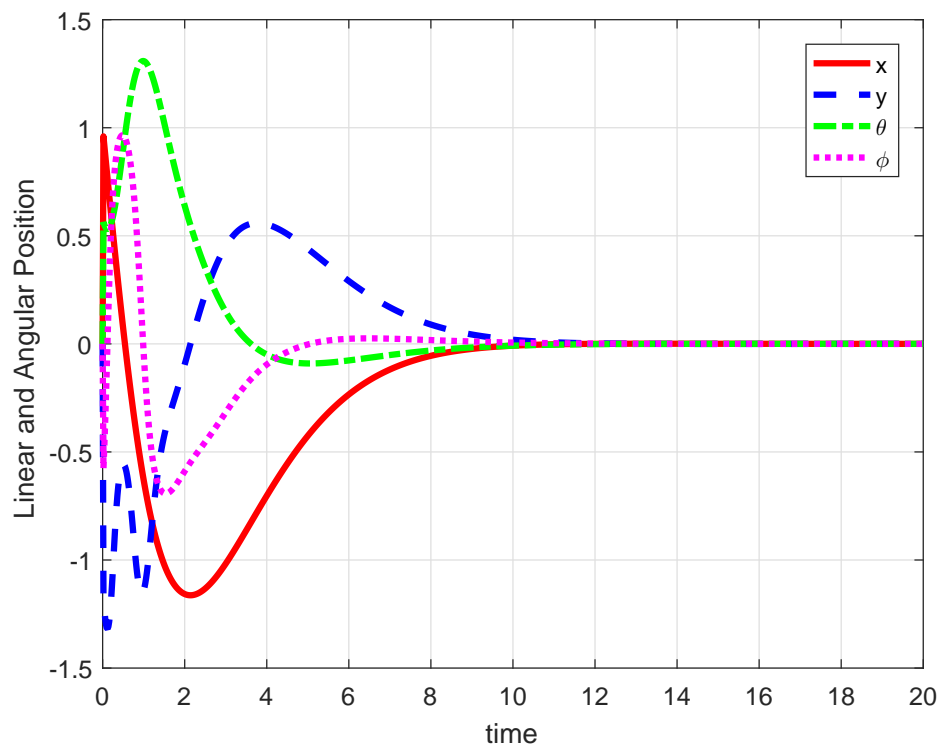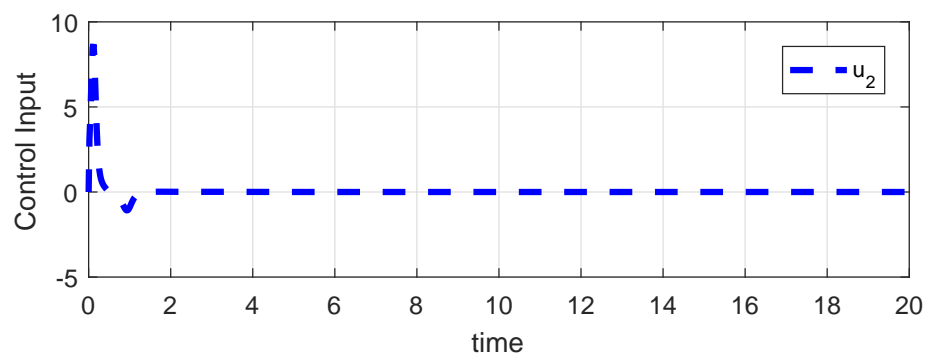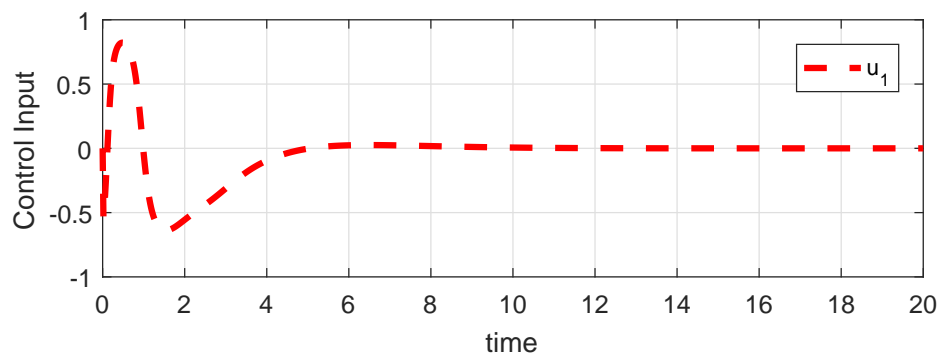
FIGURE 4.5: (a) Time response of four-wheel car corresponding to initial condition (1,-2,pi/6,-pi/4) (b) Time response of the control effort

where

$$
Y_1(x) =
\begin{bmatrix}
1 \\
0 \\
0 \\
\tan x_2 \sec x_4 \\
-\sin(x_3 - x_4 + x_5)\sec x_3 \sec x_4 \\
\tan x_4
\end{bmatrix}
, \quad
Y_2(x) =
\begin{bmatrix}
0 \\
1 \\
0 \\
0 \\
0 \\
0
\end{bmatrix}
, \quad
Y_3(x) =
\begin{bmatrix}
0 \\
0 \\
1 \\
0 \\
0 \\
0
\end{bmatrix}
$$

In order to verify the second proposition given in Sec 4.2.2., it is sufficient to calculate the following Lie brackets:

$$
Y_4(x) \overset{def}{=} [Y_1, Y_2](x) =
\begin{bmatrix}
0 \\
0 \\
0 \\
-(\sec x_2)^2 \sec x_4 \\
0 \\
0
\end{bmatrix}
,
$$

$$
Y_5(x) \overset{def}{=} [Y_1, Y_3](x) =
\begin{bmatrix}
0 \\
0 \\
0 \\
0 \\
\sec x_3 \sec x_4 \cos(x_3 - x_4 + x_5) + \sin(x_3 - x_4 + x_5)\tan x_3 \\
0
\end{bmatrix}
$$

$$
Y_6(x) \overset{def}{=} [Y_1, [Y_1, Y_2]](x)
$$

$$
= \begin{bmatrix}
0 \\
0 \\
0 \\
0 \\
(\sec x_2 \sec x_4)^2 \sec x_3 \cos(x_3 - x_4 + x_5) - \sin(x_3 - x_4 + x_5) \tan x_4 \\
(\sec x_2)^2 (\sec x_5)^3
\end{bmatrix}
$$

It is evident that if the system motion of is restricted to the manifold

$$
M \overset{def}{=} \{x \in \mathbb{R}^6 : |x_i| < \frac{\pi}{2}, i = 2,\ 3,\ 4\}
$$

then the LARC condition is satisfied.

The following transformation, given in [81]

$$
z_1 = x_1
$$

$$
z_2 = \sec^3 x_4 \tan x_3
$$

$$
z_3 = \tan x_4
$$

$$
z_4 = x_2
$$

$$
z_5 = -\sin(x_5 - x_4 + x_6) \sec x_4 \sec x_5
$$

$$
z_6 = x_6
$$

$$
v_1 = \bar{u}_1 = \cos x_4 u_1
$$

$$
v_2 = a_1 \bar{u}_1 + a_2 u_2
$$

$$
v_3 = a_3 \bar{u}_1 + a_4 u_3
$$

where

$$
a_1 = 3 \tan^2 x_3 \tan x_4 \sec^4 x_4, \quad a_2 = \sec^2 x_3 \sec^3 x_4
$$

$$
a_3 = \cos(x_5 - x_4 + x_6) \tan x_3 \sec x_5 \sec^2 x_4 + \cos(x_5 - x_4 + x_6) \sin(x_5 - x_4 + x_6)
$$

$$
\sec^2 x_5 \sec^2 x_4 - \sin(x_5 - x_4 + x_6) \sec x_5 \sec^2 x_4 \tan x_3 \tan x_4
$$

$$a_4 = -\cos(x_5 - x_4 + x_6)\sec x_4 \sec x_5 - \sin(x_5 - x_4 + x_6)\sec x_5 \sec x_4 \tan x_5$$

converts the nonholonomic firetruck model system into the following chained form system:

$$\dot{x}_1 = v_1$$
$$\dot{x}_2 = v_2$$
$$\dot{x}_3 = x_2 v_1 \tag{4.24}$$
$$\dot{x}_4 = x_3 v_1$$
$$\dot{x}_5 = v_3$$
$$\dot{x}_6 = x_5 v_1$$

After applying the steps 1 - 6 as mentioned in Section 4.3.4 on the firetruck system in chained form, we achieve the desired results given in the following subsection.

Simulation Results

Figure 4.6 shows simulation results of the applied algorithm on the model of firetruck. Here, the verification has been carried out for various initial conditions of state including (1,2,-pi/4,pi/4,pi/3,-pi/3). Time trajectories show that all the states are going towards zero for the initial condition, thus validating the correctness of the proposed algorithm.

Next, we consider the perturbed FONHS in chained form. An underwater vehicle model is considered as a model example. Two different kinds of perturbation are investigated as case studies.

4.4 Problem Formulation : Perturbed FONHS in Chained Form

Recently, there has been an increasing interest in designing and implementation of robust controllers for FONHS such as underwater vehicles. The underwater
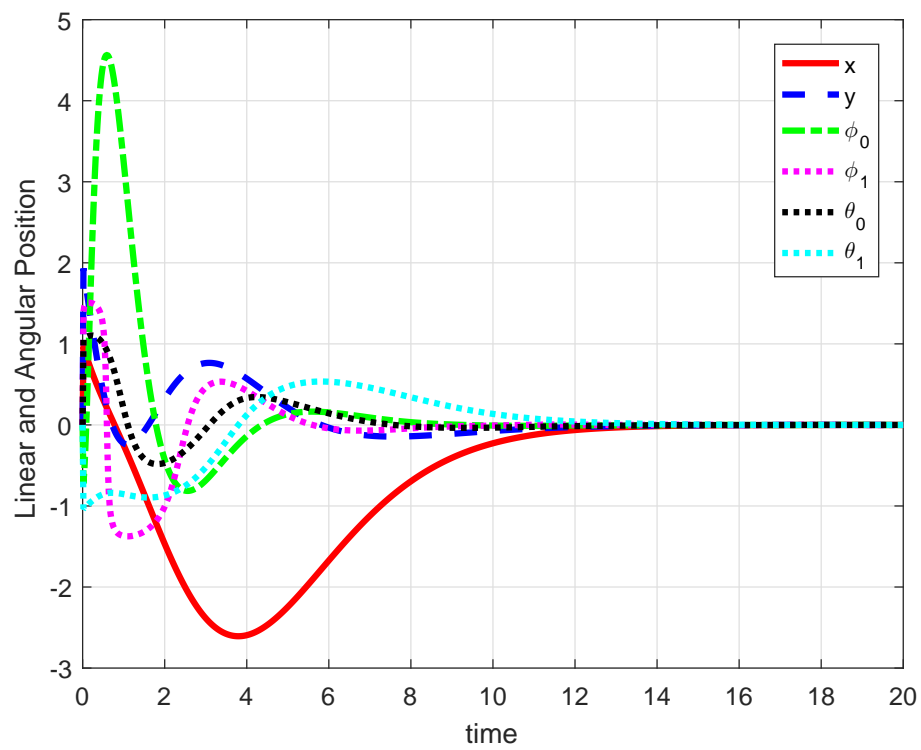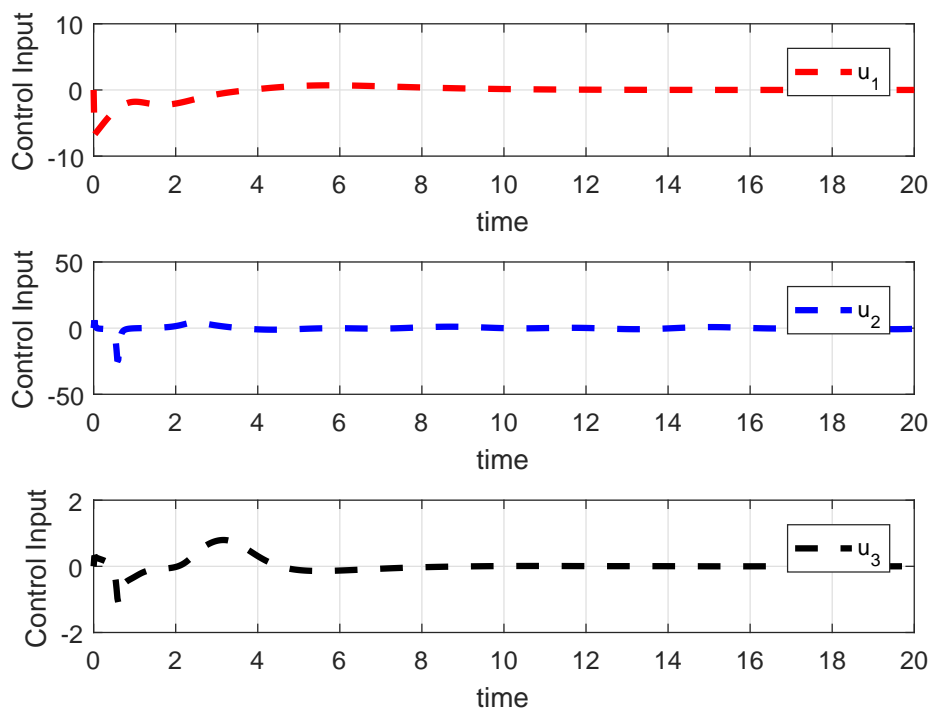
FIGURE 4.6: (a) Time response of four-wheel car corresponding to initial condition (1,2,-pi/4,pi/4,pi/3,-pi/3) (b) Time response of the control effort

vehicles are useful in performing vital roles in the monitoring of coastal shallow-water regions, environmental surveying, offshore oil installations, undersea cable/pipeline inspection, oil/mineral explorations, homeland security and many other underwater tasks ([82], [83]). These survey papers provide a useful and relevant overview on the control of Autonomous Underwater Vehicles (AUVs). In [84], a tracking control of under-actuated AUV was designed in the presence of unknown ocean currents; whereas, position-based control of an underwater robotic system for maintaining position in the presence of ocean currents was presented in [85]. A hybrid control for dynamic positioning of an under-actuated marine system was proposed in [86] and a second-order sliding mode controller was designed for AUV in the presence of unknown disturbances in [87]. Neural network based control technique for controlling the trajectory of AUVs was presented in [88]. A backstepping based adaptive tracking control design for under-actuated AUVs has been reported in [89]. In [90], a robust control of variable speed AUV was designed. Also, point stabilization for an underwater vessel in the presence of sea currents was proposed by [91]. Some recent practical applications of sliding mode control include control of steerable needles [92], nonlinear control of an unmanned agricultural tractor [93] and impedance control of a piezoelectric microgripper [94].

Owing to the presence of nonholonomic constraints, the kinematic model of AUVs is best described by:

$$\dot{z} = \sum_{i=1}^{m} g_i(z)\, u_i, \quad z \in \mathbb{R}^n \tag{4.25}$$

where $u_i, \;\; i = 1, \cdots, m, \, m < n$ are locally bounded piece-wise continuous control functions defined on the interval $[0, \infty)$ and g_i are independent vector fields on $\mathbb{R}^n$. An important feature of nonholonomic mechanical systems described by (4.25) is that the number of inputs is fewer than the degrees of freedom.

4.4.1 Kinematic Model of Underwater Vehicle

Consider a model of an underwater vehicle as shown in Figure 4.7.
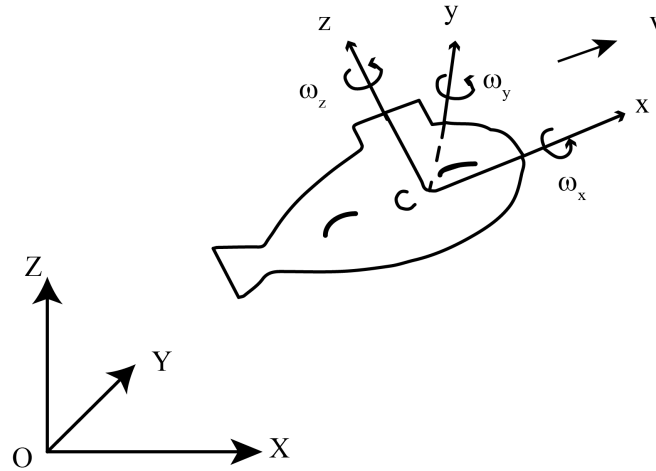
FIGURE 4.7: Autonomous Underwater Vehicle.

The two frames of reference used for deriving the AUV model include the inertial frame $(O - XYZ)$ and the local frame $(c - xyz)$. The local frame is attached to the vehicle at its centre c. Motion of the vehicle is described by using six coordinates, three for position $(x,\ y,\ z)$ and three for the vehicle orientation $(\varphi,\ \theta,\ \psi)$. The Euler angle φ corresponds to the roll motion, while ψ and θ represent yaw and pitch motions respectively.

The velocity of underwater vehicle is represented by v and its components along the x, y and z axes are given by [95]:

$$
\begin{bmatrix} \dot{x} \\ \dot{y} \\ \dot{z} \end{bmatrix} = \begin{bmatrix} v\ \cos\psi\ \cos\theta \\ v\ \sin\psi\ \cos\theta \\ -v\ \sin\theta \end{bmatrix}
\tag{4.26}
$$

The relationship between the angular velocity $\omega\ =\ (\omega_x,\ \omega_y,\ \omega_z)^T$ and time rate of the Euler angles in the local frame is given as:

$$
\begin{bmatrix} \dot{\varphi} \\ \dot{\theta} \\ \dot{\psi} \end{bmatrix} = \begin{bmatrix} 1 & \sin\varphi\ \tan\theta & \cos\varphi\ \tan\theta \\ 0 & \cos\varphi & -\sin\varphi \\ 0 & \sin\varphi\ \sec\theta & \cos\varphi\ \sec\theta \end{bmatrix} \begin{bmatrix} \omega_x \\ \omega_y \\ \omega_z \end{bmatrix}
\tag{4.27}
$$

After combining (4.26) and (4.27) and using a modified set of state and control variables as $\eta = (x, y, z, \varphi, \theta, \psi)^T$ and $(u_1, u_2, u_3, u_4) = (v, \omega_x, \omega_y, \omega_z)$ yields kinematic model for the underwater vehicle as:

$$\dot{\eta} = \begin{bmatrix} \dot{x} \\ \dot{y} \\ \dot{z} \\ \dot{\varphi} \\ \dot{\theta} \\ \dot{\psi} \end{bmatrix} = \begin{bmatrix} \cos\psi\cos\theta \\ \sin\psi\cos\theta \\ -\sin\theta \\ 0 \\ 0 \\ 0 \end{bmatrix} u_1 + \begin{bmatrix} 0 \\ 0 \\ 0 \\ 1 \\ 0 \\ 0 \end{bmatrix} u_2 + \begin{bmatrix} 0 \\ 0 \\ 0 \\ \sin\varphi\tan\theta \\ \cos\varphi \\ \sin\varphi\sec\theta \end{bmatrix} u_3 + \begin{bmatrix} 0 \\ 0 \\ 0 \\ \cos\varphi\tan\theta \\ -\sin\varphi \\ \cos\varphi\sec\theta \end{bmatrix} u_4$$

or in compact form as:

$$\dot{\eta} = g_1(\eta)\ u_1 + g_2(\eta)\ u_2 + g_3(\eta)\ u_3 + g_4(\eta)\ u_4 \tag{4.28}$$

4.4.2 Case Studies

Two different cases of uncertainties are considered here and robust stabilizing control algorithm is developed for both cases. Details of the case studies are as follows:

Case Study 1: Here, it is assumed that the perturbation is present only in one control input. Consider the above system (4.28) and choose

$$u_1 = \frac{1}{\cos\psi\cos\theta}\bar{u}_1,$$

where $\psi, \theta \neq \frac{\pi}{2}$ and $\bar{u}_1$ is the new input. Then, system (4.28) can be written as:

$$\dot{\eta} = \bar{g}_1(\eta)\ \bar{u}_1 + g_2(\eta)\ u_2 + g_3(\eta)\ u_3 + g_4(\eta)\ u_4 \tag{4.29}$$

where

$$\bar{g}_1(\eta) = \begin{bmatrix} 1 & \tan\psi & -\sec\psi\tan\theta & 0 & 0 & 0 \end{bmatrix}^T$$

$$g_2(\eta) = \begin{bmatrix} 0 & 0 & 0 & 1 & 0 & 0 \end{bmatrix}^T$$

$$g_3(\eta) = \begin{bmatrix} 0 & 0 & 0 & \sin\varphi\tan\theta & \cos\varphi & \sin\varphi\sec\theta \end{bmatrix}^T$$

$$g_4(\eta) = \begin{bmatrix} 0 & 0 & 0 & \cos\varphi\tan\theta & -\sin\varphi & \cos\varphi\sec\theta \end{bmatrix}^T$$

with $\eta \in \mathbb{R}^n$ and u_i, $i = 1, \cdots, 4$ are scalar control inputs.

Now, u_4 is assumed to be perturbed as

$$u_4 = \bar{u}_4 + \Delta(\eta, t)$$

where $\Delta(\eta, t)$ is an unknown scalar function bounded by time derivatives and known bound i.e. $|\Delta(\eta, t)| < M$.

Case Study 2: In this case, the perturbation is considered to be present in the overall system model. Therefore, the underwater vehicle model (4.29) with some nonlinear uncertainties can be written as:

$$\dot{\eta} = \bar{g}_1(\eta) \ \bar{u}_1 + g_2(\eta) \ u_2 + g_3(\eta) \ u_3 + g_4(\eta) \ u_4 + p(\eta, t) \tag{4.30}$$

where $p(\eta, t) \in \mathbb{R}^6$ is an additive perturbation in the system model. Also, it is assumed that the additive uncertainties are in matched form.

4.4.3 The Control Problem

Given a desired point $\eta_{des} \in \mathbb{R}^n$, design stabilizing control laws in form of inputs $u_i : \mathbb{R}^n \to \mathbb{R}$, $i = 1, \cdots, 4$ so that the desired point η_{des} is an attractive set for (4.29) and (4.30) in spite of the additive uncertainties and there exists an $\varepsilon > 0$ such that $\eta(t \ ; \ 0, \ \eta_0) \to \eta_{des}$ as $t \to \infty$ for any $\eta_0 \in B(\eta_{des} \ ; \varepsilon)$.

Also, it is assumed without any loss of generality that $\eta_{des} = 0$ can be obtained by a suitable translation of the coordinate system.

The kinematic model of AUV given by (4.28) satisfies the two propositions mentioned in Section 4.2.2, i.e. the vector fields g_1, g_2, g_3 and g_4 are linearly independent and the system (4.28) is completely controllable on the manifold $M = \{\eta = (x, y, z, \varphi, \theta, \psi)^T \in \mathbb{R}^6 \ : \ |\varphi| < \frac{\pi}{2} \ \}$ as it satisfies the LARC for controllability on M. In order to prove this, it is sufficient to compute the Lie brackets given below:

$$g_5(\eta) = [g_1, g_3](\eta) = \begin{bmatrix} \sin\theta\cos\psi\cos\varphi + \sin\varphi\sin\psi \\ \sin\theta\sin\psi\cos\varphi - \sin\varphi\cos\psi \\ \cos\varphi\cos\theta \\ 0 \\ 0 \\ 0 \end{bmatrix}$$

$$g_6(\eta) = [g_1, g_4](\eta) = \begin{bmatrix} -\sin\varphi\sin\theta\cos\psi + \cos\varphi\sin\psi \\ -\sin\varphi\sin\theta\sin\psi - \cos\varphi\cos\psi \\ -\sin\varphi\cos\theta \\ 0 \\ 0 \\ 0 \end{bmatrix}$$

It is now straight-forward to verify that if the system motion is restricted to the manifold M, then $\{g_1, g_2, g_3, g_4, g_5, g_6\}$ are linearly independent, thus, satisfying the LARC condition, i.e.

$$span\{g_1(\eta), \ \cdots, \ g_6(\eta)\} = \mathbb{R}^6 \quad \forall \ \eta \in M$$

4.4.4 Conversion into Chained Form

The original system is, first of all, transformed into a perturbed chained form system. Then the perturbed chained form is further modified into a special structure

comprising nominal portion and unknowns through input transformation.

Using the following state transformation,

$$x_1 = x$$
$$x_2 = \tan \psi$$
$$x_3 = y \qquad (4.31)$$
$$x_4 = -\tan \theta \sec \psi$$
$$x_5 = z$$
$$x_6 = \varphi$$

i.e. $x = \begin{bmatrix} x_1 & x_2 & x_3 & x_4 & x_5 & x_6 \end{bmatrix}^T$ and input transformation,

$$\begin{bmatrix} v_1 \\ v_2 \\ v_3 \\ v_4 \end{bmatrix} = \begin{bmatrix} 1 & 0 & 0 & 0 \\ 0 & 0 & a_1 & a_2 \\ 0 & 0 & a_3 & a_4 \\ 0 & 1 & a_5 & a_6 \end{bmatrix} \begin{bmatrix} \bar{u}_1 \\ u_2 \\ u_3 \\ u_4 \end{bmatrix} \qquad \text{i.e. } v = Au \qquad (4.32)$$

where

$$a_1 = \frac{\sin \theta}{\cos \varphi \cos^2 \psi}, \quad a_2 = \frac{\cos \theta}{\cos \varphi \cos^2 \psi}, \quad a_3 = \frac{-\cos \varphi \cos \psi - \sin \varphi \sin \theta \sin \psi}{\cos^2 \theta \cos^2 \psi}$$

$$a_4 = \frac{\sin \varphi \cos \psi - \cos \varphi \sin \theta \sin \psi}{\cos^2 \theta \cos^2 \psi}, \quad a_5 = \frac{\sin \varphi \sin \theta}{\cos \theta}, \quad a_6 = \frac{\cos \varphi \sin \theta}{\cos \theta}$$

$$|A| = \frac{1}{(\cos \theta \cos \psi)^3} \neq 0 \text{ if } \psi, \theta \neq \frac{\pi}{2}$$

the system (4.29) can be written in chained form as:

$$\dot{x}_1 = v_1$$
$$\dot{x}_2 = v_2$$
$$\dot{x}_3 = x_2 v_1$$
$$\dot{x}_4 = v_3 \qquad\qquad (4.33)$$
$$\dot{x}_5 = x_4 v_1$$
$$\dot{x}_6 = v_4$$

4.4.4.1 Bounded Uncertainty in Control Input

The control problem is resolved by first modifying the model (4.29) into the following chained form containing the uncertainty term with v_4. The system is, therefore, complicated by the presence of a bounded disturbance affecting the last equation,

$$\dot{x}_1 = v_1$$
$$\dot{x}_2 = v_2$$
$$\dot{x}_3 = x_2 v_1$$
$$\dot{x}_4 = v_3 \qquad\qquad (4.34)$$
$$\dot{x}_5 = x_4 v_1$$
$$\dot{x}_6 = v_4 + \Delta(x, t)$$

where $\Delta(x, t)$ is unknown scalar function bounded with first time derivatives and with known bound i.e. $|\Delta(x, t)| < M$.

4.4.4.2 Model-Level Perturbation

Here, consider system (4.30) along with model level perturbation as:

$$\dot{\eta} = \bar{g}_1(\eta) \ \bar{u}_1 + g_2(\eta) \ u_2 + g_3(\eta) \ u_3 + g_4(\eta) \ u_4 + p(\eta, t) \tag{4.35}$$

where

$$\bar{g}_1(\eta) = \begin{bmatrix} 1 & \tan \psi & -\sec \psi \tan \theta & 0 & 0 & 0 \end{bmatrix}^T$$

$$g_2(\eta) = \begin{bmatrix} 0 & 0 & 0 & 1 & 0 & 0 \end{bmatrix}^T$$

$$g_3(\eta) = \begin{bmatrix} 0 & 0 & 0 & \sin \varphi \tan \theta & \cos \varphi & \sin \varphi \sec \theta \end{bmatrix}^T$$

$$g_4(\eta) = \begin{bmatrix} 0 & 0 & 0 & \cos \varphi \tan \theta & -\sin \varphi & \cos \varphi \sec \theta \end{bmatrix}^T$$

and $p(\eta, t) \in span\{\bar{g}_1(\eta), g_2(\eta), g_3(\eta), g_4(\eta)\}, \ \forall \ t$

According to [96], if $p(\eta, t) \in span\{\bar{g}_1(\eta), g_2(\eta), g_3(\eta), g_4(\eta)\}$ is in matched form, then under coordinate change and state feedback (4.35) can, locally or globally, be transformed into:

$$\begin{aligned}
\dot{x}_1 &= v_1 + p_1(x, t) \\
\dot{x}_2 &= v_2 + p_2(x, t) \\
\dot{x}_3 &= x_2(v_1 + p_1(x, t)) \\
\dot{x}_4 &= v_3 + p_3(x, t) \\
\dot{x}_5 &= x_4(v_1 + p_1(x, t)) \\
\dot{x}_6 &= v_4 + p_4(x, t)
\end{aligned} \tag{4.36}$$

where the perturbations are $p_1(x, t) = x_1\varphi_1(x, t)\theta_1$, $p_2(x, t) = x_2\varphi_2(x, t)\theta_2$, $p_3(x, t) = x_4\varphi_3(x, t)\theta_3$ and $p_4(x, t) = x_6\varphi_4(x, t)\theta_4$ with known nonlinear functions $\varphi_i(x, t)$, $i = 1, \cdots, 4$ and unknown constants θ_i, $i = 1, \cdots, 4$. Let $\hat{\theta}_i$ be estimates of θ_i and let $\tilde{\theta}_i = \theta_i - \hat{\theta}_i$, $i = 1, \cdots, 4$ be errors in estimation of θ_i.

4.4.5 Case Study 1: Stabilizing Algorithm for Perturbed Control Input

The original underwater vehicle system (4.29) is, first of all, transformed into a perturbed chained form system (4.34). Then, the perturbed chained form is further modified into a special structure comprising nominal portion and some unknowns through input transformation. Adaptive method is used to compute the unknowns and the transformed system is stabilized using ISMC. The controller for the transformed system consists of nominal and compensator control. Details of the stabilizing algorithm are presented in the subsection.

4.4.5.1 Control Algorithm

Primarily the algorithm is an application of proposed Method-2 earlier presented in detail in Section 4.3.5.

Step 1: Choose $v_1 = x_2$, $v_2 = x_3$, $v_3 = x_5$ and $v_4 = v$. Then, system (4.34) becomes:

$$\begin{aligned}
\dot{x}_1 &= x_2 \\
\dot{x}_2 &= x_3 \\
\dot{x}_3 &= x_2^2 \\
\dot{x}_4 &= x_5 \\
\dot{x}_5 &= x_3 x_2 \\
\dot{x}_6 &= v + \Delta(t)
\end{aligned} \tag{4.37}$$

Step 2: After some manipulation, the above system (4.37) can be written as:

$$\dot{x}_1 = x_2$$
$$\dot{x}_2 = x_3$$
$$\dot{x}_3 = x_4 + F_3 \qquad (4.38)$$
$$\dot{x}_4 = x_5$$
$$\dot{x}_5 = x_6 + F_5$$
$$\dot{x}_6 = v + \Delta(t)$$

where $F_3 = -x_4 + x_2^2$, $F_5 = -x_6 + x_3 x_2$

Step 3: Now, assume that F_3 and F_5 are unknowns and can be computed adaptively. Let $\hat{F}_i$ be an estimate of F_i, $i = 3, 5$ respectively and $\tilde{F}_i = F_i - \hat{F}_i$ be the errors in estimation of F_i, $i = 3, 5$ respectively. Then, system (4.38) can be written as:

$$\dot{x}_1 = x_2$$
$$\dot{x}_2 = x_3$$
$$\dot{x}_3 = x_4 + \hat{F}_3 + \tilde{F}_3 \qquad (4.39)$$
$$\dot{x}_4 = x_5$$
$$\dot{x}_5 = x_6 + \hat{F}_5 + \tilde{F}_5$$
$$\dot{x}_6 = v + \Delta(t)$$

Step 4: The nominal system for (4.39) becomes:

$$\dot{x}_i = x_{i+1}, \ i = 1, \cdots, 5$$
$$\dot{x}_6 = v_0 \qquad (4.40)$$

Now, choose a sliding surface for (4.40) as $\sigma_0 = \left(1 + \frac{d}{dt}\right)^5 x_1$, i.e.

$$\sigma_0 = x_1 + 5x_2 + 10x_3 + 10x_4 + 5x_5 + x_6$$

and

$$\dot{\sigma}_0 = \dot{x}_1 + 5\dot{x}_2 + 10\dot{x}_3 + 10\dot{x}_4 + 5\dot{x}_5 + \dot{x}_6$$
$$= x_2 + 5x_3 + 10x_4 + 10x_5 + 5x_6 + v_0$$

Then, by taking

$$v_0 = -x_2 - 5x_3 - 10x_4 - 10x_5 - 5x_6 - k\sigma_0, \quad k > 0$$

we get $\dot{\sigma}_0 = -k\sigma_0$. Thus, the nominal system (4.40) is asymptotically stable.

Step 5: Select the sliding surface for (4.39) as $\sigma = \sigma_0 + \beta$, where β is computed later and it is the integral term. Select $\beta(0)$ such that $\sigma(0) = 0$ to avoid the reaching phase. Take $v = v_0 + v_s$, where v_0 is the nominal part and v_s is compensator part that is computed afterwards. Then,

$$\dot{\sigma} = \dot{\sigma}_0 + \dot{\beta} = \dot{x}_1 + 5\dot{x}_2 + 10\dot{x}_3 + 10\dot{x}_4 + 5\dot{x}_5 + \dot{x}_6 + \dot{\beta}$$
$$= x_2 + 5x_3 + 10x_4 + 10\hat{F}_3 + 10\tilde{F}_3 + 10x_5 + 5x_6 + 5\hat{F}_5 + 5\tilde{F}_5$$
$$+ v_0 + v_s + \Delta(t) + \dot{\beta} \tag{4.41}$$

Step 6: Now, by choosing a Lyapunov function $V = \frac{1}{2}\sigma^2 + \frac{1}{2}\tilde{F}_3^2 + \frac{1}{2}\tilde{F}_5^2$, design the adaptive laws for $\tilde{F}_i$ and $\hat{F}_i$, $i = 3, 5$ and compute v_s such that $\dot{V} < 0$.

Since,

$$\dot{V} = \sigma\dot{\sigma} + \tilde{F}_3\dot{\tilde{F}}_3 + \tilde{F}_5\dot{\tilde{F}}_5$$
$$= \sigma(x_2 + 5x_3 + 10x_4 + 10\hat{F}_3 + 10\tilde{F}_3 + 10x_5 + 5x_6 + 5\hat{F}_5 + 5\tilde{F}_5$$
$$+ v_0 + v_s + \dot{\beta}) + \tilde{F}_3\dot{\tilde{F}}_3 + \tilde{F}_5\dot{\tilde{F}}_5$$
$$= \sigma(x_2 + 5x_3 + 10x_4 + 10x_5 + 5x_6 + 10\hat{F}_3 + 5\hat{F}_5 + v_0 + v_s$$
$$+ \Delta(t) + \dot{\beta}) + \tilde{F}_3(\dot{\tilde{F}}_3 + 10\sigma) + \tilde{F}_5(\dot{\tilde{F}}_5 + 5\sigma)$$

Therefore, by using

$$\dot{\beta} = -x_2 - 5x_3 - 10x_4 - 10x_5 - 5x_6 - v_0$$

$$v_s = -10\hat{F}_3 - 5\hat{F}_5 - k\,\text{sgn}(\sigma),\ \ k > M$$

$$\dot{\tilde{F}}_5 = -10\sigma - k_1\,\tilde{F}_3$$

$$\dot{\tilde{F}}_5 = -5\sigma - k_2\,\tilde{F}_5$$

$$\dot{\hat{F}}_3 = -\dot{\tilde{F}}_3\ ,\ \ \dot{\hat{F}}_5 = -\dot{\tilde{F}}_5$$

we have $\dot{V} = -k\,\sigma\,\text{sgn}(\sigma) - k_1\tilde{F}_3^2 - k_2\tilde{F}_5^2 < 0$. From this we conclude that $\sigma,\ \tilde{F}_3,\ \tilde{F}_5 \to 0$. Since $\sigma \to 0$, therefore $x \to 0$.

4.4.5.2   Simulation Results

Figures 4.8 and 4.9 show simulation results for the underwater vehicle without and with the uncertainty term added in the control input. The simulations are carried out for the same initial conditions $(x(0), y(0), z(0), \varphi(0), \theta(0), \psi(0)) = (2,\ 0,\ -2, \pi/6,\ \pi/8, \pi/5)$ so that the effect of uncertainty can be observed. The applied uncertainty in the control input is $0.5\sin(2t) + 0.4\cos(t) + x_3\,x_2\,t$. As can be seen, the system states converge to zero for both the systems with and without the uncertainty, thus, validating the correctness of the applied algorithm. Therefore, the control objective to stabilize the underwater vehicle having any random initial condition has been achieved.

4.4.6   Case Study 2: Stabilizing Algorithm for Perturbed System Model

Again the original system (4.30) is, first of all, transformed into a perturbed chained form system (4.36). Afterwards, the perturbed chained form is further modified into a special structure comprising of nominal portion and unknowns through input transformation. Details of the proposed algorithm are presented next in the subsection.
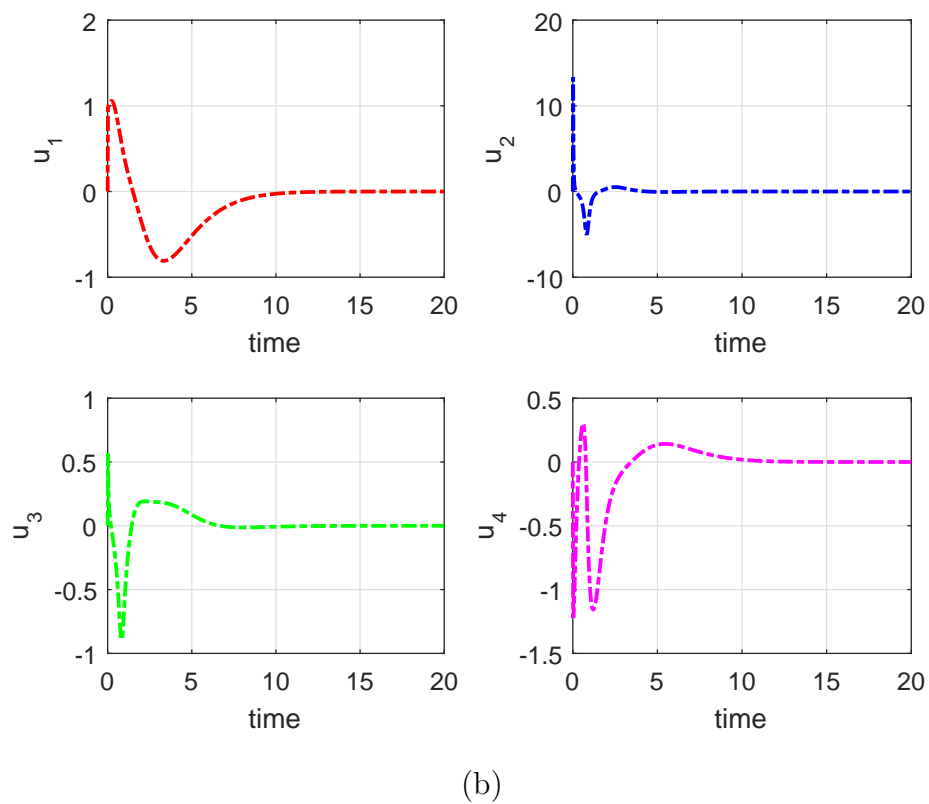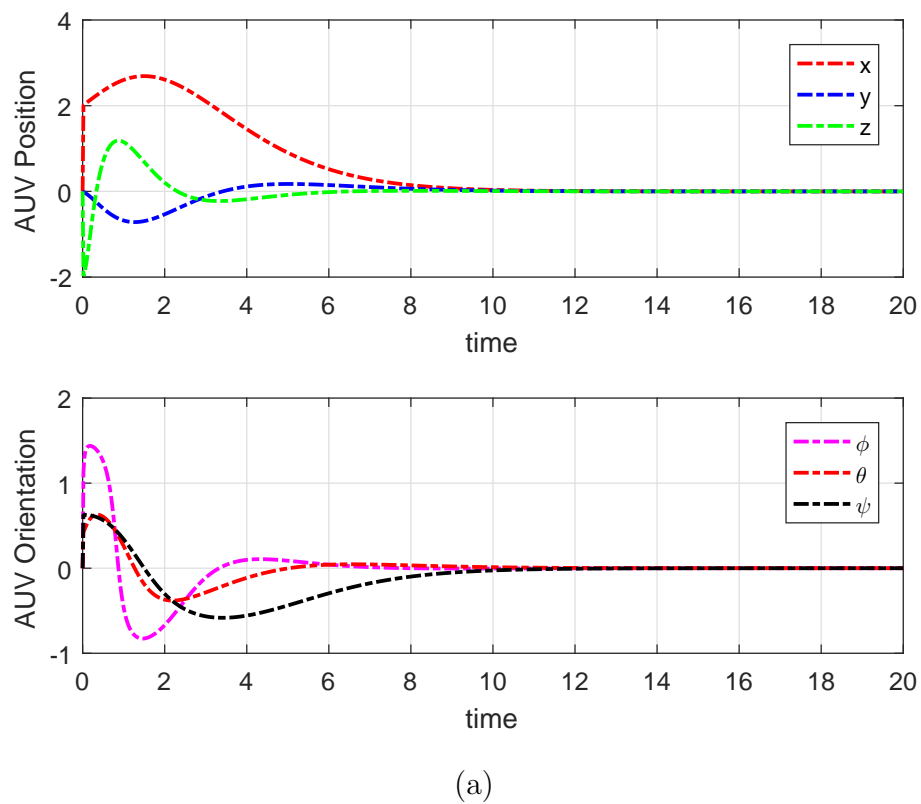
FIGURE 4.8: System Trajectory without any uncertainty (a) System states corresponding to initial condition $(2, 0, -2, \pi/6, \pi/8, \pi/5)$ (b) Control effort $u = (u_1, u_2, u_3, u_4)^T$
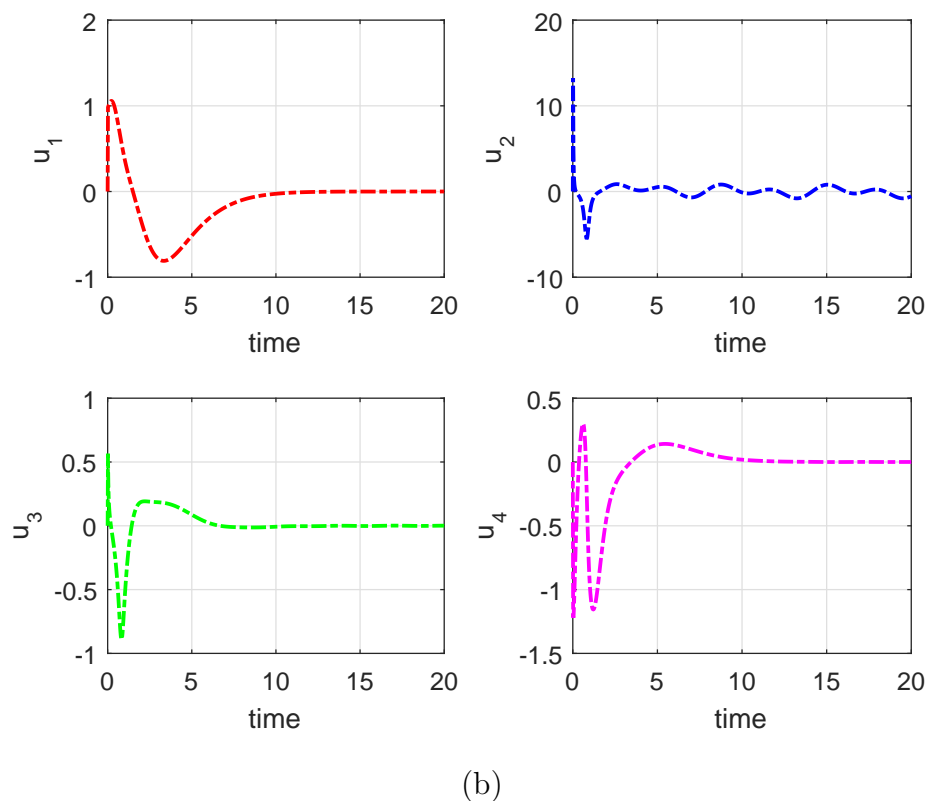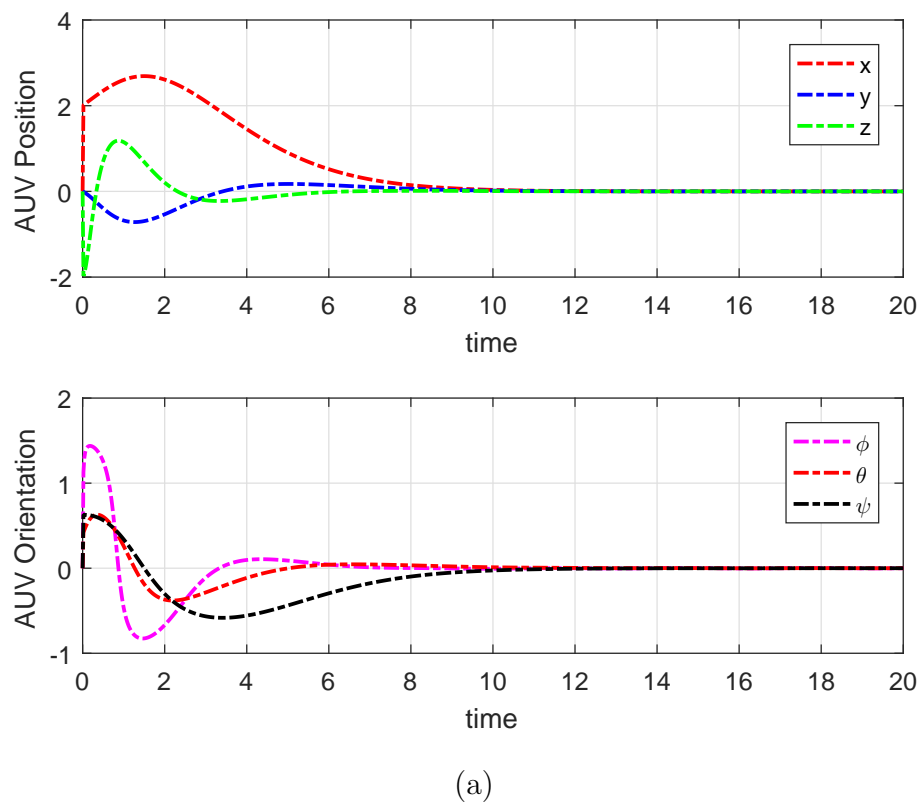
FIGURE 4.9: System Trajectory with Uncertainty (a) System states corresponding to initial condition $(2,\ 0,\ -2, \pi/6,\ \pi/8, \pi/5)$ (b) Control Effort $u = (u_1, u_2, u_3, u_4)^T$

4.4.6.1 Control Algorithm

Step 1: After decomposing unknown constants into estimated values and errors in estimated values, the system (4.36) can be rewritten as:

$$
\begin{aligned}
\dot{x}_1 &= v_1 + x_1\varphi_1(x,t)\hat{\theta}_1 + x_1\varphi_1(x,t)\tilde{\theta}_1 \\
\dot{x}_2 &= v_2 + x_2\varphi_2(x,t)\hat{\theta}_2 + x_2\varphi_2(x,t)\tilde{\theta}_2 \\
\dot{x}_3 &= x_2(v_1 + x_1\varphi_1(x,t)\hat{\theta}_1 + x_1\varphi_1(x,t)\tilde{\theta}_1) \\
\dot{x}_4 &= v_3 + x_4\varphi_3(x,t)\hat{\theta}_3 + x_4\varphi_3(x,t)\tilde{\theta}_3 \\
\dot{x}_5 &= x_3(v_1 + x_1\varphi_1(x,t)\hat{\theta}_1 + x_1\varphi_1(x,t)\tilde{\theta}_1) \\
\dot{x}_6 &= v_4 + x_6\varphi_4(x,t)\hat{\theta}_4 + x_6\varphi_4(x,t)\tilde{\theta}_4
\end{aligned}
\tag{4.42}
$$

By choosing $v_1 = x_2 - x_1\varphi_1(x,t)\hat{\theta}_1$, $v_2 = x_3 - x_2\varphi_2(x,t)\hat{\theta}_2$, $v_3 = x_5 - x_4\varphi_3(x,t)\hat{\theta}_3$ and $v_4 = v - x_6\varphi_4(x,t)\hat{\theta}_4$, system (4.42) becomes,

$$
\begin{aligned}
\dot{x}_1 &= x_2 + x_1\varphi_1(x,t)\tilde{\theta}_1 \\
\dot{x}_2 &= x_3 + x_2\varphi_2(x,t)\tilde{\theta}_2 \\
\dot{x}_3 &= x_2(x_2 + x_1\varphi_1(x,t)\tilde{\theta}_1) \\
\dot{x}_4 &= x_5 + x_4\varphi_3(x,t)\tilde{\theta}_3 \\
\dot{x}_5 &= x_3(x_2 + x_1\varphi_1(x,t)\tilde{\theta}_1) \\
\dot{x}_6 &= v + x_6\varphi_4(x,t)\tilde{\theta}_4
\end{aligned}
\tag{4.43}
$$

Step 2: After some manipulation, the above system (4.43) can be written as:

$$\dot{x}_1 = x_2 + x_1\varphi_1(x,t)\tilde{\theta}_1$$
$$\dot{x}_2 = x_3 + x_2\varphi_2(x,t)\tilde{\theta}_2$$
$$\dot{x}_3 = x_4 + F_3 + x_2x_1\varphi_1(x,t)\tilde{\theta}_1 \tag{4.44}$$
$$\dot{x}_4 = x_5 + x_4\varphi_3(x,t)\tilde{\theta}_3$$
$$\dot{x}_5 = x_6 + F_5 + x_2x_1\varphi_1(x,t)\tilde{\theta}_1$$
$$\dot{x}_6 = v + x_6\varphi_4(x,t)\tilde{\theta}_4$$

where $F_3 = -x_4 + x_2x_2$, $F_5 = -x_6 + x_3x_2$

Step 3: Now, assume that F_3 and F_5 are unknown and can be computed adaptively. Let $\hat{F}_i$ be an estimate of F_i, $i = 3, 5$ respectively and $\tilde{F}_i = F_i - \hat{F}_i$ be the errors in estimation of F_i, $i = 3, 5$ respectively. Then, system (4.44) can be written as:

$$\dot{x}_1 = x_2 + x_1\varphi_1(x,t)\tilde{\theta}_1$$
$$\dot{x}_2 = x_3 + x_2\varphi_2(x,t)\tilde{\theta}_2$$
$$\dot{x}_3 = x_4 + \hat{F}_3 + \tilde{F}_3 + x_2x_1\varphi_1(x,t)\tilde{\theta}_1 \tag{4.45}$$
$$\dot{x}_4 = x_5 + x_4\varphi_3(x,t)\tilde{\theta}_3$$
$$\dot{x}_5 = x_6 + \hat{F}_5 + \tilde{F}_5 + x_2x_1\varphi_1(x,t)\tilde{\theta}_1$$
$$\dot{x}_6 = v + x_6\varphi_4(x,t)\tilde{\theta}_4$$

Step 4: The nominal system for (4.45) is given as:

$$\dot{x}_i = x_{i+1}, \ i = 1, \cdots, 5$$
$$\dot{x}_6 = v_0 \tag{4.46}$$

Select the sliding surface for (4.46) as $\sigma_0 = (1 + \dfrac{d}{dt})^5 x_1$ i.e.

$$\sigma_0 = x_1 + 5x_2 + 10x_3 + 10x_4 + 5x_5 + x_6$$

then

$$\dot{\sigma}_0 = \dot{x}_1 + 5\dot{x}_2 + 10\dot{x}_3 + 10\dot{x}_4 + 5\dot{x}_5 + \dot{x}_6$$
$$= x_2 + 5x_3 + 10x_4 + 10x_5 + 5x_6 + v_0$$

Therefore, by taking

$$v_0 = -x_2 - 5x_3 - 10x_4 - 10x_5 - 5x_6 - k\sigma_0, \;\; k > 0$$

we get $\dot{\sigma}_0 = -k\sigma_0$. Hence, the nominal system (4.46) is asymptotically stable.

Step 5: Select the sliding surface for (4.45) as $\sigma = \sigma_0 + \beta$ where β is the integral part computed afterwards. Select $\beta(0)$ so that $\sigma(0) = 0$ to avoid the reaching phase,. Taking $v = v_0 + v_s$, where v_0 is the nominal part and v_s is compensator part that is computed afterwards. Therefore,

$$\begin{aligned}
\dot{\sigma} = \dot{\sigma}_0 + \dot{\beta} &= \dot{x}_1 + 5\dot{x}_2 + 10\dot{x}_3 + 10\dot{x}_4 + 5\dot{x}_5 + \dot{x}_6 + \dot{\beta} \\
&= x_2 + x_1\varphi_1(x,t)\tilde{\theta}_1 + 5x_3 + 5x_2\varphi_2(x,t)\tilde{\theta}_2 + 10x_4 + 10\hat{F}_3 + 10\tilde{F}_3 \\
&\quad + 10x_2x_1\varphi_1(x,t)\tilde{\theta}_1 + 10x_5 + 10x_4\varphi_3(x,t)\tilde{\theta}_3 + 5x_6 + 5\hat{F}_5 + 5\tilde{F}_5 \\
&\quad + 5x_2x_1\varphi_1(x,t)\tilde{\theta}_1 + x_6\varphi_4(x,t)\tilde{\theta}_4 + v_0 + v_s + \dot{\beta}
\end{aligned}$$

Step 6: By choosing a Lyapunov function

$$V = \frac{1}{2}\sigma^2 + \frac{1}{2}\tilde{F}_3^2 + \frac{1}{2}\tilde{F}_5^2 + \frac{1}{2}\tilde{\theta}_1^2 + \frac{1}{2}\tilde{\theta}_2^2 + \frac{1}{2}\tilde{\theta}_3^2 + \frac{1}{2}\tilde{\theta}_4^2$$

design the adaptive laws for $\tilde{F}_i$ and $\hat{F}_i$, $i = 3, 5$, $\tilde{\theta}_i$ and $\hat{\theta}_i$, $i = 1, ..., 4$ and compute v_s such that $\dot{V} < 0$.

Since

$$\dot{V} = \sigma\dot{\sigma} + \tilde{F}_3\dot{\tilde{F}}_3 + \tilde{F}_5\dot{\tilde{F}}_5 + \tilde{\theta}_1\dot{\tilde{\theta}}_1 + \tilde{\theta}_2\dot{\tilde{\theta}}_2 + \tilde{\theta}_3\dot{\tilde{\theta}}_3 + \tilde{\theta}_4\dot{\tilde{\theta}}_4$$

$$= \sigma[x_2 + x_1\varphi_1(x,t)\tilde{\theta}_1 + 5x_3 + 5x_2\varphi_2(x,t)\tilde{\theta}_2 + 10x_4 + 10\hat{F}_3 + 10\tilde{F}_3$$

$$+ 10x_2x_1\varphi_1(x,t)\tilde{\theta}_1 + 10x_5 + 10x_4\varphi_3(x,t)\tilde{\theta}_3 + 5x_6 + 5\hat{F}_5 + 5\tilde{F}_5$$

$$+ 5x_2x_1\varphi_1(x,t)\tilde{\theta}_1 + x_6\varphi_4(x,t)\tilde{\theta}_4 + v_0 + v_s + \dot{\beta}] + \tilde{F}_3\dot{\tilde{F}}_3 + \tilde{F}_5\dot{\tilde{F}}_5$$

$$+ \tilde{\theta}_1\dot{\tilde{\theta}}_1 + \tilde{\theta}_2\dot{\tilde{\theta}}_2 + \tilde{\theta}_3\dot{\tilde{\theta}}_3 + \tilde{\theta}_4\dot{\tilde{\theta}}_4$$

$$= \sigma[x_2 + 5x_3 + 10x_4 + 10x_5 + 5x_6 + 10\hat{F}_3 + 5\hat{F}_5 + v_0 + v_s + \dot{\beta}] + \tilde{F}_3(\dot{\tilde{F}}_3 + 10\sigma)$$

$$+ \tilde{F}_5(\dot{\tilde{F}}_5 + 5\sigma) + \tilde{\theta}_1(\dot{\tilde{\theta}}_1 + \sigma x_1\varphi_1(x,t) + 10\sigma x_2x_1\varphi_1(x,t) + 5\sigma x_2x_1\varphi_1(x,t))$$

$$+ \tilde{\theta}_2(\dot{\tilde{\theta}}_2 + 5\sigma x_2\varphi_2(x,t)) + \tilde{\theta}_3(\dot{\tilde{\theta}}_3 + 10\sigma x_4\varphi_3(x,t)) + \tilde{\theta}_4(\dot{\tilde{\theta}}_4 + \sigma x_6\varphi_4(x,t))$$

Then, by using

$$\dot{\beta} = -x_2 - 5x_3 - 10x_4 - 10x_5 - 5x_6 - v_0$$

$$v_s = -10\hat{F}_3 - 5\hat{F}_5 - k\,\mathrm{sgn}(\sigma)$$

$$\dot{\tilde{F}}_3 = -10\sigma - k_1\,\tilde{F}_3\,, \quad \dot{\tilde{F}}_5 = -5\sigma - k_2\,\tilde{F}_5, \quad \dot{\hat{F}}_3 = -\dot{\tilde{F}}_3, \quad \dot{\hat{F}}_5 = -\dot{\tilde{F}}_5,$$

$$\dot{\tilde{\theta}}_1 = -\sigma x_1\varphi_1(x,t) - 10\sigma x_2x_1\varphi_1(x,t) - 5\sigma x_2x_1\varphi_1(x,t) - l_1\tilde{\theta}_1, \quad \dot{\hat{\theta}}_1 = -\dot{\tilde{\theta}}_1$$

$$\dot{\tilde{\theta}}_2 = -5\sigma x_2\varphi_2(x,t) - l_2\tilde{\theta}_2, \quad \dot{\hat{\theta}}_2 = -\dot{\tilde{\theta}}_2$$

$$\dot{\tilde{\theta}}_3 = -10\sigma x_4\varphi_3(x,t) - l_3\tilde{\theta}_3, \quad \dot{\hat{\theta}}_3 = -\dot{\tilde{\theta}}_3$$

$$\dot{\tilde{\theta}}_4 = -\sigma x_6\varphi_4(x,t) - l_4\tilde{\theta}_4, \quad \dot{\hat{\theta}}_4 = -\dot{\tilde{\theta}}_4, \quad l_i > 0,\, i = 1, 2, 3, 4$$

we have $\dot{V} = -k\,\sigma\,\mathrm{sgn}(\sigma) - k_1\tilde{F}_3^2 - k_2\tilde{F}_5^2 - l_1\tilde{\theta}_1^2 - l_2\tilde{\theta}_2^2 - l_3\tilde{\theta}_3^2 - l_4\tilde{\theta}_4^2 < 0$. From this, we conclude that $\sigma,\ \tilde{F}_3,\ \tilde{F}_5,\ \tilde{\theta}_i \to 0$. Since $\sigma \to 0$, therefore $x \to 0$.

4.4.6.2 Simulation Results

Figures 4.10 and 4.11 show simulation results for underwater vehicle model affected with uncertainties. The simulations are carried out for two different initial conditions:
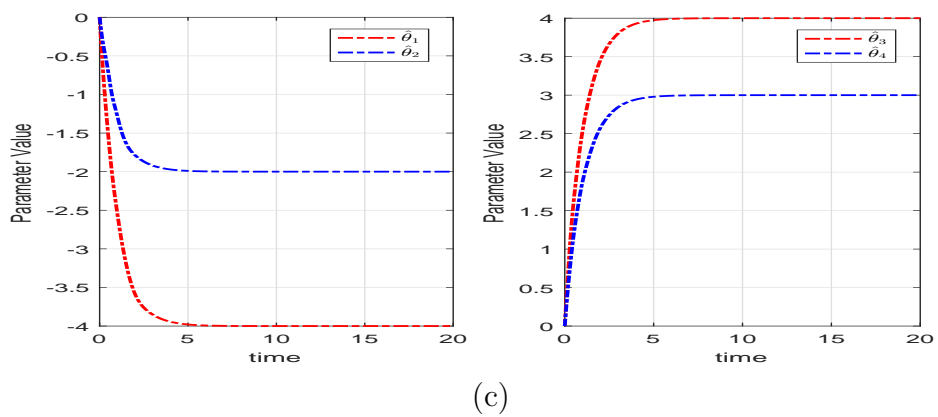
i) $(0,1,-1,\pi\,/5,\pi\,/8,\pi\,/6)$

FIGURE 4.10: System Trajectory with perturbation in system model (a) System states corresponding to initial condition (0,1,-1,π /5,π /8,π /6) (b) Control effort (c) Estimated values of parameters $\theta_i, i = 1, ..., 4$

ii) (1,-1,1,π /6,π /10,π /8)

Also, following sinusoidal/nonlinear functions are used for the known functions in the perturbations.

$$\varphi_1(x,t) = 0.5\sin(x_1) + 0.3\sin(2x_2)$$

$$\varphi_2(x,t) = x_1 + t\,x_3$$

$$\varphi_3(x,t) = 0.2\cos(x_5) + 0.5\sin(x_4)$$

$$\varphi_4(x,t) = x_5 + x_4 x_5 + t\,x_6$$

The unknown parameters for Figure 4.10 are chosen as $(\theta_1, \theta_2, \theta_3, \theta_4) = (-4,-2,4,3)$, whereas the unknown parameters for Figure 4.11 are taken as $(\theta_1, \theta_2, \theta_3, \theta_4) = (4,-3,-2,1)$. As can be seen from the simulation results, all the system states converge to zero for both systems with perturbations and the estimates of θ_i, $i = 1, \cdots, 4$ converge to their actual values, thus validating the correctness of the applied algorithm.

4.5   Summary

In this chapter, different forms of FONHS are considered and proposed algorithms are applied under various conditions to prove the robustness of the control methodologies. The effectiveness of the proposed technique is verified through simulation studies. The chapter also presents a robust method for stabilization of nonholonomic AUVs affected with uncertainties. The importance of this research is further highlighted by the fact that the proposed methodology is general and can be applied to other nonholonomic mechanical systems such as wheeled mobile robots (WMRs), helicopters, Vertical Take Off and Landing (VTOL) aircraft, robotic manipulators and surface vehicles. At the same time, the proposed methodology provides robustness for the whole state space as the reaching phase is eliminated because of integral SMC.
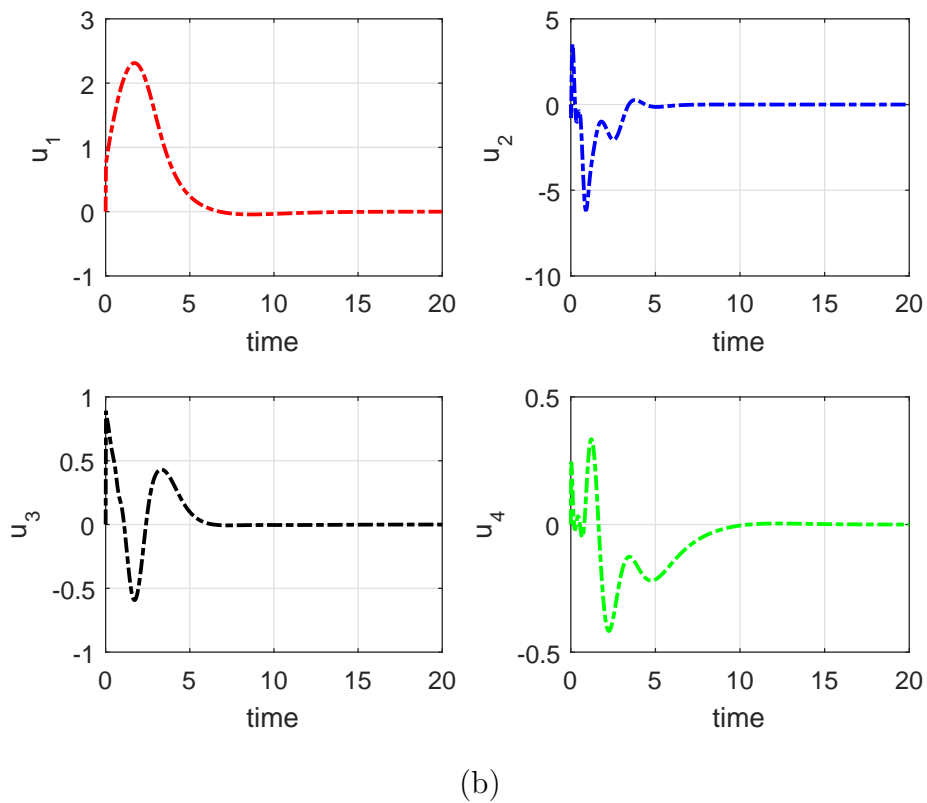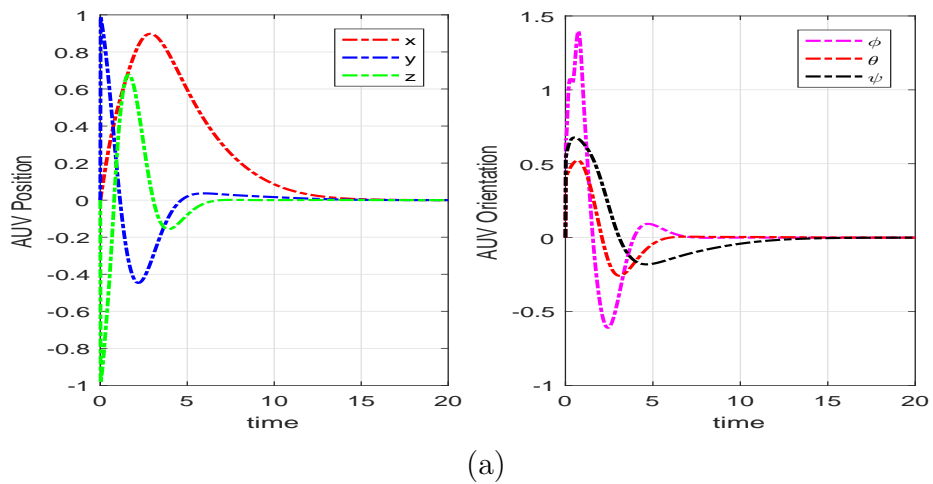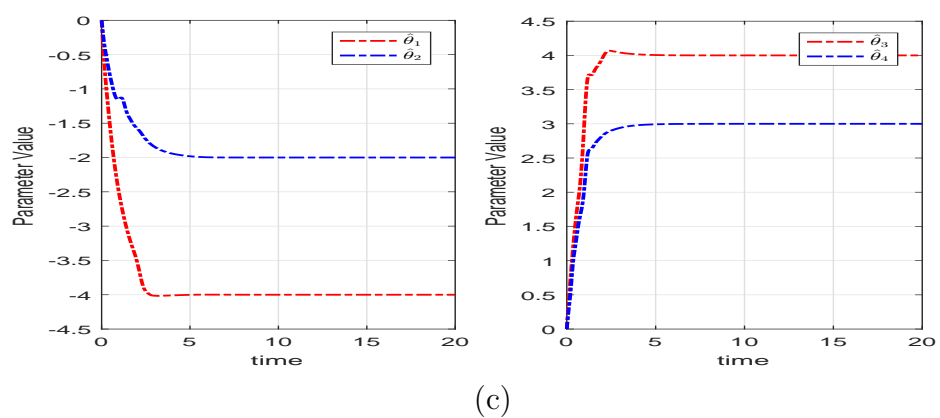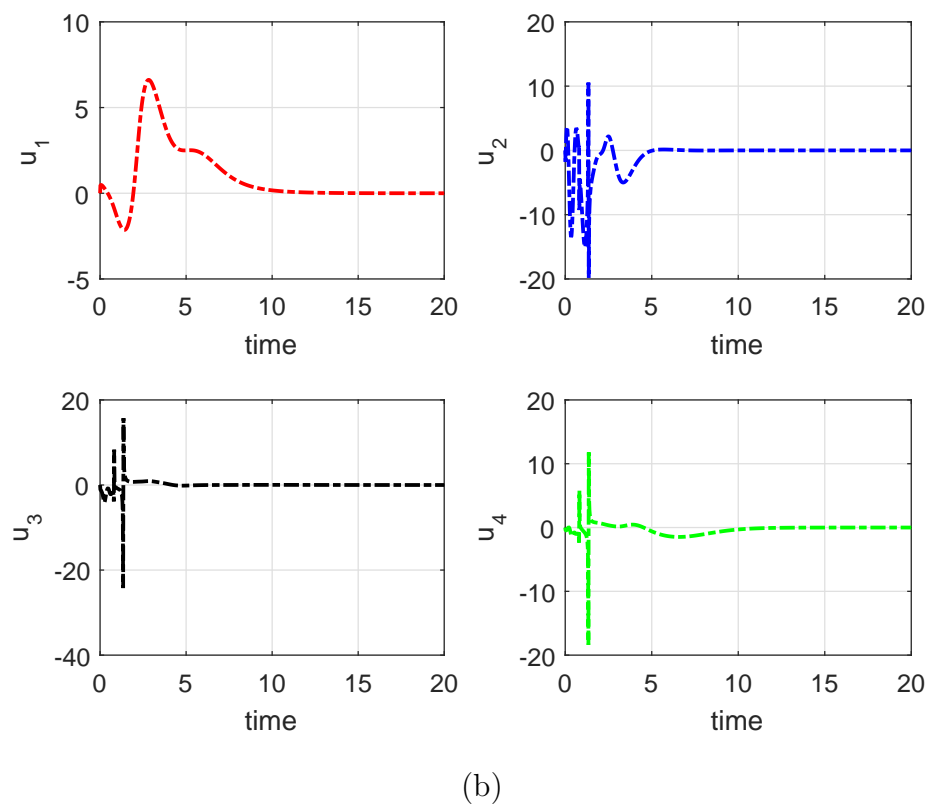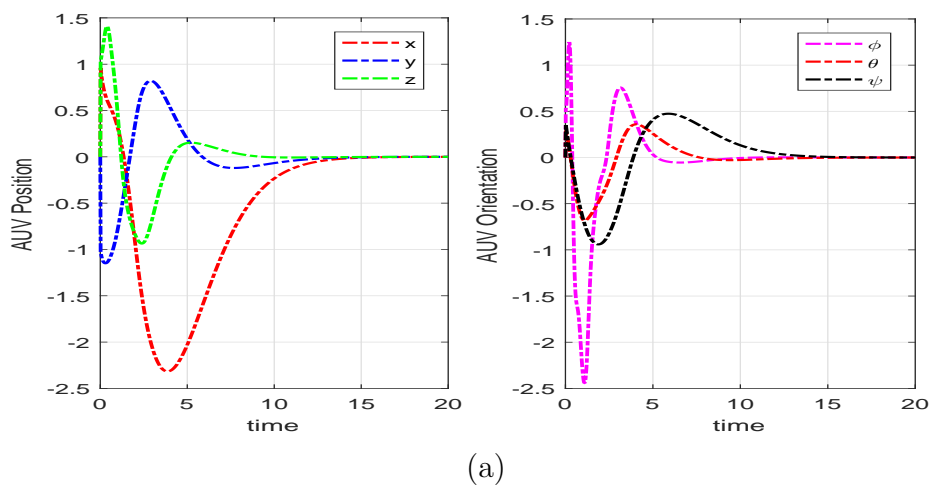
FIGURE 4.11: System Trajectory with perturbation in system model (a) System states corresponding to initial condition (1,-1,1,π /6,π /10,π /8) (b) Control effort (c) Estimated values of parameters $\theta_i, i = 1, ..., 4$

Chapter 5

Stabilization of Second-Order Perturbed Nonholonomic Systems in Chained Form

This chapter presents novel solutions to the problem of stabilizing nonholonomic systems that are expressed in canonical chained form. The methodologies are based on adaptive ISMC. Firstly, the chained form system is converted into a special structure, comprising nominal portion and unknowns through input transformation. Then the transformed system is stabilized using ISMC control and the unknown terms are computed adaptively. The controller for the transformed system consists of nominal and compensator control. The proposed method is tested on two different second-order nonholonomic systems including a 3-DOF manipulator and a planar PPR manipulator model. Subsequently, perturbations are included in the control input and robust stabilizing algorithm is developed in order to overcome the uncertainties. The performance of the proposed methods is verified through simulations.

5.1   Second-Order Nonholonomic Systems

During the last couple of decades, most of the publications in the literature on non-holonomic systems have been on mechanical systems with first-order nonholonomic constraints. Only recently, the underactuated systems with second-order nonholonomic constraints have received the attention of researchers. In [97], the authors discovered a class of UMS with second-order nonholonomic constraints. The underactuated robot manipulators, Autonomous Underwater Vehicles (AUVs), underactuated surface vessels and the planar vertical take-off and landing aircraft are examples of underactuated systems belonging to this class [97]. The main difference between the two types is that the second-order nonholonomic systems include drift terms that make control of these much more difficult. Whereas, in general, the second-order nonholonomic systems also do not satisfy Brockett's necessary condition for smooth time-invariant stabilizing static state-feedback [7] similar to the first-order nonholonomic systems.

5.2   Second-Order Chained Form Systems

A special canonical form called the second-order chained form system is defined as:

$$
\begin{aligned}
\ddot{y}_1 &= v_1 \\
\ddot{y}_2 &= v_2 \\
\ddot{y}_3 &= y_2 v_1
\end{aligned}
\tag{5.1}
$$

This second-order chained form plays the same role for the second-order nonholonomic systems as the simple chained form system for the first-order nonholonomic systems. Thus, the dynamics of second-order chained form system are considerably simplified and, therefore, easier to control. It is well known that a class of UMS can be transformed to second-order canonical form (5.1) by constructing

input and coordinate transformations [11]. Systems that can be transformed into the second-order chained form include: an underactuated planar horizontal 3-link serial-drive PPR manipulator (PPR means two prismatic and one revolute joint), an underactuated planar horizontal PPR manipulator with a spring-coupled third link, an underactuated planar horizontal 3-link serial-drive RRR manipulator, a manipulator driven by end-effector forces, an underactuated planar horizontal parallel drive RRR manipulator with any two joints unactuated, a planar rigid body with an unactuated DOF, an underactuated surface vessel [8] etc.

5.3 Problem Formulation : Unperturbed Case

5.3.1 Dynamic Model of a Second-Order Nonholonomic System

Taking a general second-order nonholonomic system described as:

$$D(q)\ddot{q} + C(q,\dot{q})\dot{q} + G(q) = F(q)u \tag{5.2}$$

where $q \in \mathbb{R}^n$ is the configuration vector, $D(q) \in \mathbb{R}^{n \times n}$ is inertia matrix which is positive definite symmetric matrix, $C(q,\dot{q})\dot{q} \in \mathbb{R}^n$ are the Centrifugal and Coriolis terms and $G(q)$ is the gravity term. Assuming $F(q) = \begin{bmatrix} I_m & 0 \end{bmatrix}^T$ and $u \in \mathbb{R}^m$ is the actuator input vector in above (5.2).

5.3.2 The Stabilization Problem

Given a desired set point $z_{des} = \begin{bmatrix} q_{des} \\ \dot{q}_{des} \end{bmatrix} \in \mathbb{R}^{2n}$, design feedback controller $u(q,\dot{q})$ such that the desired set point z_{des} is an attractive set for system (5.2), such that there exists an $\varepsilon > 0$ and $z(t;\ t_0,\ z_0) \to z_{des},\ as\ t \to \infty$ for any $(t_0,\ q_0) \in \mathbb{R}^+ \times B(z_{des};\varepsilon)$.

The stabilization problem is solved by converting the system (5.2) into the second-order chained form (5.1).

5.3.3 Adaptive ISMC

The SMC has attracted the attention of researchers in recent years due to its simplicity, fast response and robustness to external noise ([98], [99], [100]). Properties of the SMC just depend on the design of the switching surface and have nothing to do with external interferences [101]. The two phases of the SMC are the reaching phase and the sliding phase. During the reaching phase, the system has no insensitivity property. Whereas during the sliding phase the system trajectory is forced to slide on the sliding surface. The system response depends on the parameters of the surface and remains insensitive to parameter variations and external disturbances.

ISMC guarantees the robustness of motion in the whole state space ([100], [101]) because of elimination of the reaching phase. The robustness of the system, therefore, can be guaranteed throughout the system response starting from the initial time instance. The integral sliding mode control combines the nominal control that stabilizes the nominal system and a discontinuous control that rejects the uncertainty. In this research, adaptive algorithms based on Lyapunov theory are developed with ISMC in order to provide the solution for the whole state-space.

5.3.3.1 Proposed Algorithm : Method-1

Step 1: Define

$$Y = \begin{bmatrix} y_1 & y_2 & y_3 \end{bmatrix}^T \text{ and } \dot{Y} = \begin{bmatrix} \dot{y}_1 & \dot{y}_2 & \dot{y}_3 \end{bmatrix}^T$$

as the state vector. Now, using the new state vector, the second-order form system (5.1) can be stated as:

$$\ddot{Y} = \begin{bmatrix} 1 \\ 0 \\ y_2 \end{bmatrix} v_1 + \begin{bmatrix} 0 \\ 1 \\ 0 \end{bmatrix} v_2 = g_1(Y)v_1 + g_2(Y)v_2 \tag{5.3}$$

where,

$$g_1(Y) = \begin{bmatrix} 1 & 0 & y_2 \end{bmatrix}^T \text{and } g_2(Y) = \begin{bmatrix} 0 & 1 & 0 \end{bmatrix}^T$$

Step 2: Compute the Lie bracket

$$g_3(Y) = [g_1(Y), g_2(Y)] = \begin{bmatrix} 0 & 0 & 1 \end{bmatrix}^T.$$

Now, by adding and subtracting $g_3(Y)v_3$, the system (5.3) can be stated as:

$$\ddot{Y} = g_1(Y)v_1 + g_2(Y)v_2 + g_3(Y)v_3 - g_3(Y)v_3 = Gw - v \tag{5.4}$$

where, $G = \begin{bmatrix} 1 & 0 & 0 \\ 0 & 1 & 0 \\ y_2 & 0 & 1 \end{bmatrix}$, $w = \begin{bmatrix} v_1 \\ v_2 \\ v_3 \end{bmatrix}$ and $v = \begin{bmatrix} 0 \\ 0 \\ v_3 \end{bmatrix}$.

Now, assume that v is unknown and can be computed adaptively. Let $\hat{v}$ be estimate of v and $\tilde{v} = v - \hat{v}$ be error in the estimation. Then, (5.4) can be written as:

$$\ddot{Y} = Gw - \hat{v} - \tilde{v} \tag{5.5}$$

Step 3: Take first part of system (5.5) as the nominal system and use subscript form w_0 for the nominal input, we get:

$$\ddot{Y} = G w_0 \tag{5.6}$$

Choose the sliding surface for the nominal system (5.6) as:

$$S_0 = \begin{bmatrix} s_{01} \\ s_{02} \\ s_{03} \end{bmatrix} = 2Y + \dot{Y}$$

Then,

$$\dot{S}_0 = 2\dot{Y} + \ddot{Y} = 2\dot{Y} + Gw_0$$

and the choice of

$$w_0 = -G^{-1}(2\dot{Y} + kS_0) \tag{5.7}$$

gives $\dot{S}_0 = -kS_0$. Now take $V = \frac{1}{2}S_0^T S_0$ as a Lyapunov function for (5.6), which makes $\dot{V} = S_0^T \dot{S}_0 = -k\, S_0^T S_0 < 0$. Thus, the nominal system (5.6) is asymptotically stable.

Step 4: Now, consider complete system (5.5). Choose $w = w_0 + w_s$, where w_0 is the nominal control given at (5.7) and w_s is the switching control designated as compensator control that is determined during next step. Also, define the sliding surface as $S = S_0 + R$, where $R = \begin{bmatrix} r_1 \\ r_2 \\ r_3 \end{bmatrix}$ is the integral vector term. Then,

$$\dot{S} = \dot{S}_0 + \dot{R} = 2\dot{Y} + Gw_0 + Gw_s - \hat{v} - \tilde{v} + \dot{R} \tag{5.8}$$

Step 5: By choosing a Lyapunov function $V = \frac{1}{2}S^T S + \frac{1}{2}\tilde{v}^T \Gamma \tilde{v}$, where, Γ is a 3×3 positive diagonal matrix, design the input w_s and the adaptive laws for $\tilde{v}$ and $\hat{v}$ such that $\dot{V} < 0$.

Theorem 5.1: *Consider a Lyapunov function* $V = \frac{1}{2}S^T S + \frac{1}{2}\tilde{v}^T \Gamma \tilde{v}$. *Then* $\dot{V} < 0$ *if the input* w_s *and the adaptive laws for* $\tilde{v}$ *and* $\hat{v}$ *are chosen as:*

$$\dot{R} = -2\dot{Y} - Gw_0$$

$$w_s = G^{-1}(\hat{v} - k\,\text{sgn}(S)), \quad k > 0 \tag{5.9}$$

$$\dot{\tilde{v}} = \Gamma^{-1}(S - \Gamma\tilde{v}), \quad \dot{\hat{v}} = -\dot{\tilde{v}}$$

Proof. Since

$$\dot{V} = S^T \dot{S} + \tilde{v}^T \Gamma \dot{\tilde{v}} = S^T(2\dot{Y} + Gw_0 + Gw_s - \hat{v} - \tilde{v} + \dot{R}) + \tilde{v}^T \Gamma \dot{\tilde{v}}$$

$$= S^T(2\dot{Y} + Gw_0 + Gw_s - \hat{v} + \dot{R}) + \tilde{v}^T(\Gamma\dot{\tilde{v}} - S)$$

By using,

$$\dot{R} = -2\dot{Y} - Gw_0$$

$$w_s = G^{-1}(\hat{v} - k\,\text{sgn}(S)), \quad k > 0$$

$$\dot{\tilde{v}} = \Gamma^{-1}(S - \Gamma\tilde{v}), \quad \dot{\hat{v}} = -\dot{\tilde{v}}$$

we have, $\dot{V} = -k\,S^T S - \tilde{v}^T \Gamma \tilde{v} < 0.$ □

From this we conclude that S and $\tilde{v} \to 0$. Since $S = \begin{bmatrix} s_1 \\ s_2 \\ s_3 \end{bmatrix} = \begin{bmatrix} 2y_1 + y_4 \\ 2y_2 + y_5 \\ 2y_3 + y_6 \end{bmatrix} \to 0$,

$2y_1 + y_4$, $2y_2 + y_5$ and $2y_3 + y_6$ are Hurwitz polynomial, therefore, y_i , $i = 1, .., 6 \to 0$.

5.3.3.2 Proposed Algorithm : Method-2

Step 1: Define the state vector

$$x = \begin{bmatrix} x_1 = y_1 & x_2 = \dot{y}_1 & x_3 = y_3 & x_4 = \dot{y}_3 & x_5 = y_2 & x_6 = \dot{y}_2 \end{bmatrix}^T$$

Now, the second-order chained form system (5.1) can be written in state-space form as:

$$\dot{x}_1 = x_2$$
$$\dot{x}_2 = v_1$$
$$\dot{x}_3 = x_4 \qquad\qquad (5.10)$$
$$\dot{x}_4 = x_5 v_1$$
$$\dot{x}_5 = x_6$$
$$\dot{x}_6 = v_2$$

Step 2: Transform system (5.10) into the following form by choosing $v_1 = x_3$ and $v_2 = v$, where v is the new input:

$$\dot{x}_i = x_{i+1} \quad i = 1, 2, 3$$
$$\dot{x}_4 = x_5 x_3 \qquad\qquad (5.11)$$
$$\dot{x}_5 = x_6$$
$$\dot{x}_6 = v$$

Now, write system (5.11) as:

$$\dot{x}_i = x_{i+1} \quad i = 1, 2, 3$$
$$\dot{x}_4 = x_5 + F \qquad\qquad (5.12)$$
$$\dot{x}_5 = x_6$$
$$\dot{x}_6 = v$$

where $F = -x_5 + h(x)$ and $h(x) : \mathbb{R}^n \times \mathbb{R}^m \to \mathbb{R}$ is a nonlinear function.

Step 3: Assume that F is the uncertainty in chained form system and let $\hat{F}$ be an estimate of F and $\tilde{F} = F - \hat{F}$. Now apply function approximation technique presented in [102] to represent F and the estimate $\hat{F}$ as $F = w^T \phi(t)$ and $\hat{F} = \hat{w}^T \phi(t)$

respectively. Here we have $\phi(t) = [\phi_1(t) \cdots \phi_n(t)]^T$ as basis vector function and $w(t) = [w_1(t) \cdots w_n(t)]^T$ as weight vector. Let $\hat{w}$ be an estimate of w. Then we can estimate F by estimating the weight vector as $\hat{F} = \hat{w}^T \phi(t)$. Define $\tilde{w} = w - \hat{w}$, then system (5.12) can be written as:

$$
\begin{aligned}
\dot{x}_i &= x_{i+1} \quad i = 1, 2, 3 \\
\dot{x}_4 &= x_5 + \hat{w}^T(t)\phi(t) + \tilde{w}^T(t)\phi(t) \\
\dot{x}_5 &= x_6 \\
\dot{x}_6 &= v
\end{aligned}
\tag{5.13}
$$

Step 4: Select the nominal system for (5.13) as:

$$
\begin{aligned}
\dot{x}_i &= x_{i+1}, \ i = 1, \cdots, 5 \\
\dot{x}_6 &= v_0
\end{aligned}
\tag{5.14}
$$

Step 5: Now, define the surface for nominal part (5.14) as

$$
s_0 = x_1 + 5x_2 + 10x_3 + 10x_4 + 5x_5 + x_6
$$

Then,

$$
\begin{aligned}
\dot{s}_0 &= \dot{x}_1 + 5\dot{x}_2 + 10\dot{x}_3 + 10\dot{x}_4 + 5\dot{x}_5 + \dot{x}_6 \\
&= x_2 + 5x_3 + 10x_4 + 10x_5 + 5x_6 + v_0
\end{aligned}
\tag{5.15}
$$

By choosing

$$
v_0 = -x_2 - 5x_3 - 10x_4 - 10x_5 - 5x_6 - k\, s_0, \ \ k > 0
$$

we get $\dot{s}_0 = -k\, s_0$. Therefore, the nominal part (5.14) is stable in asymptotic way.

Step 6: Now, define sliding surface for complete model (5.13) as:

$$s = s_0 + z = x_1 + 5x_2 + 10x_3 + 10x_4 + 5x_5 + x_6 + z \qquad (5.16)$$

where z is integral part computed afterwards. Select $z(0)$ such that $s(0) = 0$ to avoid the reaching phase. Choose $v = v_0 + v_s$, where v_0 is the nominal input and v_s is compensator term computed later. Then

$$\dot{s} = \dot{x}_1 + 5\dot{x}_2 + 10\dot{x}_3 + 10\dot{x}_4 + 5\dot{x}_5 + \dot{x}_6 + \dot{z}$$

$$= x_2 + 5x_3 + 10x_4 + 10x_5 + 10\hat{w}^T\varphi + 10\tilde{w}^T\varphi + 5x_6 + v_0 + v_s + \dot{z} \qquad (5.17)$$

Step 7: Take a Lyapunov function $V = \frac{1}{2}s^2 + \frac{1}{2}\tilde{w}^T\tilde{w}$, design the adaptive laws for $\tilde{w}$, $\hat{w}$ and compute v_s so that $\dot{V} < 0$.

Theorem 5.2: *Consider a Lyapunov function $V = \frac{1}{2}s^2 + \frac{1}{2}\tilde{w}^T\tilde{w}$. Then $\dot{V} < 0$ if the adaptive laws for $\tilde{w}$, $\hat{w}$ and the value of v_s are chosen as:*

$$\dot{z} = -x_2 - 5x_3 - 10x_4 - 10x_5 - 5x_6 - v_0,$$

$$v_s = -10\hat{w}^T\varphi - k\,\mathrm{sgn}(s)$$

$$\dot{\tilde{w}} = -10s\varphi - k_1\,\tilde{w}\ ,\dot{\hat{w}} = -\dot{\tilde{w}},\ \ k, k_1 > 0$$

Proof. Since

$$\dot{V} = s\dot{s} + \tilde{w}^T\dot{\tilde{w}}$$

$$= s(x_2 + 5x_3 + 10x_4 + 10x_5 + 10\hat{w}^T\varphi + 10\tilde{w}^T\varphi + 5x_6 + v_0 + v_s + \dot{z}) + \tilde{w}^T\dot{\tilde{w}}$$

$$= s(x_2 + 5x_3 + 10x_4 + 10x_5 + 10\hat{w}^T\varphi + 5x_6 + v_0 + v_s + \dot{z}) + \tilde{w}^T(\dot{\tilde{w}} + 10s)$$

By using,

$$\dot{z} = -x_2 - 5x_3 - 10x_4 - 10x_5 - 5x_6 - v_0, \quad v_s = -10\hat{w}^T\varphi - k\,\mathrm{sgn}(s)$$

$$\dot{\tilde{w}} = -10s\varphi - k_1\,\tilde{w}$$

$$\dot{\hat{w}} = -\dot{\tilde{w}}, \quad k,\ k_1 > 0$$

we have, $\dot{V} = -\,k\,s\,\mathrm{sgn}(s) - k_1\tilde{w}^T\tilde{w} < 0.$ □

From this we conclude that $s,\ \tilde{w} \to 0$. Since $s \to 0$, therefore $x \to 0$.

In the following section, the above algorithm is applied on two different second-order nonholonomic mechanical systems which are first transformed to second-order chained form systems.

5.3.4 Application Example : 3-DOF Manipulator with a Free Link
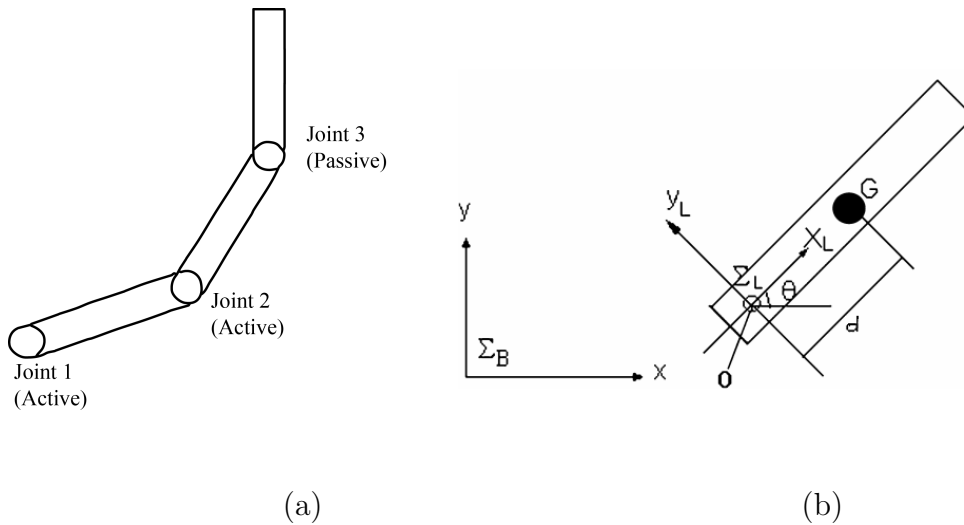

(a)

(b)

FIGURE 5.1: (a) 3-DOF Manipulator with a Free Joint. (b) Model of Passive Link.

Figure 5.1 shows a 3-DOF manipulator in horizontal plane. The manipulator has first two prismatic joints that are active and these control the third unactuated joint. It is assumed that the third free joint is a revolute around the vertical axis.

Assign the coordinate frames Σ_B, Σ_L, θ, (x, y) as given in [10]. The generalized coordinates representing the manipulator configuration are given as (x, y, θ). Therefore, the equations of motion according to the third link are given as [10]:

$$f_x = m\ddot{x} - md\ddot{\theta}\sin\theta - md\dot{\theta}^2\cos\theta$$
$$f_y = m\ddot{y} + md\ddot{\theta}\cos\theta - md\dot{\theta}^2\sin\theta \qquad (5.18)$$
$$0 = -md\ddot{x}\sin\theta + md\,\ddot{y}\cos\theta + (I + md^2)\ddot{\theta}$$

where I is the moment of inertia of third link around G, m is the mass of third link, $[f_x, f_y]$ is the translation force and d is the distance $|OG|$ between the center of gravity and the joint.

By denoting $\lambda = d + I/md$, the system constraint becomes:

$$-\ddot{x}\sin\theta + \ddot{y}\cos\theta + \lambda\ddot{\theta} = 0 \qquad (5.19)$$

The acceleration translational direction of joint 3, i.e. $(\ddot{x}, \ddot{y})$, is taken as input to the system (5.18). It is a second-order nonholonomic system as the constraint (5.19) does not have the first integral [10].

5.3.4.1 Conversion into Second-Order Chained Form

Let $\ddot{x} = \xi_1$, $\ddot{y} = \xi_2$. Then, (5.19) can be written as:

$$\ddot{x} = \xi_1$$
$$\ddot{y} = \xi_2 \qquad (5.20)$$
$$\ddot{\theta} = \frac{1}{\lambda}\sin\theta\,\xi_1 - \frac{1}{\lambda}\cos\theta\,\xi_2$$

Using the input transformation

$$\xi_1 = w_1$$

$$\xi_2 = \tan\theta\, w_1 - \lambda\sec\theta\, w_2 \qquad (5.21)$$

the system (5.20) can be transformed as:

$$\ddot{x} = w_1$$

$$\ddot{\theta} = w_2 \qquad (5.22)$$

$$\ddot{y} = \tan\theta\, w_1 - \lambda\sec\theta\, w_2$$

Using another transformation

$$y_1 = x + \lambda\cos\theta$$

$$y_2 = \tan\theta$$

$$y_3 = y + \lambda\sin\theta \qquad (5.23)$$

$$v_1 = w_1 - \lambda\sin\theta\, w_2 - \lambda\cos\theta\, \dot{\theta}^2$$

$$v_2 = \sec^2\theta\, w_2 + 2\sec^2\theta\, \tan\theta\, \dot{\theta}^2$$

where $y_i, i = 1, 2, 3$ are new coordinate variables and $v_1, \ v_2$ are new inputs, then, we have the following second-order chained form system:

$$\ddot{y}_1 = v_1$$

$$\ddot{y}_2 = v_2 \qquad (5.24)$$

$$\ddot{y}_3 = y_2 v_1$$

After applying the proposed algorithm on system (5.24), we get a stabilized non-holonomic system. Simulation results are presented with different initial conditions in the subsection below.

TABLE 5.1: Parameter Values for 3-Link Planar Model.

Parameter	Value
m	$1\ Kg$
I	$5/6\ Kgm^2$
d	$0.5\ m$

5.3.4.2 Simulation Results

After applying the proposed algorithm on system (5.24), the obtained simulation results are shown in Figs 5.2 - 5.3 for the original system. The chosen values of the parameters m, I and l are kept the same as given in [11] and are shown in Table 5.1.

The simulation results are presented for different initial conditions. Figure 5.2 shows the system states $(q(t), \dot{q}(t))$ and the corresponding control (f_x, f_y) for the initial condition (-2,2,-π/3,0,0,0). Similarly, Figure 5.3 shows the system states $(q(t), \dot{q}(t))$ and the corresponding control (f_x, f_y) for (0,0,π/6,0,0,0). The objective was to steer all the system states to zero in the simulations. It can easily be seen from the simulation results that with less control effort similar results are obtained; hence, proving the efficiency of the proposed algorithm.

5.3.5 Application Example : Planar PPR Manipulator

Consider a PPR robot as shown in Figure 5.4. For simplicity, consider that the robot is moving in a horizontal plane. All the joints of the robot are passive and the input forces are applied on the end-effector only. Let d_3 be the distance between mass center of 3rd link and the joint axis, l_3 the length of third link, m_i the mass of the ith link and I_3 the central moment of inertia.

The dynamical model of the robot [103] is:

$$M(q_3)\ddot{q} + H(q_3, \dot{q}_3) = J^T(q_3)F \tag{5.25}$$
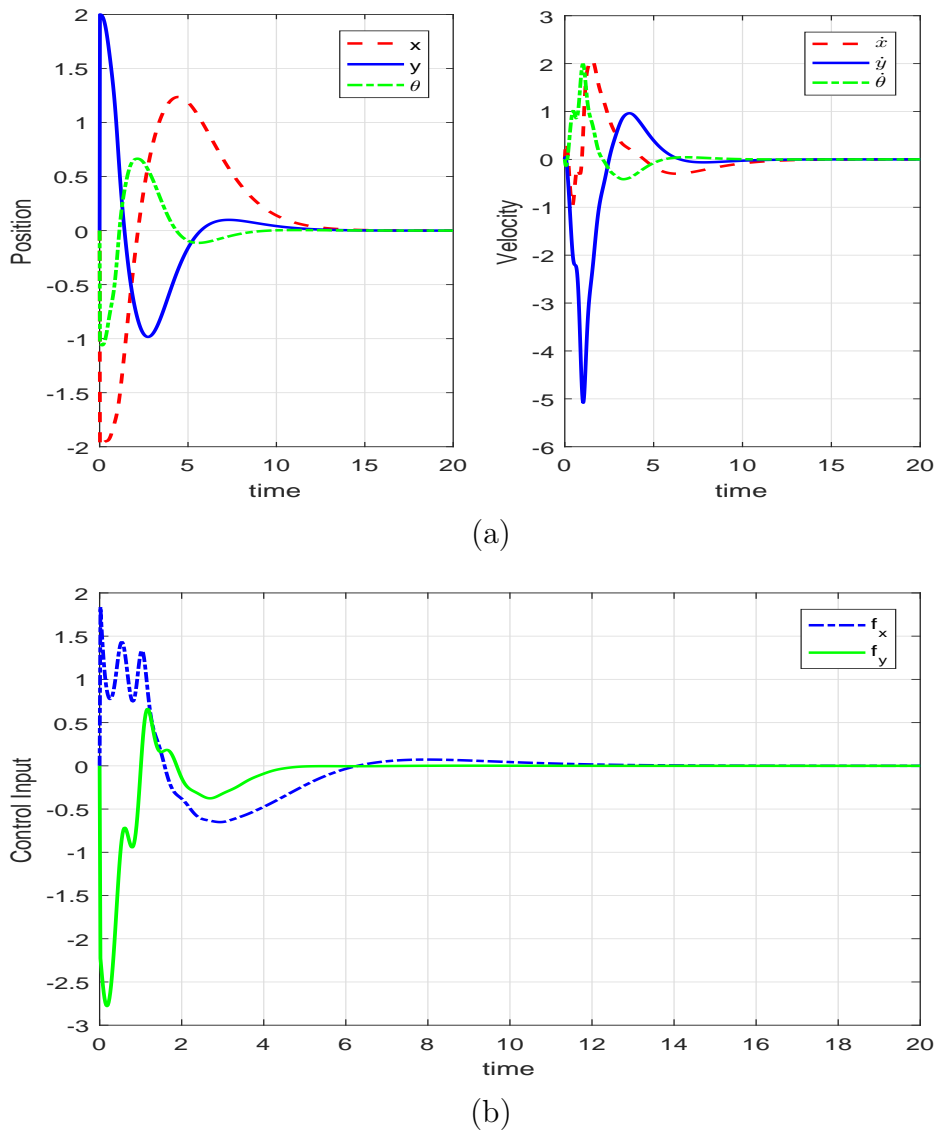
FIGURE 5.2: 3-DOF Manipulator with one Passive Joint (a) States $(q(t), \dot{q}(t))$
corresponding to $(-2,2,-\pi/3,0,0,0)$ (b) Control effort (f_x, f_y)

where $F = [F_x, \ F_y]^T$ are the cartesian forces acting on the end-effector, $q_i, \ i = 1, \ 2, \ 3$ are the generalized coordinates and

$$M(q_3) = \begin{bmatrix} a_1 & 0 & a_4 c \\ 0 & a_2 & -a_4 s \\ a_4 c & -a_4 s & a_3 \end{bmatrix}, \ H(q_3, \dot{q}_3) = -a_4 \dot{q}_3^2 \begin{bmatrix} s \\ c \\ 0 \end{bmatrix} \text{ and } J(q_3) = \begin{bmatrix} 0 & 1 & -l_3 s \\ 1 & 0 & l_3 c \end{bmatrix}$$

with $a_1 = m_1 + m_2 + m_3, \ a_2 = m_2 + m_3, \ a_3 = I_3 + m_3 d_3^2, \ c = \cos q_3,$
$s = \sin q_3$ and $a_4 = m_3 d_3$
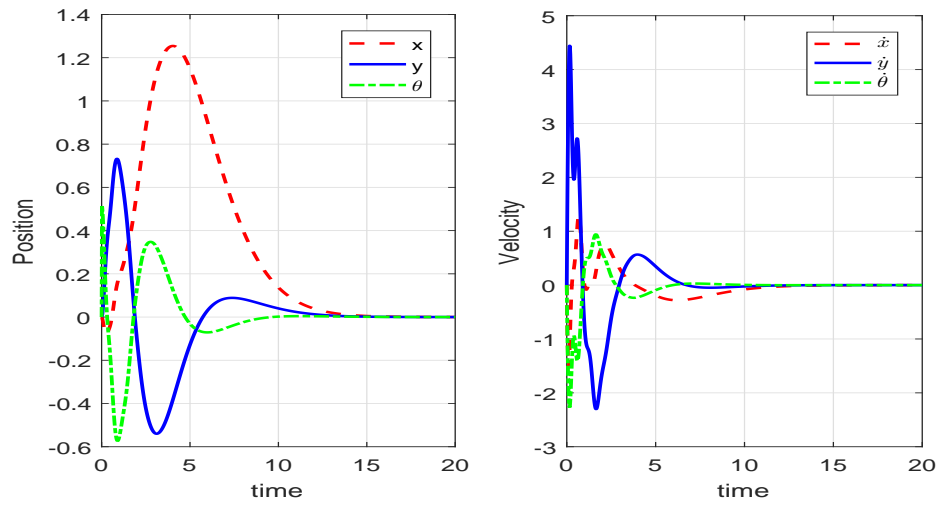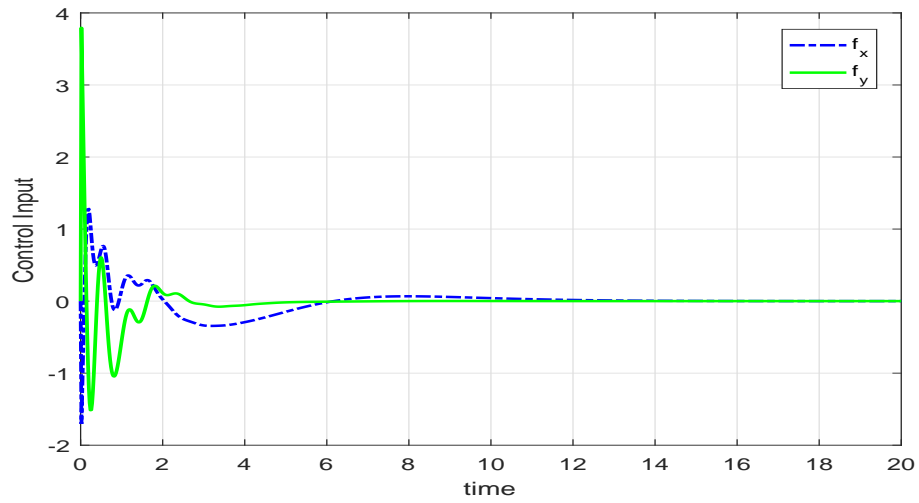
FIGURE 5.3: 3-DOF Manipulator with one Passive Joint (a) States $(q(t), \dot{q}(t))$ corresponding to $(0,0,\pi/6,0,0,0)$ (b) Control effort (f_x, f_y)

5.3.5.1 Conversion into Second-Order Chained Form

Equation (5.25) can be written as:

$$a_1\ddot{q}_1 + a_4 \cos q_3 \ddot{q}_3 - a_4 \dot{q}_3^2 \sin q_3 = F_y \tag{5.26}$$

$$a_2\ddot{q}_2 - a_4 \sin q_3 \ddot{q}_3 - a_4 \dot{q}_3^2 \cos q_3 = F_x \tag{5.27}$$

$$a_4 \cos q_3 \ddot{q}_1 - a_4 \sin q_3 \ddot{q}_2 + a_3\ddot{q}_3 = -l_3 \sin q_3 F_x + l_3 \cos q_3 F_y \tag{5.28}$$
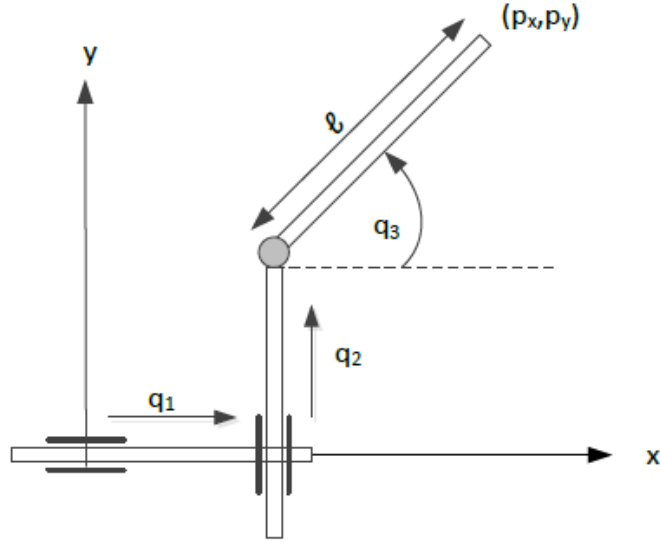
FIGURE 5.4: Planar PPR Manipulator.

After re-arranging, (5.26) gives

$$\ddot{q}_1 = -\frac{a_4}{a_1}\cos q_3 \ddot{q}_3 + \frac{a_4}{a_1}\sin q_3 \dot{q}_3^2 + \frac{1}{a_1}F_y \tag{5.29}$$

Substitute (5.29) in (5.28)

$$\ddot{q}_3 = \frac{1}{r_1}(a_2 - a_1)a_4^2 \cos q_3 \sin q_3 \dot{q}_3^2 + \frac{1}{r_1}(a_2 l_3 - a_4)a_1 \sin q_3 F_x + \frac{1}{r_1}(a_4 - a_1 l_3)a_2 \cos q_3 F_y \tag{5.30}$$

where $r_1 = a_4^2 a_2 \cos^2 q_3 + a_4^2 a_1 \sin^2 q_3 - a_1 a_2 a_3$

Again substituting (5.30) in (5.27), we get

$$\begin{aligned}\ddot{q}_2 = &\frac{1}{r_2}(a_4^2 - a_1 a_3)a_4 \cos q_3 \dot{q}_3^2 + \frac{1}{r_2}(l_3 a_1 a_4 \sin^2 q_3 + a_4^2 \cos^2 q_3 - a_1 a_3)F_x \\ &+ \frac{1}{r_2}(a_4 - a_1 l_3)a_4 \cos q_3 \sin q_3 F_y\end{aligned} \tag{5.31}$$

where $r_2 = (a_2 - a_1)a_4^2 \cos^2 q_3 + a_4^2 a_1 - a_1 a_2 a_3$

Now, substitute (5.26) and (5.27) in (5.28), we get

$$a_4 \cos q_3 \ddot{q}_1 - a_4 \sin q_3 \ddot{q}_2 + a_3 \ddot{q}_3 = -l_3 \sin q_3 (a_2 \ddot{q}_2 - a_4 \sin q_3 \ddot{q}_3 - a_4 \dot{q}_3^2 \cos q_3)$$

$$+ l_3 \cos q_3 (a_1 \ddot{q}_1 + a_4 \cos q_3 \ddot{q}_3 - a_4 \dot{q}_3^2 \sin q_3)$$

$$\ddot{q}_1 (a_4 - a_1 l_3) \cos q_3 = \ddot{q}_2 (a_4 - a_2 l_3) \sin q_3 + \ddot{q}_3 (a_4 l_3 - a_3)$$

$$\ddot{q}_1 = \ddot{q}_2 \frac{(a_4 - a_2 l_3)}{(a_4 - a_1 l_3)} \tan q_3 + \ddot{q}_3 \frac{(a_4 l_3 - a_3)}{(a_4 - a_1 l_3)} \sec q_3 \qquad (5.32)$$

By choosing

$$v_1 = \frac{1}{r_2}(a_4^2 - a_1 a_3)a_4 \cos q_3 \dot{q}_3^2 + \frac{1}{r_2}(l_3 a_1 a_4 \sin^2 q_3 + a_4^2 \cos^2 q_3 - a_1 a_3)F_x$$

$$+ \frac{1}{r_2}(a_4 - a_1 l_3)a_4 \cos q_3 \sin q_3 F_y$$

$$v_2 = \frac{1}{r_1}(a_2 - a_1)a_4^2 \cos q_3 \sin q_3 \dot{q}_3^2 + \frac{1}{r_1}(a_2 l_3 - a_4)a_1 \sin q_3 F_x$$

$$+ \frac{1}{r_1}(a_4 - a_1 l_3)a_2 \cos q_3 F_y$$

Equations (5.30), (5.31) and (5.32) reduce to the following:

$$\ddot{q}_2 = v_1$$

$$\ddot{q}_3 = v_2 \qquad (5.33)$$

$$\ddot{q}_1 = a_5 \tan q_3 v_1 + a_6 \sec q_3 v_2$$

where $a_5 = \dfrac{(a_4 - a_2 l_3)}{(a_4 - a_1 l_3)}$ and $a_6 = \dfrac{(a_4 l_3 - a_3)}{(a_4 - a_1 l_3)}$

Using the input and state transformations:

$$y_1 = q_2 - \frac{a_6}{a_5}(\cos q_3 - 1)$$

$$y_2 = a_5 \tan q_3$$

$$y_3 = q_1 - a_6 \sin q_3 \qquad (5.34)$$

$$u_1 = v_1 + \frac{a_6}{a_5} \sin q_3 v_2 + \frac{a_6}{a_5} \cos q_3 \dot{q}_3^2$$

$$u_2 = a_5 \sec^2 q_3 v_2 + 2a_5 \sec^2 q_3 \tan q_3 \dot{q}_3^2$$

TABLE 5.2: Parameter Values for Planar PPR Manipulator.

Parameter	Value
m_1	$0.5\ Kg$
m_2	$0.5\ Kg$
m_3	$1.0\ Kg$
I_3	$1.0\ Kgm^2$
d_3	$1\ m$
l_3	$2\ m$

the system (5.33) can be converted to form:

$$\ddot{y}_1 = u_1$$
$$\ddot{y}_2 = u_2 \tag{5.35}$$
$$\ddot{y}_3 = y_2 u_1$$

After applying the proposed algorithm on system (5.35), we get a stabilized non-holonomic system. Simulation results are presented with different initial conditions in the following subsection.

5.3.5.2 Results for Planar PPR Manipulator

Applying the proposed algorithm on system (5.35), the achieved simulation results are shown in Figs 6.6 - 6.7 for original system. The values of the parameters m_i, $i = 1, 2, 3$, I and l are taken from [104] and are shown in Table 5.2.

The simulations are carried out for different initial conditions. Figure 6.6 shows the system states and the corresponding control for the initial conditions (-0.5,1,$\pi/8$,0, 0,0). Also, Figure 6.7 shows the system states $(q(t), \dot{q}(t))$ and the corresponding control (f_x, f_y) for the initial condition (0.93,5.43,-0.4π,0,2.5,0). The proposed objective to steer all the system states to zero has been achieved. Also, it can be
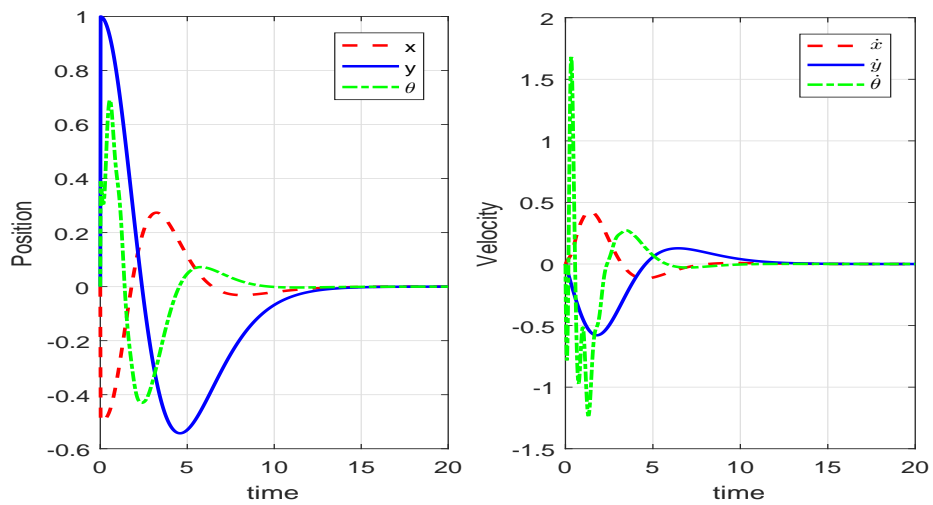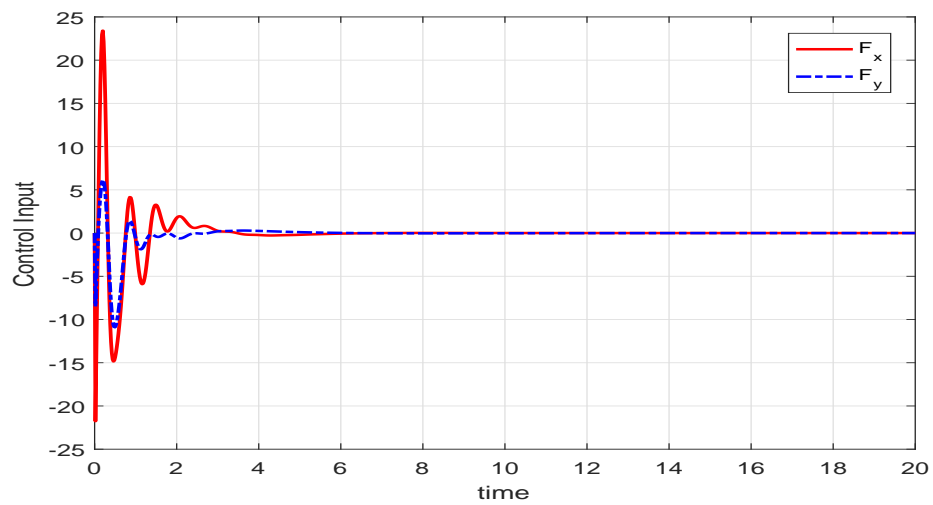
FIGURE 5.5: Planar PPR Manipulator (a) States $(q(t), \dot{q}(t))$ corresponding to (-0.5,1,$pi/8$,0,0,0) (b) Control effort (f_x, f_y)

seen that less control effort is required to achieve the desired results proving the efficiency of the proposed algorithm.
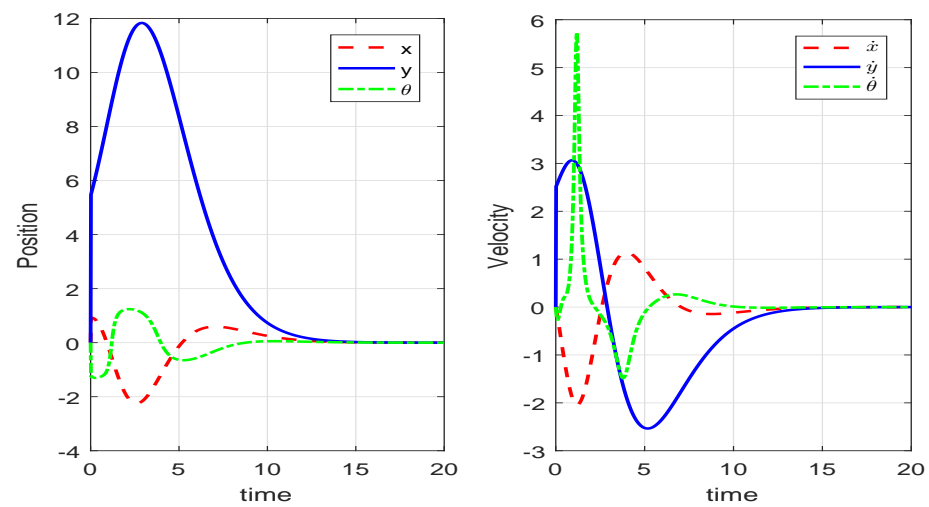
(a)
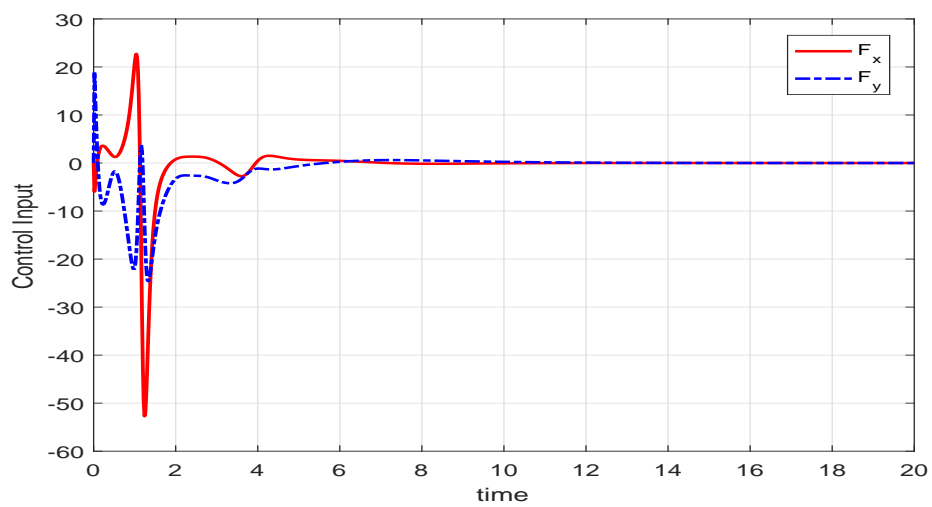
(b)

FIGURE 5.6: Planar PPR Manipulator (a) States $(q(t), \dot{q}(t))$ corresponding to $(0.93, 5.43, -0.4\pi, 0, 2.5, 0)$ (b) Control effort (f_x, f_y)

5.4 Problem Formulation : Perturbed Case

5.4.1 Dynamic Model of a Perturbed Second-Order Non-holonomic System

Consider a second-order chained form system with uncertainties in control input described as:

$$\ddot{y}_1 = v_1 + d_1$$
$$\ddot{y}_2 = v_2 + d_2 \tag{5.36}$$
$$\ddot{y}_3 = y_2 v_1 + y_2 d_1$$

where $q = [y_1 \ y_2 \ y_3]^T \in \mathbb{R}^3$ and $\dot{q} = [\dot{y}_1 \ \dot{y}_2 \ \dot{y}_3]^T \in \mathbb{R}^3$ denote the configuration vector and its derivative, $[v_1 \ v_2]^T \in \mathbb{R}^2$ is the control input vector and d_1, d_2 are unknown constant disturbances.

5.4.2 Adaptive ISMC

Integral sliding mode control (ISMC) is used in this research to stabilize perturbed second-order nonholonomic systems in chained form. ISMC guarantees the robustness of motion in the whole state space ([100], [101]) because of elimination of the reaching phase. The robustness of the system, therefore, can be guaranteed throughout the system response starting from the initial time instance. The integral sliding mode control combines the nominal control that stabilizes the nominal system and a discontinuous control that rejects the uncertainty. In this research, an adaptive algorithm based on Lyapunov theory is developed with ISMC in order to provide the solution for the whole state-space.

5.4.2.1 Proposed Algorithm

Here, in order to address the uncertainties in the input, a variant of Method-2 previously presented in Section 5.3.3. is given. The perturbed version of Method-1 can similarly be obtained with some modifications.

Let $\hat{d}_i, i = 1, 2$ be the estimate of $d_i, i = 1, 2$ respectively and let $\tilde{d}_i = d_i - \hat{d}_i$ be the estimation error. Then system (5.36) can be written as:

$$
\begin{aligned}
\ddot{y}_1 &= v_1 + \hat{d}_1 + \tilde{d}_1 \\
\ddot{y}_2 &= v_2 + \hat{d}_2 + \tilde{d}_2 \\
\ddot{y}_3 &= y_2 v_1 + y_2 \hat{d}_1 + y_2 \tilde{d}_1
\end{aligned}
\tag{5.37}
$$

Step 1: Define the state vector

$$
x = \begin{bmatrix} x_1 = y_1 & x_2 = \dot{y}_1 & x_3 = y_3 & x_4 = \dot{y}_3 & x_5 = y_2 & x_6 = \dot{y}_2 \end{bmatrix}^T
$$

Now, the second-order chained form system (5.37) can be written in state-space form as:

$$
\begin{aligned}
\dot{x}_1 &= x_2 \\
\dot{x}_2 &= v_1 + \hat{d}_1 + \tilde{d}_1 \\
\dot{x}_3 &= x_4 \\
\dot{x}_4 &= x_5 v_1 + x_5 \hat{d}_1 + x_5 \tilde{d}_1 \\
\dot{x}_5 &= x_6 \\
\dot{x}_6 &= v_2 + \hat{d}_2 + \tilde{d}_2
\end{aligned}
\tag{5.38}
$$

Step 2: Transform system (5.38) into the following form by choosing $v_1 = x_3 - \hat{d}_1$ and $v_2 = v - \hat{d}_2$, where v is the new input:

$$\dot{x}_1 = x_2$$
$$\dot{x}_2 = x_3 + \tilde{d}_1$$
$$\dot{x}_3 = x_4 \qquad\qquad (5.39)$$
$$\dot{x}_4 = x_5 x_3 + x_5 \tilde{d}_1$$
$$\dot{x}_5 = x_6$$
$$\dot{x}_6 = v + \tilde{d}_2$$

Now, write system (5.39) as:

$$\dot{x}_1 = x_2$$
$$\dot{x}_2 = x_3 + \tilde{d}_1$$
$$\dot{x}_3 = x_4 \qquad\qquad (5.40)$$
$$\dot{x}_4 = x_5 + F + x_5 \tilde{d}_1$$
$$\dot{x}_5 = x_6$$
$$\dot{x}_6 = v + \tilde{d}_2$$

where $F = -x_5 + x_5 x_3$.

Step 3: Assume that F is unknown and can be computed adaptively. Let $\hat{F}$ be an estimate of F and $\tilde{F} = F - \hat{F}$. Now apply function approximation technique presented in [102] to represent F and the estimate $\hat{F}$ as $F = w^T \phi(t)$ and $\hat{F} = \hat{w}^T \phi(t)$ respectively. Here we have $\phi(t) = [\phi_1(t) \cdots \phi_n(t)]^T$ as basis vector function and $w(t) = [w_1(t) \cdots w_n(t)]^T$ as weight vector. Let $\hat{w}$ be an estimate of w. Then we can estimate F by estimating the weight vector as $\hat{F} = \hat{w}^T \phi(t)$. Define $\tilde{w} = w - \hat{w}$,

then system (5.40) can be written as:

$$
\begin{aligned}
\dot{x}_1 &= x_2 \\
\dot{x}_2 &= x_3 + \tilde{d}_1 \\
\dot{x}_3 &= x_4 \\
\dot{x}_4 &= x_5 + \hat{w}^T(t)\phi(t) + \tilde{w}^T(t)\phi(t) + x_5\tilde{d}_1 \\
\dot{x}_5 &= x_6 \\
\dot{x}_6 &= v + \tilde{d}_2
\end{aligned}
\tag{5.41}
$$

Step 4: Choose the nominal system for (5.41) as:

$$
\begin{aligned}
\dot{x}_i &= x_{i+1}, \quad i = 1, \cdots, 5 \\
\dot{x}_6 &= v_0
\end{aligned}
\tag{5.42}
$$

Step 5: Now, taking sliding surface for nominal system (5.42) as

$$
s_0 = x_1 + 5x_2 + 10x_3 + 10x_4 + 5x_5 + x_6
$$

Then,

$$
\begin{aligned}
\dot{s}_0 &= \dot{x}_1 + 5\dot{x}_2 + 10\dot{x}_3 + 10\dot{x}_4 + 5\dot{x}_5 + \dot{x}_6 \\
&= x_2 + 5x_3 + 10x_4 + 10x_5 + 5x_6 + v_0
\end{aligned}
\tag{5.43}
$$

By choosing

$$
v_0 = -x_2 - 5x_3 - 10x_4 - 10x_5 - 5x_6 - k\,s_0, \quad k > 0
$$

we get $\dot{s}_0 = -k\,s_0$. Thus, the nominal system (5.42) is stable asymptotically.

Step 6: Furthermore, define sliding surface for complete system (5.41) as:

$$
s = s_0 + z = x_1 + 5x_2 + 10x_3 + 10x_4 + 5x_5 + x_6 + z
\tag{5.44}
$$

where z is some integral term that is computed afterwards. Choose $z(0)$ such that $s(0) = 0$ in order to avoid the reaching phase. Choose $v = v_0 + v_s$, where v_0 is the nominal term and v_s is the compensator term that is computed afterwards. Then

$$\dot{s} = \dot{x}_1 + 5\dot{x}_2 + 10\dot{x}_3 + 10\dot{x}_4 + 5\dot{x}_5 + \dot{x}_6 + \dot{z}$$

$$= x_2 + 5x_3 + 5\tilde{d}_1 + 10x_4 + 10x_5 + 10\hat{w}^T\varphi + 10\tilde{w}^T\varphi + 10x_5\tilde{d}_1 + 5x_6 \quad (5.45)$$

$$+ v_0 + v_s + \tilde{d}_2 + \dot{z} \quad (5.46)$$

Step 7: Choose a Lyapunov function $V = \frac{1}{2}s^2 + \frac{1}{2}\tilde{w}^T\tilde{w} + \frac{1}{2}\tilde{d}_1^2 + \frac{1}{2}\tilde{d}_2^2$, design the adaptive laws for $\tilde{w}$, $\hat{w}, \tilde{d}_1, \tilde{d}_2$ and compute v_s so that $\dot{V} < 0$.

Theorem 5.3: *Taking a Lyapunov function* $V = \frac{1}{2}s^2 + \frac{1}{2}\tilde{w}^T\tilde{w} + \frac{1}{2}\tilde{d}_1^2 + \frac{1}{2}\tilde{d}_2^2$. *Then* $\dot{V} < 0$ *if the adaptive laws for* $\tilde{w}$, $\hat{w}, \tilde{d}_1, \tilde{d}_2$ *and the value of* v_s *are taken as:*

$$\dot{z} = -x_2 - 5x_3 - 10x_4 - 10x_5 - 5x_6 - v_0, \quad v_s = -10\hat{w}^T\varphi - k\,\mathrm{sgn}(s)$$

$$\dot{\tilde{w}} = -10s\varphi - k_1\tilde{w}, \ \dot{\hat{w}} = -\dot{\tilde{w}}$$

$$\dot{\tilde{d}}_1 = -5s - 10sx_5 - k_2\tilde{d}_1, \ \dot{\hat{d}}_1 = -\dot{\tilde{d}}_1$$

$$\dot{\tilde{d}}_2 = -s - k_3\tilde{d}_2, \ \dot{\hat{d}}_2 = -\dot{\tilde{d}}_2, \quad k, \ k_i > 0, \ i = 1, 2, 3$$

Proof. Since

$$\dot{V} = s\dot{s} + \tilde{w}^T\dot{\tilde{w}} + \tilde{d}_1\dot{\tilde{d}}_1 + \tilde{d}_2\dot{\tilde{d}}_2$$

$$= s(x_2 + 5x_3 + 5\tilde{d}_1 + 10x_4 + 10x_5 + 10\hat{w}^T\varphi + 10\tilde{w}^T\varphi + 10x_5\tilde{d}_1 + 5x_6 + v_0$$

$$+ v_s + \tilde{d}_2 + \dot{z}) + \tilde{w}^T\dot{\tilde{w}} + \tilde{d}_1\dot{\tilde{d}}_1 + \tilde{d}_2\dot{\tilde{d}}_2$$

$$= s(x_2 + 5x_3 + 10x_4 + 10x_5 + 10\hat{w}^T\varphi + 5x_6 + v_0 + v_s + \tilde{d}_2 + \dot{z})$$

$$+ \tilde{w}^T(\dot{\tilde{w}} + 10s\varphi) + \tilde{d}_1(\dot{\tilde{d}}_1 + 5s + 10sx_5) + \tilde{d}_2(\dot{\tilde{d}}_2 + s)$$

By using,

$$\dot{z} = -x_2 - 5x_3 - 10x_4 - 10x_5 - 5x_6 - v_0, \quad v_s = -10\hat{w}^T\varphi - k\,\mathrm{sgn}(s)$$

$$\dot{\hat{w}} = -10s\varphi - k_1\tilde{w}, \;\; \dot{\hat{w}} = -\dot{\tilde{w}}$$

$$\dot{\hat{d}}_1 = -5s - 10sx_5 - k_2\tilde{d}_1, \;\; \dot{\hat{d}}_1 = -\dot{\tilde{d}}_1$$

$$\dot{\hat{d}}_2 = -s - k_3\tilde{d}_2, \;\; \dot{\hat{d}}_2 = -\dot{\tilde{d}}_2, \quad k, \; k_i > 0, \; i = 1,2,3$$

we have, $\dot{V} = -k\,s\,\mathrm{sgn}(s) - k_1\tilde{w}^T\tilde{w} - k_2\tilde{d}_1^{\,2} - k_3\tilde{d}_2^{\,2} < 0.$ $\qquad\square$

From this we conclude that $s,\; \tilde{w} \to 0$. Since $s \to 0$, therefore $x \to 0$.

In the following section, the above algorithm is applied on second-order perturbed nonholonomic mechanical systems that are first transformed to second-order chained form systems.

5.4.3 Application Examples

After applying the proposed algorithm on 3-DOF manipulator with a passive joint and PPR manipulator, we get following results.

5.4.3.1 Simulation Results : 3-DOF Manipulator with a Passive Joint

After applying the proposed algorithm on system (5.24), the obtained simulation results are shown in Figs 5.2 - 5.3 for the original system. The chosen values of the parameters m, I and l are kept the same as used in Section 5.3.4.

The simulation results are presented for the initial condition (-2,2,-π/3,0,0,0). Figure 5.7 shows the system states $(q(t), \dot{q}(t))$ and the corresponding control (f_x, f_y) The objective was to steer all the system states to zero in the simulations.
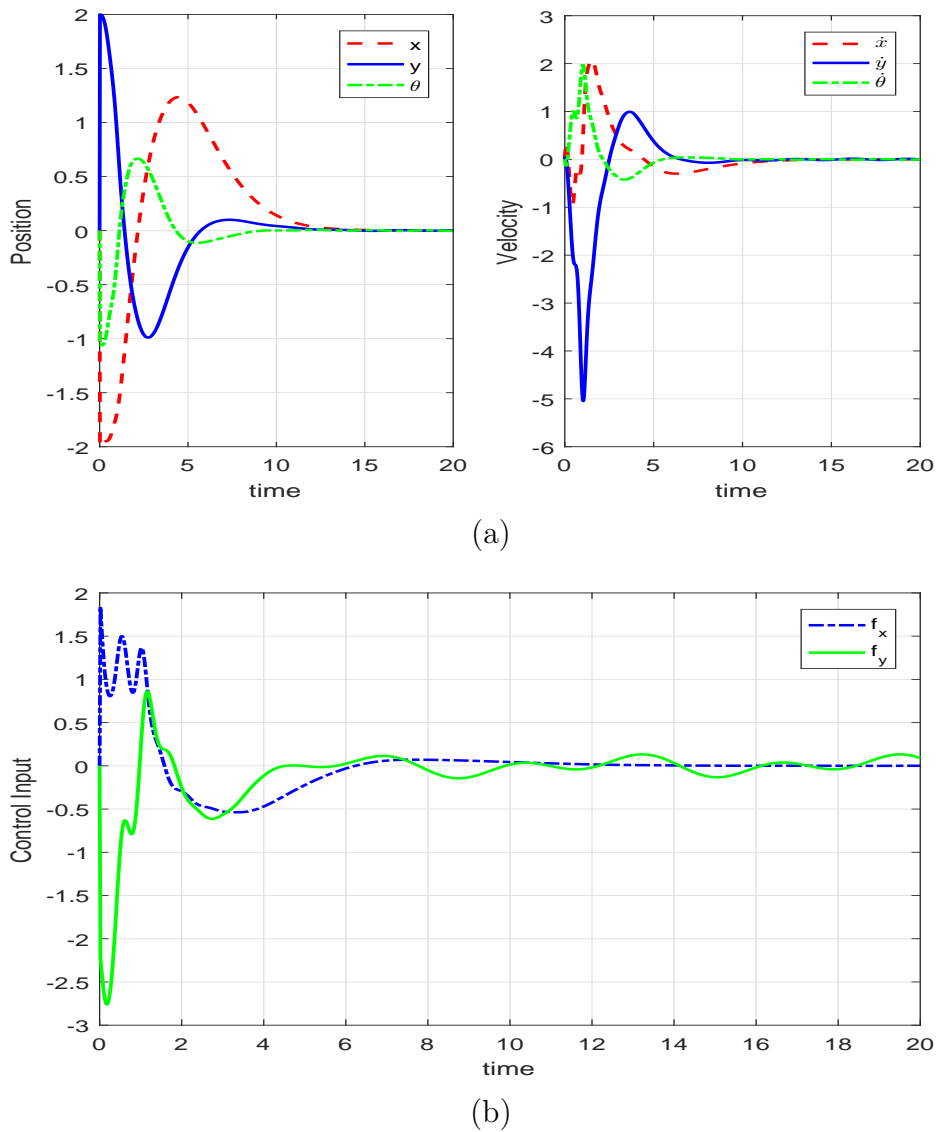
FIGURE 5.7: 3-DOF Manipulator with one Passive Joint (a) States $(q(t), \dot{q}(t))$ corresponding to (-2,2,-π/3,0,0,0) (b) Control effort (f_x, f_y)

5.4.3.2 Simulation Results : Planar PPR Manipulator

Applying the proposed algorithm on system (5.35), the achieved simulation results are shown in Figs 5.8 for original system. The values of the parameters m_i, $i = 1, 2, 3$, I and l are taken from [103] and are shown in Table 5.2.

The simulations are carried out for different initial conditions. Figure 5.8 shows the system states and the corresponding control for the initial conditions (2,-2,π/4,0,0,0). The proposed objective to steer all the system states to zero has
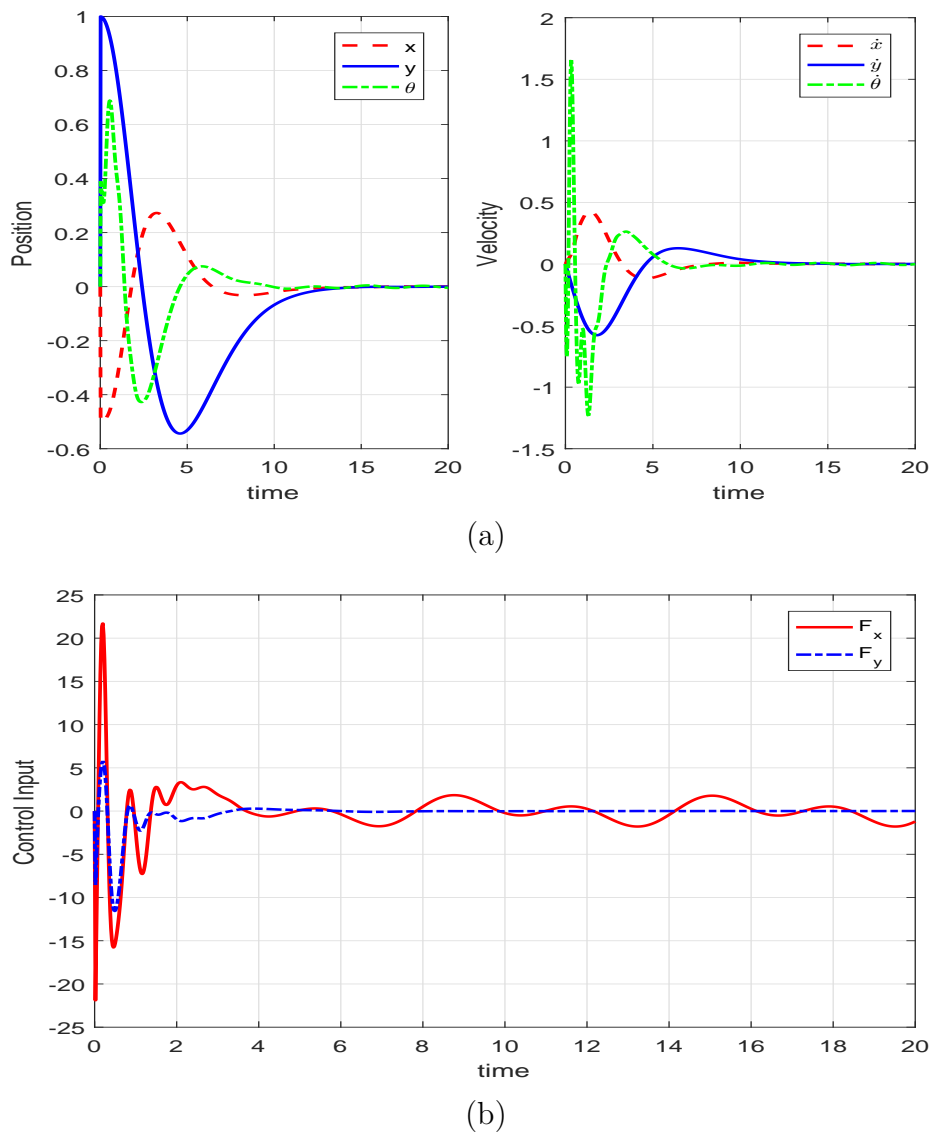
FIGURE 5.8: Planar PPR Manipulator (a) States $(q(t), \dot{q}(t))$ corresponding to $(2,-2,\pi/4,0,0,0)$ (b) Control effort (f_x, f_y)

been achieved.

5.5   Summary

Adaptive integral sliding mode based stabilizing control algorithms for the second-order nonholonomic mechanical system are presented in this chapter. The proposed methods are tested on two different second-order nonholonomic systems; a

three DOF manipulator with a passive joint model and a planar PPR manipulator model. Both models belong to the second-order nonholonomic family that are transferable into second-order chained form systems. The effectiveness of the proposed method is verified through simulations when applied to the original models. The aim was to steer the systems from any starting configuration state to a desired one. Also, robustness of the proposed algorithms is verified by introducing uncertainties in the control input. Simulation results validate that the control objective has been successfully accomplished.

Chapter 6

Stabilization of Higher-Order Perturbed Nonholonomic Systems

Systems that satisfy non-integrable constraints of order greater than two are known as higher-order nonholonomic systems. These systems are strongly accessible and small-time locally controllable, under certain conditions, at any equilibrium point. In this chapter, the stabilization problem of a PPR robot manipulator is explored under a third-order non-integrable jerk constraint. By maintaining the transverse jerk component at zero, the control objective is to move the robot end-effector from any starting configuration to the equilibrium configuration. The control methodology is based on adaptive integral sliding mode control (AISMC) technique. Firstly, the higher-order nonholonomic system is augmented by adding its missing Lie brackets and some unknown adaptive parameters. Secondly, the control and the adaptive laws are designed in such a way that the behaviour of the augmented system is similar to that of the nominal system on the sliding surface and the addition of missing Lie brackets in the original system can be compensated for adaptively. Similarly, a second algorithm is developed using function approximation approach. A TONHS such as a planar PPR manipulator subject to a jerk constraint is used to verify the presented algorithm. Towards the end, perturbed version of the third-order NHS is also proposed in order to handle the uncertainties in the control input.

6.1 Third-Order Nonholonomic System

Since the beginning of the last century, considerable effort has been put in to formulate the theory with respect to higher-order nonholonomic constraints ([59], [105]). The constraints, defined as program constraints, occur by imposing specific conditions on the allowable trajectories [59]. For example, second- and third-order constraints occur by imposing torsion and curvature constraints on robot trajectories. Recently, interest has been shown in stabilizing systems with performance and task requirements that involve higher-order derivatives of the configuration variables ([106], [43], [107]). In industrial robotic applications [106], program constraints are imposed on the permissible jerk in order to reduce the jerk. Also, a variety of optimization techniques have been proposed for generating minimum-snap trajectories [107] and minimum-jerk trajectories [43]. By exploiting the inherent geometric configuration in these systems, the theoretical framework for the stabilization of these systems was carried out by [108].

6.1.1 Mathematical Model of a PPR Manipulator

By following ([59], [60]) and after suitable nonlinear control and state transformations [42], higher-order non-holonomic systems can be given as:

$$q_1^{(p)} = u \tag{6.1}$$

$$q_2^{(p)} = J(q, \dot{q}, ..., q^{(p-1)})u + R(q, \dot{q}, ..., q^{(p-1)}) \tag{6.2}$$

where $q_1 \in \mathbb{R}^m$, $m \geq 2$ represents the directly actuated configuration variables, $u \in \mathbb{R}^m$ denotes the control for the directly actuated DoF and $q_2 \in \mathbb{R}^{n-m}$ represents the variables where control is achieved through system coupling.

Let us take a planar Prismatic-Prismatic-Revolute robot manipulator as illustrated in Figure 6.1. The movement of robot manipulator is restricted on a horizontal plane so that the gravity term can be ignored. The problem objective is to control the manipulator from any given (x_0, y_0, θ_0) to final configuration (x_f, y_f, θ_f) by

maintaining the resultant transverse jerk at the end-effector is zero, i.e.

$$\dddot{x}\sin\theta - \dddot{y}\cos\theta = 0 \tag{6.3}$$

The above condition is a design constraint. Here, in this particular example
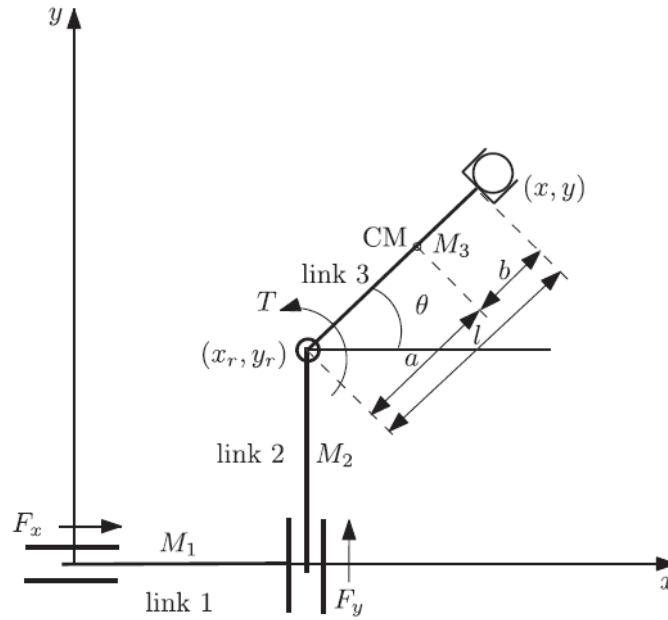
FIGURE 6.1: Planar PPR Manipulator.

$p = n = 3$ and $m = 2$. Using the results of [108], it can be seen that (6.3) represents a non-integrable constraint of order 3. Jerk is envisioned as rapidly changing actuator force in the robot manipulators which causes premature degradation of the actuators, leads to unnecessary oscillations in the robotic structure and most importantly difficult to track by the controller. The constrained equations of motion [42] are given as:

$$m_x\ddot{x} + m_{x\theta}(\ddot{\theta}\sin\theta + \dot{\theta}^2\cos\theta) = F_x + \lambda\sin\theta \tag{6.4}$$

$$m_y\ddot{y} - m_{y\theta}(\ddot{\theta}\cos\theta - \dot{\theta}^2\sin\theta) = F_y - \lambda\cos\theta \tag{6.5}$$

$$I\ddot{\theta} + m_{x\theta}\ddot{x}\sin\theta - m_{y\theta}\ddot{y}\cos\theta + M_1 l^2\dot{\theta}^2\sin\theta\cos\theta = T + l(F_x\sin\theta - F_y\cos\theta) \tag{6.6}$$

Assuming $\theta \in (-\pi/2, \pi/2)$, the above system (6.4) to (6.6) can be rewritten in the normal form:

$$
\begin{aligned}
\dddot{x} &= u_1 \\
\dddot{\theta} &= u_2 \\
\ddot{y} &= \tan\theta \, u_1
\end{aligned}
\tag{6.7}
$$

where, we have used

$$
F_y = m_y \ddot{y}
\tag{6.8}
$$

$$
\dot{F}_x = m_x u_1 + m_{y\theta}\dot{\theta}\sec\theta(2\ddot{\theta} + \dot{\theta}^2\tan\theta) + M_1 l\left[(u_2 - \dot{\theta}^3)\sin\theta + 3\dot{\theta}\,\ddot{\theta}\cos\theta\right]
\tag{6.9}
$$

and

$$
\begin{aligned}
\dot{\tau}_\theta =& \bar{I}\, u_2 + \bar{m}\dot{\theta}(\dddot{x}\cos\theta - \ddot{y}\sin\theta) - m_{y\theta}l\dot{\theta}(2\ddot{\theta}\tan\theta + \dot{\theta}^2\sec^2\theta) \\
& - 2M_1 l^2\dot{\theta}(\dot{\theta}^2\cos 2\theta + \ddot{\theta}\sin 2\theta)
\end{aligned}
\tag{6.10}
$$

with

$$
\begin{aligned}
\bar{I} &= I - M_1 l^2\sin^2\theta = I_3 + M_2 l^2 + M_3 b^2 \\
\bar{m} &= m_{x\theta} - m_x l = m_{y\theta} - m_y l = M_3(b - l) - ml
\end{aligned}
$$

The control objective is transformed to constructing controls u_i, $i = 1, 2$ for the system (6.7). Once the controls are constructed, we can use relations (6.8), (6.9) and (6.10) to ascertain the controls F_x, F_y and T respectively.

Let $q = [x, \theta, y]^T$, defined by $(q, \dot{q}, \ddot{q}) \in M = \mathbb{R} \times (-\frac{\pi}{2}, \frac{\pi}{2}) \times \mathbb{R} \times \mathbb{R}^3 \times \mathbb{R}^3$, denote the configuration vector. The set of equilibrium solutions corresponding to $u = 0$ is given by $M_e = \{(q, \dot{q}, \ddot{q}) \in M | \dot{q} = \ddot{q} = 0\}$.

The higher-order nonholonomic mechanical system can be written as:

$$
\dot{x} = f(x) + \sum_{i=1}^{m} g_i(x)u_i
\tag{6.11}
$$

such that the control and drift vector fields are given by:

$$f = \dot{x}\frac{\partial}{\partial x} + \dot{\theta}\frac{\partial}{\partial \theta} + \dot{y}\frac{\partial}{\partial y} + \ddot{x}\frac{\partial}{\partial \dot{x}} + \ddot{\theta}\frac{\partial}{\partial \dot{\theta}} + \ddot{y}\frac{\partial}{\partial \dot{y}},$$

$$g_1 = \frac{\partial}{\partial \ddot{x}} + \tan\theta\frac{\partial}{\partial \ddot{y}},$$

$$g_2 = \frac{\partial}{\partial \ddot{\theta}}$$

As $R \equiv 0$, therefore, no time-invariant feedback control law exists which is able to stabilize the system in an asymptotic way to a required equilibrium position $(q_e, 0, 0)$. Otherwise, space spanned by the vector fields

$$g_1, g_2, [f, g_1], [f, g_2], [f, [f, g_1]], [f, [f, g_2]], [g_2, [f, [f, g_1]]], [f, [g_2, [f, [f, g_1]]]],$$

$$[f, [f, [g_2, [f, [f, g_1]]]]]$$

has dimension 9 at any $(q, \dot{q}, \ddot{q}) \in M \times \mathbb{R}$ and therefore system under consideration is strongly accessible [108] and small time local controllable [34]. There exists both discontinuous time-invariant and smooth time varying feedback laws which asymptotically stabilize the equilibrium point [42]. The controllability property guarantees the existence of a solution to control the manipulator with zero transverse jerk at its end-effector.

6.1.2   The Stabilization Problem

Given a desired set point $z_{des} = \begin{bmatrix} q_{des} \\ \dot{q}_{des} \\ \ddot{q}_{des} \end{bmatrix} \in M \times \mathbb{R}$, construct control laws such that the desired set point z_{des} is an attractive set for system (6.7) and there exists an $\varepsilon > 0$, such that $z(t, t_0, z_0) \to z_{des}$, as $t \to \infty$ for any $(t_0, z_0) \in \mathbb{R} \times B(z_{des}; \varepsilon)$. For stabilization problem, we can take $z_{des} = 0$ attained by a suitable translation of coordinates.

6.1.3 Adaptive Integral Sliding Mode Controller Design

In SMC, there is no guarantee for robustness during the reaching phase; whereas, ISMC ensures elimination of the reaching phase by enforcing sliding mode for the entire response duration. The drawback of using SMC is the chattering phenomenon which makes implementation of SMC in real applications very difficult. Following algorithms are proposed for third-order nonholonomic systems.

6.1.4 Proposed Algorithm : Method-1

Step 1: Define

$$\begin{bmatrix} x_1 = x & x_2 = \theta & x_3 = y & x_4 = \dot{x} & x_5 = \dot{\theta} & x_6 = \dot{y} & x_7 = \ddot{x} & x_8 = \ddot{\theta} & x_9 = \ddot{y} \end{bmatrix}^T$$

$$Z = \begin{bmatrix} x_1 & x_2 & x_3 \end{bmatrix}^T, \dot{Z} = \begin{bmatrix} x_4 & x_5 & x_6 \end{bmatrix}^T \text{ and } \ddot{Z} = \begin{bmatrix} x_7 & x_8 & x_9 \end{bmatrix}^T$$

as the state vector. Now, using the new state vector, the third-order chained form system (6.7) can be written as:

$$\dddot{Z} = \begin{bmatrix} 1 \\ 0 \\ \tan x_2 \end{bmatrix} u_1 + \begin{bmatrix} 0 \\ 1 \\ 0 \end{bmatrix} u_2 = g_1(Z)u_1 + g_2(Z)u_2 \tag{6.12}$$

where,

$$g_1(Z) = \begin{bmatrix} 1 & 0 & \tan x_2 \end{bmatrix}^T \text{ and } g_2(Z) = \begin{bmatrix} 0 & 1 & 0 \end{bmatrix}^T$$

Step 2: Compute the following Lie bracket

$$g_3(Z) = [g_1(Z), g_2(Z)] = \begin{bmatrix} 0 & 0 & \sec^2 x_2 \end{bmatrix}^T.$$

Now, by adding and subtracting $g_3(Z)u_3$, the system (6.12) can be written as:

$$\dddot{Z} = g_1(Z)u_1 + g_2(Z)u_2 + g_3(Z)u_3 - g_3(Z)u_3 = Gu - v \tag{6.13}$$

$$\text{where, } G = \begin{bmatrix} 1 & 0 & 0 \\ 0 & 1 & 0 \\ \tan x_2 & 0 & \sec^2 x_2 \end{bmatrix}, \ u = \begin{bmatrix} u_1 \\ u_2 \\ u_3 \end{bmatrix} \text{ and } v = \begin{bmatrix} 0 \\ 0 \\ \sec^2 x_2 \end{bmatrix} u_3 = \begin{bmatrix} 0 \\ 0 \\ \sec^2 x_2 u_3 \end{bmatrix}.$$

In order to reduce the state dependence and to make G matrix invertible, the third column of the matrix is taken as a constant $v = \begin{bmatrix} 0 & 0 & u_3 \end{bmatrix}^T$. Now, assume that v is unknown and can be computed adaptively. Let $\hat{v}$ be estimate of v and $\tilde{v} = v - \hat{v}$ be error in the estimation. Then (6.13) can be written as:

$$\ddot{Z} = Gu - \hat{v} - \tilde{v} \tag{6.14}$$

Step 3: Take first part of system (6.14) as the nominal system and use subscript form w_0 for the nominal input, we get:

$$\ddot{Z} = G w_0 \tag{6.15}$$

Take the sliding surface for the nominal system (6.15) as:

$$S_0 = \begin{bmatrix} s_{01} \\ s_{02} \\ s_{03} \end{bmatrix} = Z + 2\dot{Z} + \ddot{Z} = \begin{bmatrix} x_1 + 2x_4 + x_7 \\ x_2 + 2x_5 + x_8 \\ x_3 + 2x_6 + x_9 \end{bmatrix}$$

Then,

$$\dot{S}_0 = \dot{Z} + 2\ddot{Z} + \dddot{Z} = \dot{Z} + 2\ddot{Z} + Gw_0$$

and the choice of

$$w_0 = -G^{-1}(\dot{Z} + 2\ddot{Z} + k\operatorname{sgn}(S_0) + kS_0) \tag{6.16}$$

gives $\dot{S}_0 = -k\operatorname{sgn}(S_0) - kS_0$. Now take $V = \frac{1}{2}S_0^T S_0$ as a Lyapunov function for (6.15), which makes $\dot{V} = S_0^T \dot{S}_0 = -k\,S_0^T \operatorname{sgn}(S_0) - k\,S_0^T S_0 < 0$. Thus, the nominal system (6.15) is asymptotically stable.

Step 4: Now, consider complete system (6.14). Choose $w = w_0 + w_s$, where w_0 is the nominal control given at (6.16) and w_s is the switching control designated as compensator control that is determined during next step. Also, define the sliding surface as $S = S_0 + R$, where $R = \begin{bmatrix} r_1 \\ r_2 \\ r_3 \end{bmatrix}$ is the integral vector term. Then,

$$\dot{S} = \dot{S}_0 + \dot{R} = \dot{Z} + 2\ddot{Z} + Gw_0 + Gw_s - \hat{v} - \tilde{v} + \dot{R} \tag{6.17}$$

Step 5: By choosing a Lyapunov function $V = \frac{1}{2}S^T S + \frac{1}{2}\tilde{v}^T \Gamma \tilde{v}$, where, Γ is a 3×3 positive diagonal matrix, design the input w_s and the adaptive laws for $\tilde{v}$ and $\hat{v}$ such that $\dot{V} < 0$.

Theorem 6.1: *Taking a Lyapunov function $V = \frac{1}{2}S^T S + \frac{1}{2}\tilde{v}^T \Gamma \tilde{v}$. Then $\dot{V} < 0$ if the input w_s and the adaptive laws for $\tilde{v}$ and $\hat{v}$ are chosen as:*

$$\dot{R} = -\dot{Z} - 2\ddot{Z} - Gw_0$$
$$w_s = G^{-1}(\hat{v} - k\,\mathrm{sgn}(S)), \quad k > 0 \tag{6.18}$$
$$\dot{\tilde{v}} = \Gamma^{-1}(S - \Gamma\tilde{v}), \quad \dot{\hat{v}} = -\dot{\tilde{v}}$$

Proof. Since

$$\dot{V} = S^T \dot{S} + \tilde{v}^T \Gamma \dot{\tilde{v}} = S^T(\dot{Z} + 2\ddot{Z} + Gw_0 + Gw_s - \hat{v} - \tilde{v} + \dot{R}) + \tilde{v}^T \Gamma \dot{\tilde{v}}$$
$$= S^T(\dot{Z} + 2\ddot{Z} + Gw_0 + Gw_s - \hat{v} + \dot{R}) + \tilde{v}^T(\Gamma\dot{\tilde{v}} - S)$$

By using,

$$\dot{R} = -\dot{Z} - 2\ddot{Z} - Gw_0$$
$$w_s = G^{-1}(\hat{v} - k\,\mathrm{sgn}(S)), \quad k > 0$$
$$\dot{\tilde{v}} = \Gamma^{-1}(S - \Gamma\tilde{v}), \quad \dot{\hat{v}} = -\dot{\tilde{v}}$$

we have, $\dot{V} = -k\,S^T S - \tilde{v}^T \Gamma \tilde{v} < 0.$ $\square$

From this we conclude that S and $\tilde{v} \to 0$. Since $S = \begin{bmatrix} s_1 \\ s_2 \\ s_3 \end{bmatrix} = \begin{bmatrix} x_1 + 2x_4 + x_7 \\ x_2 + 2x_5 + x_8 \\ x_3 + 2x_6 + x_9 \end{bmatrix} \to 0,$

$x_1 + 2x_4 + x_7$, $x_2 + 2x_5 + x_8$ and $x_3 + 2x_6 + x_9$ are Hurwitz polynomial, therefore, x_i, $i = 1,..,9 \to 0$. The simulation results are shown for two different initial conditions. In all these simulations, the objective was to steer the systems states to zero.

6.1.4.1 Simulation Results

Figures 6.4 and 6.5 show simulation results for planar PPR manipulator with a jerk constraint. The simulations are carried out for two different initial conditions:

i) $(3, \pi/4, -2, 2, -\pi/3, 3, 1, \pi/5, 2)$

ii) $(1, \pi/4, -1, 0, 0, 0, 0, 0, 0)$

As can be seen from the simulation results, all the system states converge to zero for systems with different initial conditions, thus validating the correctness of the applied algorithm.

6.1.5 Proposed Algorithm : Method-2

Step 1: Define

$$\begin{bmatrix} x_1 = x & x_2 = \dot{x} & x_3 = \ddot{x} & x_4 = y & x_5 = \dot{y} & x_6 = \ddot{y} & x_7 = \theta & x_8 = \dot{\theta} & x_9 = \ddot{\theta} \end{bmatrix}^T$$
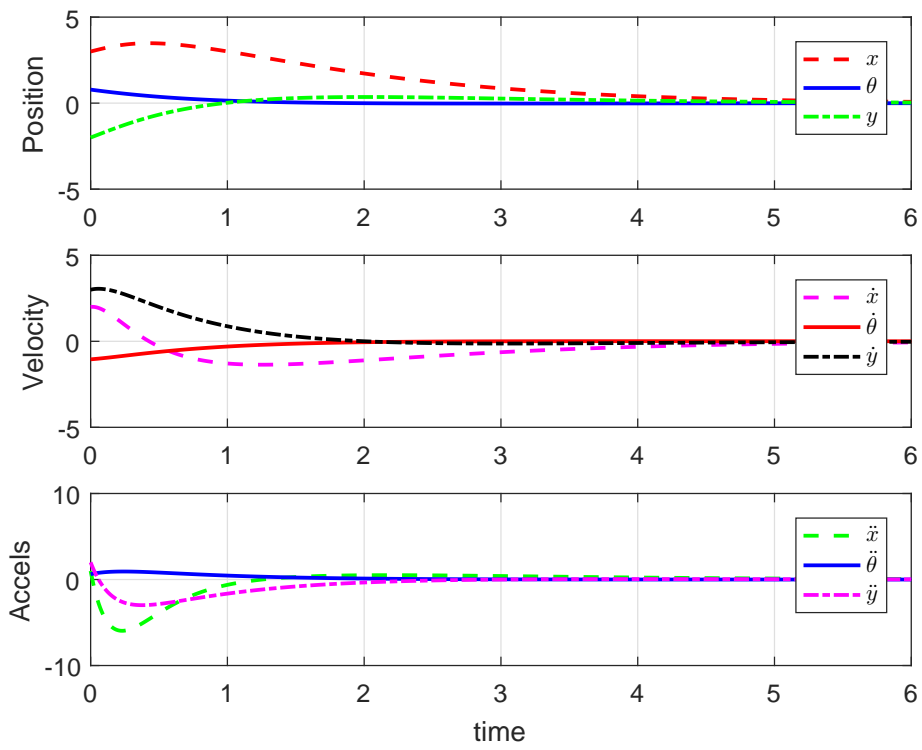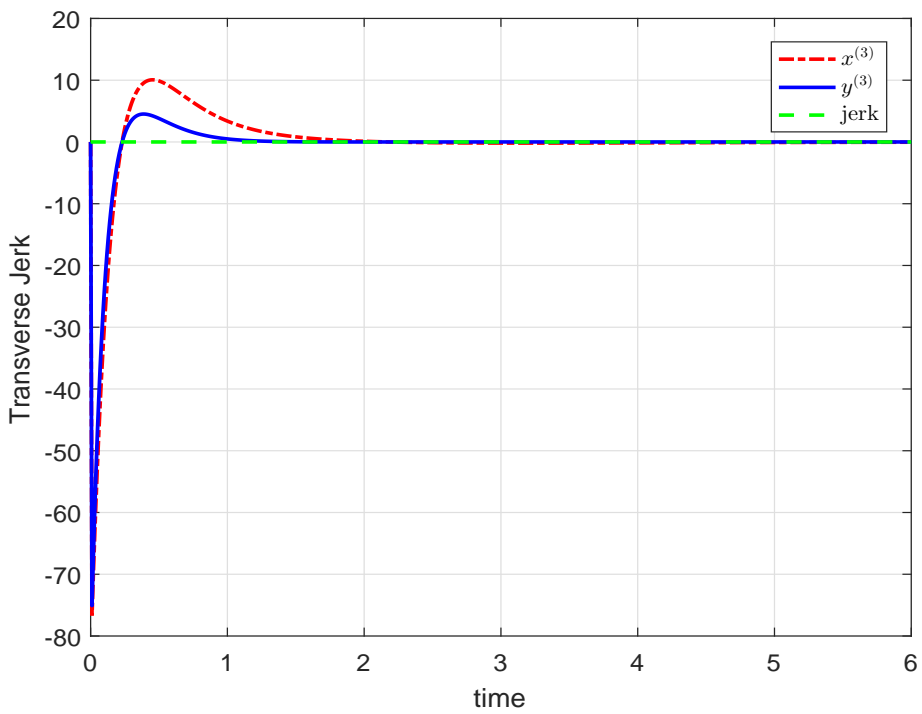
FIGURE 6.2: System Trajectory with jerk constraint (a) System states corresponding to initial condition (3,π /4,-2, 2,-π /3, 3, 1,π /5, 2) (b) Time history of jerk $\dddot{\sin}\theta - \dddot{\cos}\theta$
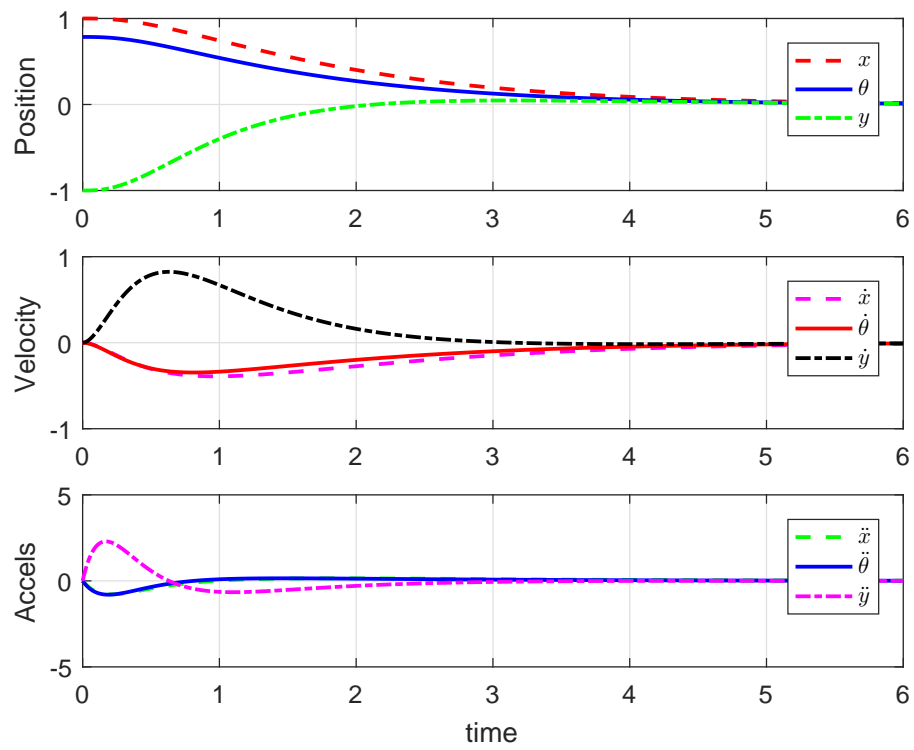
(a)
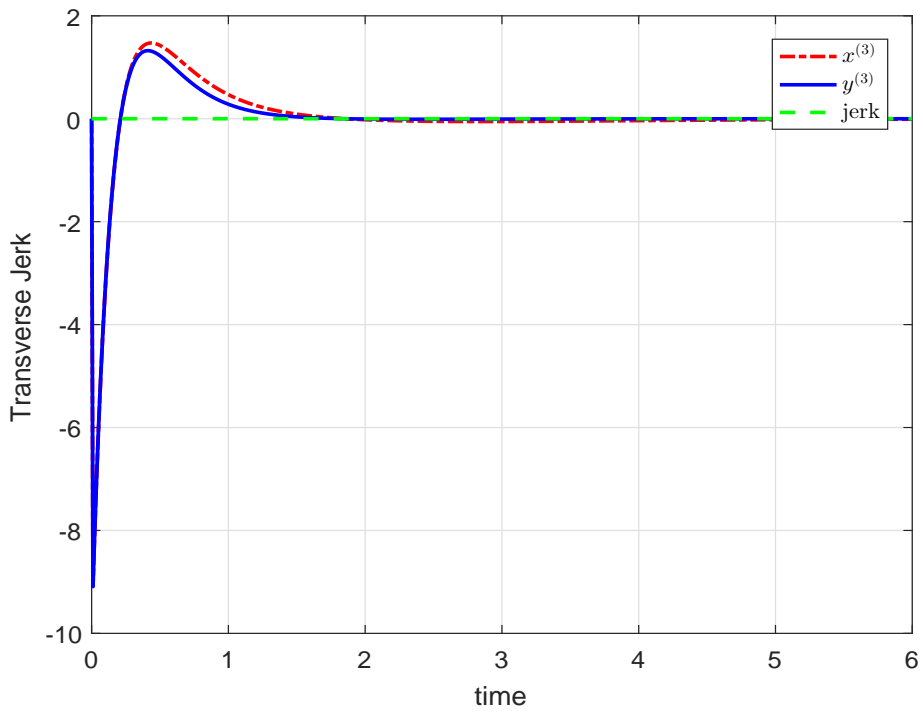
(b)

FIGURE 6.3: System Trajectory with jerk constraint (a) System states corresponding to initial condition $(1, \pi/4, -1, 0, 0, 0, 0, 0, 0)$ (b) Time history of jerk $\dddot{x} \sin\theta - \dddot{y} \cos\theta$

Now, the third-order chained form system (6.7) can be written in state-space form as:

$$\dot{x}_1 = x_2$$
$$\dot{x}_2 = x_3$$
$$\dot{x}_3 = v_1$$
$$\dot{x}_4 = x_5 \qquad\qquad (6.19)$$
$$\dot{x}_5 = x_6$$
$$\dot{x}_6 = \tan(x_7)v_1$$
$$\dot{x}_7 = x_8$$
$$\dot{x}_8 = x_9$$
$$\dot{x}_9 = v_2$$

Step 2: Transform system (6.19) into the following form by choosing $v_1 = x_4$ and $v_2 = v$, where v is the new input:

$$\dot{x}_i = x_{i+1} \quad i = 1, \cdots, 5$$
$$\dot{x}_6 = \tan(x_7)x_4 \qquad\qquad (6.20)$$
$$\dot{x}_7 = x_8$$
$$\dot{x}_8 = x_9$$
$$\dot{x}_9 = v$$

Now, write system (6.20) as:

$$\dot{x}_i = x_{i+1} \quad i = 1, \cdots, 5$$
$$\dot{x}_6 = x_7 + F \qquad\qquad (6.21)$$
$$\dot{x}_7 = x_8$$
$$\dot{x}_8 = x_9$$
$$\dot{x}_9 = v$$

where $F = -x_7 + h(x)$ and $h(x) : \mathbb{R}^n \times \mathbb{R}^m \to \mathbb{R}$ is a nonlinear function.

Step 3: Assume that F is the uncertainty in chained form system and let $\hat{F}$ be an estimate of F and $\tilde{F} = F - \hat{F}$. Now apply function approximation technique presented in [102] to represent F and the estimate $\hat{F}$ as $F = w^T \phi(t)$ and $\hat{F} = \hat{w}^T \phi(t)$ respectively. Here we have $\phi(t) = [\phi_1(t) \cdots \phi_n(t)]^T$ as basis vector function and $w(t) = [w_1(t) \cdots w_n(t)]^T$ as weight vector. Let $\hat{w}$ be an estimate of w. Then we can estimate F by estimating the weight vector as $\hat{F} = \hat{w}^T \phi(t)$. Define $\tilde{w} = w - \hat{w}$, then system (6.21) can be written as:

$$
\begin{aligned}
\dot{x}_i &= x_{i+1} \quad i = 1, \cdots, 5 \\
\dot{x}_6 &= x_7 + \hat{w}^T(t)\phi(t) + \tilde{w}^T(t)\phi(t) \\
\dot{x}_7 &= x_8 \\
\dot{x}_8 &= x_9 \\
\dot{x}_9 &= v
\end{aligned}
\tag{6.22}
$$

Step 4: Take the nominal system for (6.22) as:

$$
\begin{aligned}
\dot{x}_i &= x_{i+1}, \ i = 1, \cdots, 8 \\
\dot{x}_6 &= v_0
\end{aligned}
\tag{6.23}
$$

Step 5: Now, define the sliding surface for nominal part (6.23) as

$$
s_0 = x_1 + 8x_2 + 28x_3 + 56x_4 + 70x_5 + 56x_6 + 28x_7 + 8x_8 + x_9
$$

Then,

$$
\begin{aligned}
\dot{s}_0 &= \dot{x}_1 + 8\dot{x}_2 + 28\dot{x}_3 + 56\dot{x}_4 + 70\dot{x}_5 + 56\dot{x}_6 + 28\dot{x}_7 + 8\dot{x}_8 + \dot{x}_9 \\
&= x_2 + 8x_3 + 28x_4 + 56x_5 + 70x_6 + 56x_7 + 28x_8 + 8x_9 + v_0
\end{aligned}
\tag{6.24}
$$

By choosing

$$v_0 = -x_2 - 8x_3 - 28x_4 - 56x_5 - 70x_6 - 56x_7 - 28x_8 - 8x_9 - k\,\text{sgn}(s_0),\ \ k > 0$$

we get $\dot{s}_0 = -k\,\text{sgn}(s_0)$. Therefore, the nominal system (6.23) is stable in an asymptotic way.

Step 6: Now, define sliding surface for system (6.22) as:

$$s = s_0 + z = x_1 + 8x_2 + 28x_3 + 56x_4 + 70x_5 + 56x_6 + 28x_7 + 8x_8 + x_9 + z \quad (6.25)$$

where z is some integral part that is computed afterwards. Choose $z(0)$ so that $s(0) = 0$ in order to avoid the reaching phase. Choose $v = v_0 + v_s$, where v_0 is the nominal input and v_s is compensator part that is computed afterwards. Then

$$\begin{aligned}
\dot{s} &= \dot{x}_1 + 8\dot{x}_2 + 28\dot{x}_3 + 56\dot{x}_4 + 70\dot{x}_5 + 56\dot{x}_6 + 28\dot{x}_7 + 8\dot{x}_8 + \dot{x}_9 + \dot{z} \\
&= x_2 + 8x_3 + 28x_4 + 56x_5 + 70x_6 + 56x_7 + 56\hat{w}^T\varphi + 56\tilde{w}^T\varphi + 28x_8 + 8x_9 \\
&\quad + v_0 + v_s + \dot{z}
\end{aligned} \quad (6.26)$$

Step 7: Taking a Lyapunov function $V = \frac{1}{2}s^2 + \frac{1}{2}\tilde{w}^T\tilde{w}$, design the adaptive laws for $\tilde{w}$, $\hat{w}$ and compute v_s so that $\dot{V} < 0$.

Theorem 6.2: *Take a Lyapunov function* $V = \frac{1}{2}s^2 + \frac{1}{2}\tilde{w}^T\tilde{w}$. *Then* $\dot{V} < 0$ *if the adaptive control for* $\tilde{w}$, $\hat{w}$ *and the value of* v_s *are chosen as:*

$$\begin{aligned}
\dot{z} &= -x_2 - 8x_3 - 28x_4 - 56x_5 - 70x_6 - 56x_7 - 28x_8 - 8x_9 - v_0, \\
v_s &= -56\hat{w}^T\varphi - k\,\text{sgn}(s) \\
\dot{\tilde{w}} &= -56s\varphi - k_1\tilde{w}\ ,\dot{\hat{w}} = -\dot{\tilde{w}},\ \ k, k_1 > 0
\end{aligned}$$

Proof. Since

$$\dot{V} = s\dot{s} + \tilde{w}^T \dot{\tilde{w}}$$

$$= s(x_2 + 8x_3 + 28x_4 + 56x_5 + 70x_6 + 56x_7 + 56\hat{w}^T\varphi + 56\tilde{w}^T\varphi + 28x_8 + 8x_9$$

$$+ v_0 + v_s + \dot{z}) + \tilde{w}^T \dot{\tilde{w}}$$

$$= s(x_2 + 8x_3 + 28x_4 + 56x_5 + 70x_6 + 56x_7 + 56\hat{w}^T\varphi + 28x_8 + 8x_9 + v_0 + v_s + \dot{z})$$

$$+ \tilde{w}^T(\dot{\tilde{w}} + 56s)$$

By using,

$$\dot{z} = -x_2 - 8x_3 - 28x_4 - 56x_5 - 70x_6 - 56x_7 - 28x_8 - 8x_9 - v_0,$$

$$v_s = -56\hat{w}^T\varphi - k\,\text{sgn}(s)$$

$$\dot{\tilde{w}} = -56s\varphi - k_1\tilde{w}\ ,\ \dot{\hat{w}} = -\dot{\tilde{w}},\ \ k, k_1 > 0$$

we have, $\dot{V} = -k\,s\,\text{sgn}(s) - k_1\tilde{w}^T\tilde{w} < 0.$ □

From this we conclude that $s,\ \tilde{w} \to 0$. Since $s \to 0$, therefore $x \to 0$.

6.1.5.1 Simulation Results

Figures 6.4 and 6.5 show simulation results for planar PPR manipulator with a jerk constraint. The simulations are carried out for two different initial conditions:

i) $(3,\pi\,/4,-2,\,2,-\pi\,/3,\,3,\,1,\pi\,/5,\,2)$

ii) $(1,\pi\,/4,\,-1,\,0,\,0,\,0,\,0,\,0,\,0)$

As can be seen from the simulation results, all the system states converge to zero for systems with different initial conditions, thus validating the correctness of the applied algorithm.
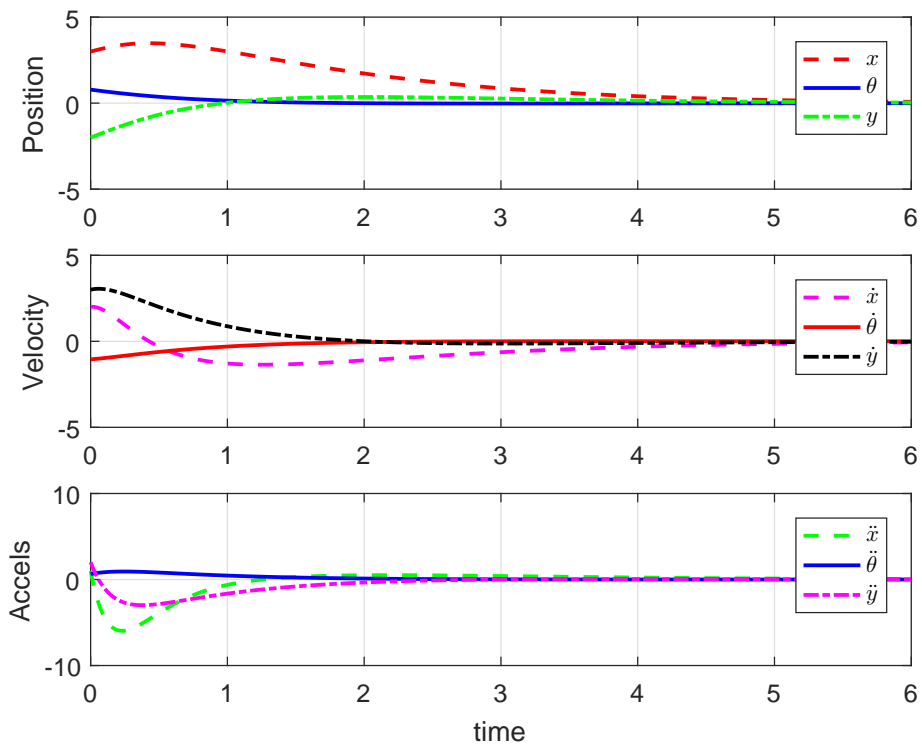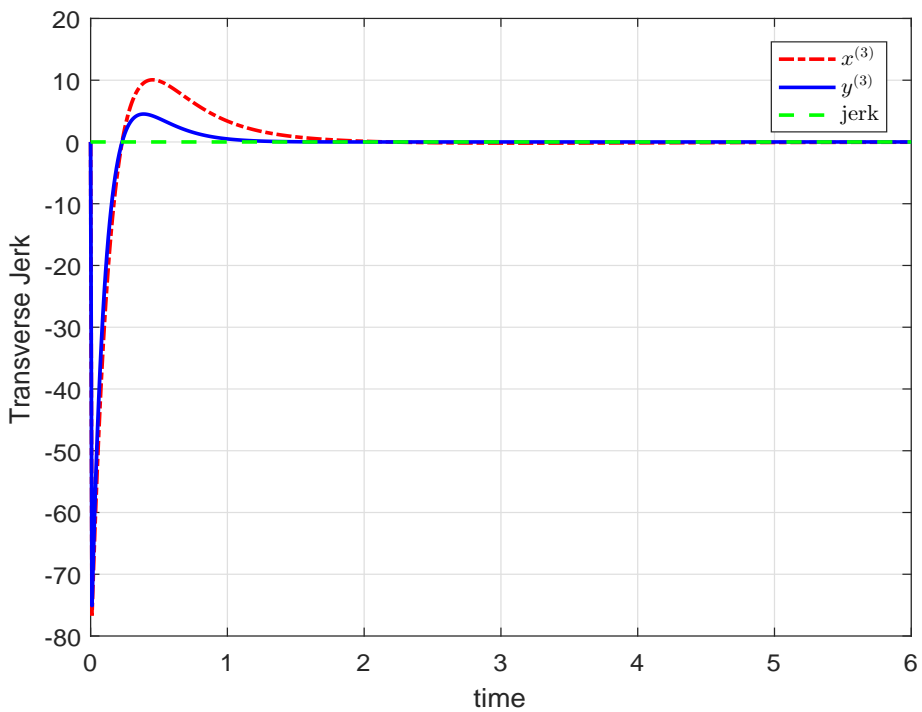
FIGURE 6.4: System Trajectory with jerk constraint (a) System states corresponding to initial condition $(3, \pi/4, -2, 2, -\pi/3, 3, 1, \pi/5, 2)$ (b) Time history of jerk $\dddot{\sin}\theta - \dddot{\cos}\theta$
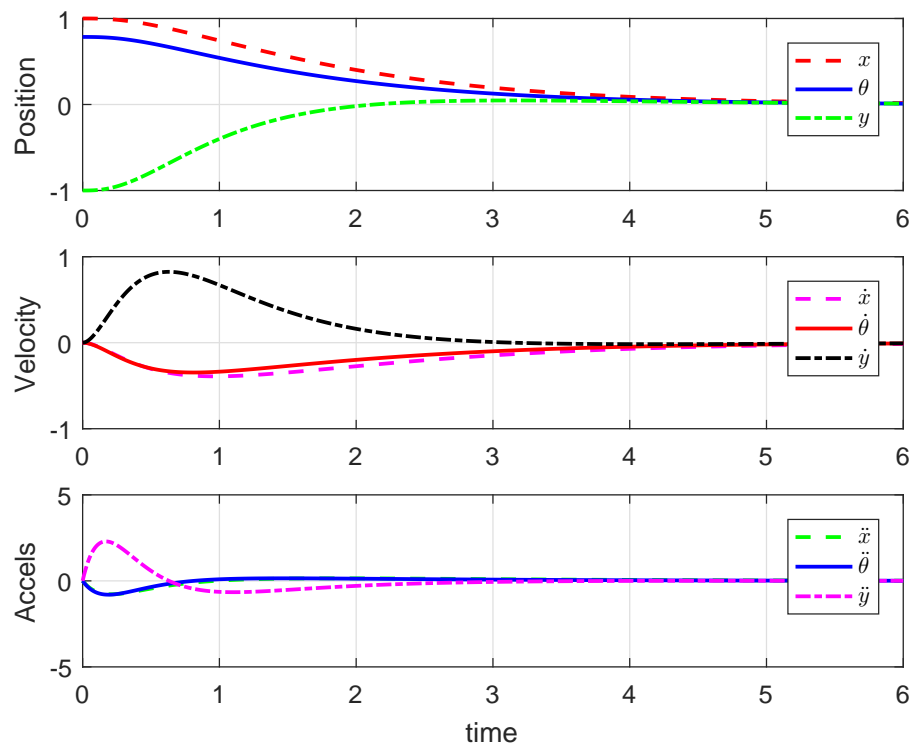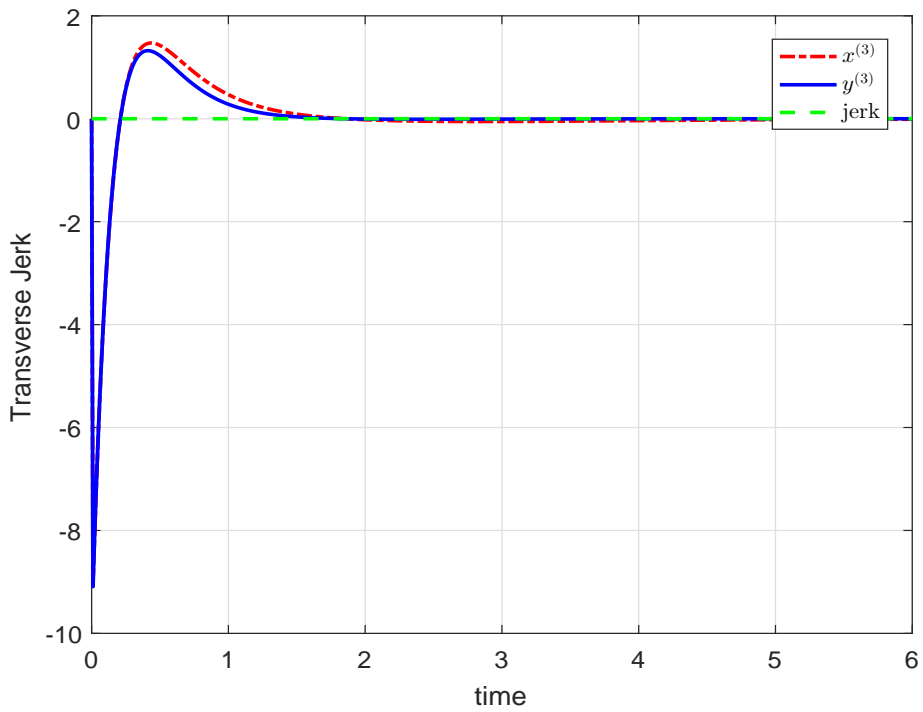
FIGURE 6.5: System Trajectory with jerk constraint (a) System states corresponding to initial condition $(1, \pi/4, -1, 0, 0, 0, 0, 0, 0)$ (b) Time history of jerk $\dddot{x} \sin\theta - \dddot{y} \cos\theta$

6.2 Problem Formulation : Peturbed Case

6.2.1 Dynamic Model of a Perturbed Third-Order Non-holonomic System

Consider a third-order chained form system with uncertainties in control input v_2 described as:

$$
\begin{aligned}
\dddot{y}_1 &= v_1 \\
\dddot{y}_2 &= v_2 + d_1 \\
\dddot{y}_3 &= y_2 v_1
\end{aligned}
\tag{6.27}
$$

where $q = [y_1 \; y_2 \; y_3]^T$, $\dot{q} = [\dot{y}_1 \; \dot{y}_2 \; \dot{y}_3]^T$ and $\ddot{q} = [\ddot{y}_1 \; \ddot{y}_2 \; \ddot{y}_3]^T \in \mathbb{R}^3$ denote the configuration vector and derivatives, $[v_1 \; v_2]^T \in \mathbb{R}^2$ is the control input vector and d_1 is unknown disturbance in control input v_2.

6.2.2 Adaptive ISMC

6.2.2.1 Proposed Algorithm

Here, in order to address the uncertainty in the control input, a variant of Method-2 previously presented in Section 6.1.5. is given. The perturbed version of Method-1 can similarly be obtained with some modifications.

Let $\hat{d}_i, i = 1, 2$ be the estimate of d_i and let $\tilde{d}_i = d_i - \hat{d}_i$ be the estimation error. Then system (6.27) can be written as:

$$
\begin{aligned}
\dddot{y}_1 &= v_1 + \hat{d}_1 + \tilde{d}_1 \\
\dddot{y}_2 &= v_2 + \hat{d}_2 + \tilde{d}_2 \\
\dddot{y}_3 &= y_2 v_1 + y_2 \hat{d}_1 + \tilde{d}_1
\end{aligned}
\tag{6.28}
$$

Step 1: Define the state vector

$$\left[x_1 = y_1 \quad x_2 = \dot{y}_1 \quad x_3 = \ddot{y}_1 \quad x_4 = y_3 \quad x_5 = \dot{y}_3 \quad x_6 = \ddot{y}_3 \quad x_7 = y_2 \quad x_8 = \dot{y}_2 \quad x_9 = \ddot{y}_2 \right]^T$$

Now, the third-order chained form system (6.28) can be written in state-space form as:

$$\begin{aligned}
\dot{x}_1 &= x_2 \\
\dot{x}_2 &= x_3 \\
\dot{x}_3 &= v_1 + \hat{d}_1 + \tilde{d}_1 \\
\dot{x}_4 &= x_5 \\
\dot{x}_5 &= x_6 \\
\dot{x}_6 &= x_7 v_1 + x_7 \hat{d}_1 + \tilde{d}_1 \\
\dot{x}_7 &= x_8 \\
\dot{x}_8 &= x_9 \\
\dot{x}_9 &= v_2 + \hat{d}_2 + \tilde{d}_2
\end{aligned} \tag{6.29}$$

Step 2: Transform system (6.29) into the following form by choosing $v_1 = x_4 - \hat{d}_1$ and $v_2 = v - \hat{d}_2$, where v is the new input:

$$\begin{aligned}
\dot{x}_1 &= x_2 \\
\dot{x}_2 &= x_3 \\
\dot{x}_3 &= x_4 + \tilde{d}_1 \\
\dot{x}_4 &= x_5 \\
\dot{x}_5 &= x_6 \\
\dot{x}_6 &= x_7 x_4 + x_7 \tilde{d}_1 \\
\dot{x}_7 &= x_8 \\
\dot{x}_8 &= x_9 \\
\dot{x}_9 &= v + \tilde{d}_2
\end{aligned} \tag{6.30}$$

Now, write system (6.30) as:

$$\dot{x}_1 = x_2$$
$$\dot{x}_2 = x_3$$
$$\dot{x}_3 = x_4 + \tilde{d}_1$$
$$\dot{x}_4 = x_5$$
$$\dot{x}_5 = x_6 \qquad (6.31)$$
$$\dot{x}_6 = x_7 + F + x_7\tilde{d}_1$$
$$\dot{x}_7 = x_8$$
$$\dot{x}_8 = x_9$$
$$\dot{x}_9 = v + \tilde{d}_2$$

where $F = -x_7 + x_7x_4$.

Step 3: Assume that F is unknown and can be computed adaptively. Let $\hat{F}$ be an estimate of F and $\tilde{F} = F - \hat{F}$. Now apply function approximation technique presented in [102] to represent F and the estimate $\hat{F}$ as $F = w^T\phi(t)$ and $\hat{F} = \hat{w}^T\phi(t)$ respectively. Here we have $\phi(t) = [\phi_1(t) \cdots \phi_n(t)]^T$ as basis vector function and $w(t) = [w_1(t) \cdots w_n(t)]^T$ as weight vector. Let $\hat{w}$ be an estimate of w. Then we can estimate F by estimating the weight vector as $\hat{F} = \hat{w}^T\phi(t)$. Define $\tilde{w} = w - \hat{w}$,

then system (6.31) can be written as:

$$\dot{x}_1 = x_2$$
$$\dot{x}_2 = x_3$$
$$\dot{x}_3 = x_4 + \tilde{d}_1$$
$$\dot{x}_4 = x_5$$
$$\dot{x}_5 = x_6 \qquad (6.32)$$
$$\dot{x}_6 = x_7 + \hat{w}^T(t)\phi(t) + \tilde{w}^T(t)\phi(t) + x_7\tilde{d}_1$$
$$\dot{x}_7 = x_8$$
$$\dot{x}_8 = x_9$$
$$\dot{x}_9 = v + \tilde{d}_2$$

Step 4: Take the nominal system for (6.32) as:

$$\dot{x}_i = x_{i+1}, \;\; i = 1, \cdots, 8$$
$$\dot{x}_6 = v_0 \qquad (6.33)$$

Step 5: Now, define the sliding surface for nominal system (6.33) as

$$s_0 = x_1 + 8x_2 + 28x_3 + 56x_4 + 70x_5 + 56x_6 + 28x_7 + 8x_8 + x_9$$

Then,

$$\dot{s}_0 = \dot{x}_1 + 8\dot{x}_2 + 28\dot{x}_3 + 56\dot{x}_4 + 70\dot{x}_5 + 56\dot{x}_6 + 28\dot{x}_7 + 8\dot{x}_8 + \dot{x}_9 \qquad (6.34)$$
$$= x_2 + 8x_3 + 28x_4 + 56x_5 + 70x_6 + 56x_7 + 28x_8 + 8x_9 + v_0$$

By choosing

$$v_0 = -x_2 - 8x_3 - 28x_4 - 56x_5 - 70x_6 - 56x_7 - 28x_8 - 8x_9 - k\, s_0, \;\; k > 0$$

we get $\dot{s}_0 = -k\,s_0$. Therefore, the nominal system (6.33) is stable in an asymptotic way.

Step 6: Now, define sliding surface for system (6.32) as:

$$s = s_0 + z = x_1 + 8x_2 + 28x_3 + 56x_4 + 70x_5 + 56x_6 + 28x_7 + 8x_8 + x_9 + z \quad (6.35)$$

where z is some integral part computed afterwards. Choose $z(0)$ so that $s(0) = 0$ in order to avoid the reaching phase. Choose $v = v_0 + v_s$, where v_0 is the nominal input and v_s is compensator part that is computed afterwards. Then

$$
\begin{aligned}
\dot{s} =& \dot{x}_1 + 8\dot{x}_2 + 28\dot{x}_3 + 56\dot{x}_4 + 70\dot{x}_5 + 56\dot{x}_6 + 28\dot{x}_7 + 8\dot{x}_8 + \dot{x}_9 + \dot{z} \\
=& x_2 + 8x_3 + 28(x_4 + \tilde{d}_1) + 56x_5 + 70x_6 + 56(x_7 + \hat{w}^T\varphi + \tilde{w}^T\varphi + x_7\tilde{d}_1) + 28x_8 \\
&+ 8x_9 + v_0 + v_s + \tilde{d}_2 + \dot{z} \quad (6.36)
\end{aligned}
$$

Step 7: Take a Lyapunov function $V = \frac{1}{2}s^2 + \frac{1}{2}\tilde{w}^T\tilde{w} + \frac{1}{2}\tilde{d}_1^{\,2} + \frac{1}{2}\tilde{d}_2^{\,2}$, design the adaptive laws for $\tilde{w},\ \hat{w}, \tilde{d}_1, \tilde{d}_2$ and compute v_s so that $\dot{V} < 0$.

Theorem 6.3: *Take a Lyapunov function $V = \frac{1}{2}s^2 + \frac{1}{2}\tilde{w}^T\tilde{w} + \frac{1}{2}\tilde{d}_1^{\,2} + \frac{1}{2}\tilde{d}_2^{\,2}$. Then $\dot{V} < 0$ if the adaptive control for $\tilde{w},\ \hat{w},\ \tilde{d}_1,\ \tilde{d}_2$ and the value of v_s are chosen as:*

$$
\begin{aligned}
\dot{z} &= -x_2 - 8x_3 - 28x_4 - 56x_5 - 70x_6 - 56x_7 - 28x_8 - 8x_9 - v_0 \\
v_s &= -56\hat{w}^T\varphi - k\,\mathrm{sgn}(s) \\
\dot{\tilde{w}} &= -56s\varphi - k_1\tilde{w}, \ \ \dot{\hat{w}} = -\dot{\tilde{w}} \\
\dot{\tilde{d}}_1 &= -28s - 56x_7s - k_2\tilde{d}_1, \ \ \dot{\hat{d}}_1 = -\dot{\tilde{d}}_1 \\
\dot{\tilde{d}}_2 &= -s - k_3\tilde{d}_2, \ \ \dot{\hat{d}}_2 = -\dot{\tilde{d}}_2, \ \ k, k_1, k_2, k_3 > 0
\end{aligned}
$$

Proof. Since

$$\dot{V} = s\dot{s} + \tilde{w}^T\dot{\tilde{w}} + \tilde{d}_1\dot{\tilde{d}}_1 + \tilde{d}_2\dot{\tilde{d}}_2$$

$$= s(x_2 + 8x_3 + 28(x_4 + \tilde{d}_1) + 56x_5 + 70x_6 + 56(x_7 + \hat{w}^T\varphi + \tilde{w}^T\varphi + x_7\tilde{d}_1) + 28x_8$$

$$+ 8x_9 + v_0 + v_s + \tilde{d}_2 + \dot{z}) + \tilde{w}^T\dot{\tilde{w}} + \tilde{d}_1\dot{\tilde{d}}_1 + \tilde{d}_2\dot{\tilde{d}}_2$$

$$= s(x_2 + 8x_3 + 28x_4 + 56x_5 + 70x_6 + 56x_7 + 56\hat{w}^T\varphi + 28x_8 + 8x_9$$

$$+ v_0 + v_s + \dot{z}) + \tilde{w}^T(\dot{\tilde{w}} + 56s\varphi) + \tilde{d}_1(\dot{\tilde{d}}_1 + 28s + 56x_7s) + \tilde{d}_2(\dot{\tilde{d}}_2 + s)$$

By using,

$$\dot{z} = -x_2 - 8x_3 - 28x_4 - 56x_5 - 70x_6 - 56x_7 - 28x_8 - 8x_9 - v_0$$

$$v_s = -56\hat{w}^T\varphi - k\,\text{sgn}(s)$$

$$\dot{\tilde{w}} = -56s\varphi - k_1\tilde{w}, \quad \dot{\hat{w}} = -\dot{\tilde{w}}$$

$$\dot{\tilde{d}}_1 = -28s - 56x_7s - k_2\tilde{d}_1, \quad \dot{\hat{d}}_1 = -\dot{\tilde{d}}_1$$

$$\dot{\tilde{d}}_2 = -s - k_3\tilde{d}_2, \quad \dot{\hat{d}}_2 = -\dot{\tilde{d}}_2, \quad k, k_1, k_2, k_3 > 0$$

we have, $\dot{V} = -k\,s\,\text{sgn}(s) - k_1\tilde{w}^T\tilde{w} - k_2\tilde{d}_1^2 - k_3\tilde{d}_2^2 < 0.$ $\qquad\square$

From this we conclude that $s, \tilde{w} \to 0$. Since $s \to 0$, therefore $x \to 0$.

6.2.2.2   Results for Planar PPR Manipulator

Applying the proposed algorithm on perturbed system, the achieved simulation results are shown in Figs 6.6 - 6.7 for original system.

The simulations are carried out for different initial conditions. Figure 6.6 shows the system states and the corresponding control for the initial conditions (3,π /4,-2, 2,-π /3, 3, 1,π /5, 2). Also, Figure 6.7 shows the system states $(q(t), \dot{q}(t))$ and the corresponding control (f_x, f_y) for the initial condition (1,π /4, -1, 0, 0, 0, 0, 0, 0). The proposed objective to steer all the system states to zero has been achieved.
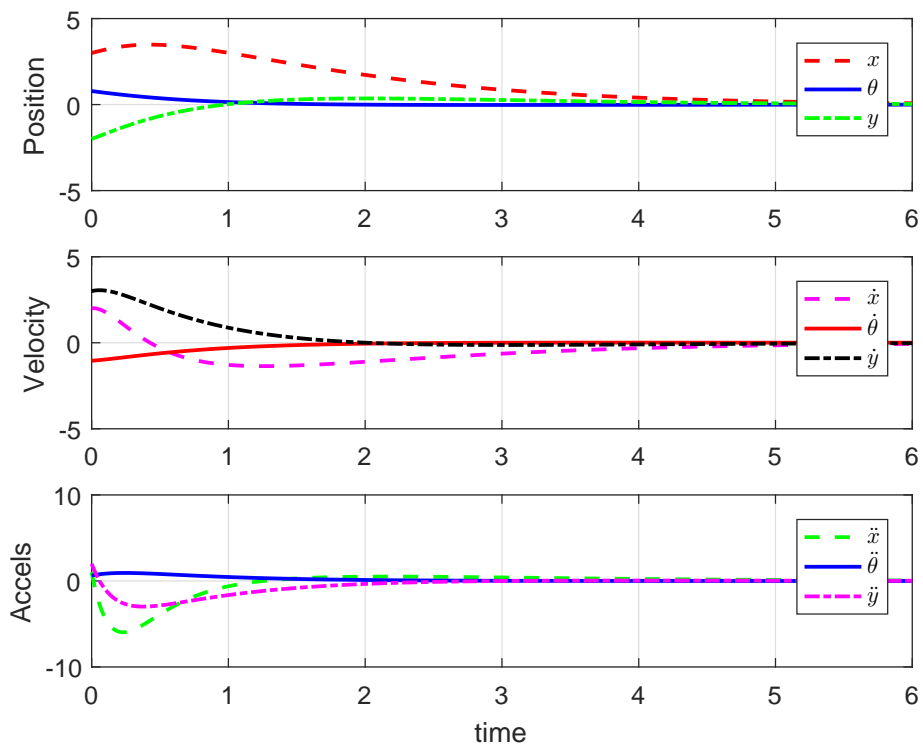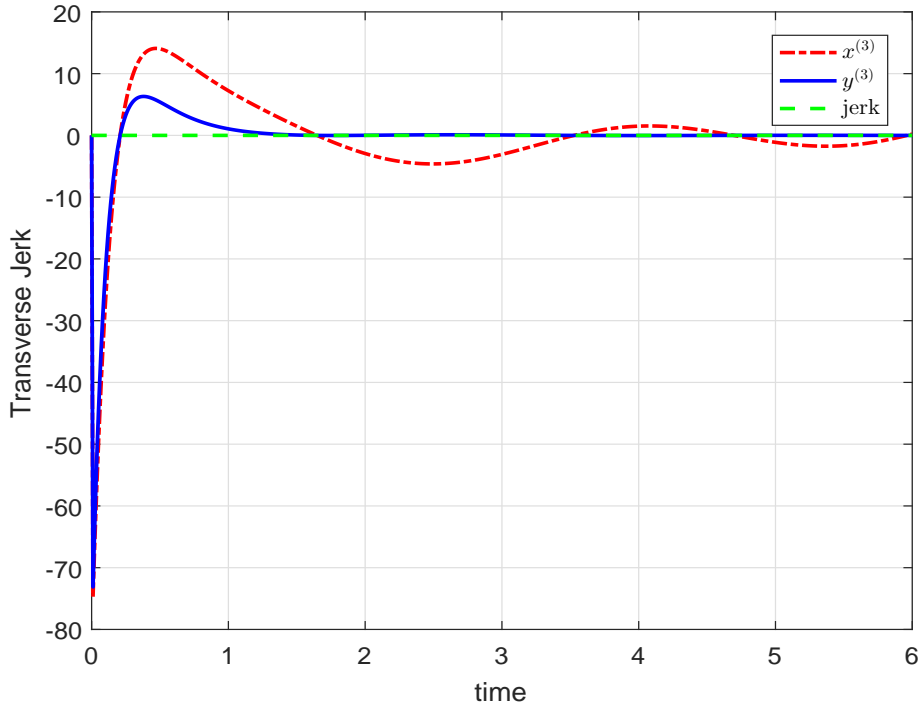
FIGURE 6.6: Third-Order NHS (a) States $(q(t), \dot{q}(t))$ corresponding to $(3, \pi /4, -2, 2, -\pi /3, 3, 1, \pi /5, 2)$ (b) Control effort (f_x, f_y)
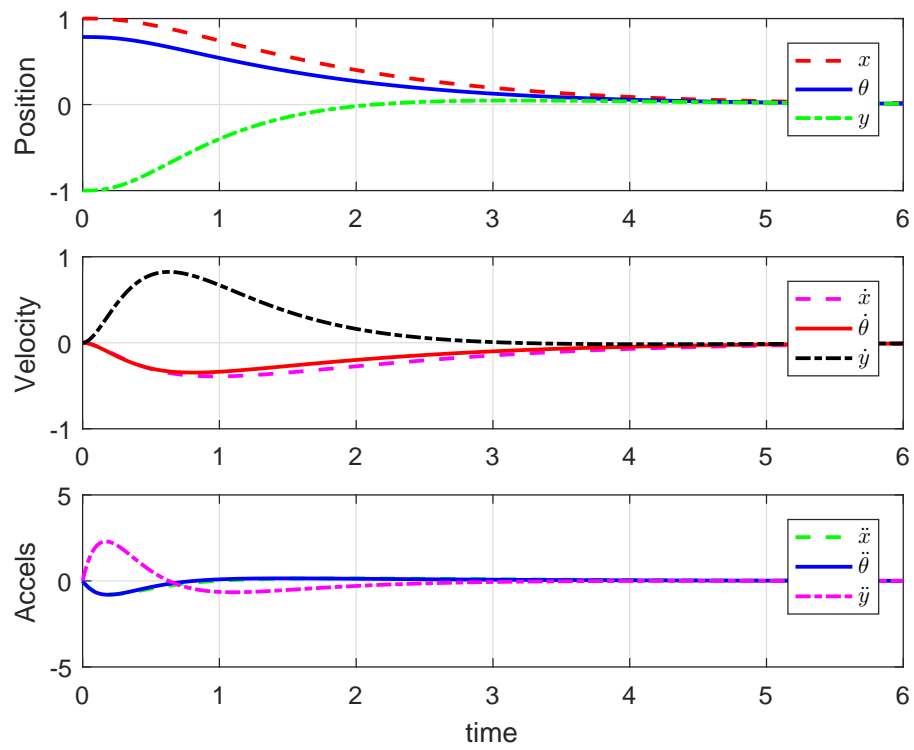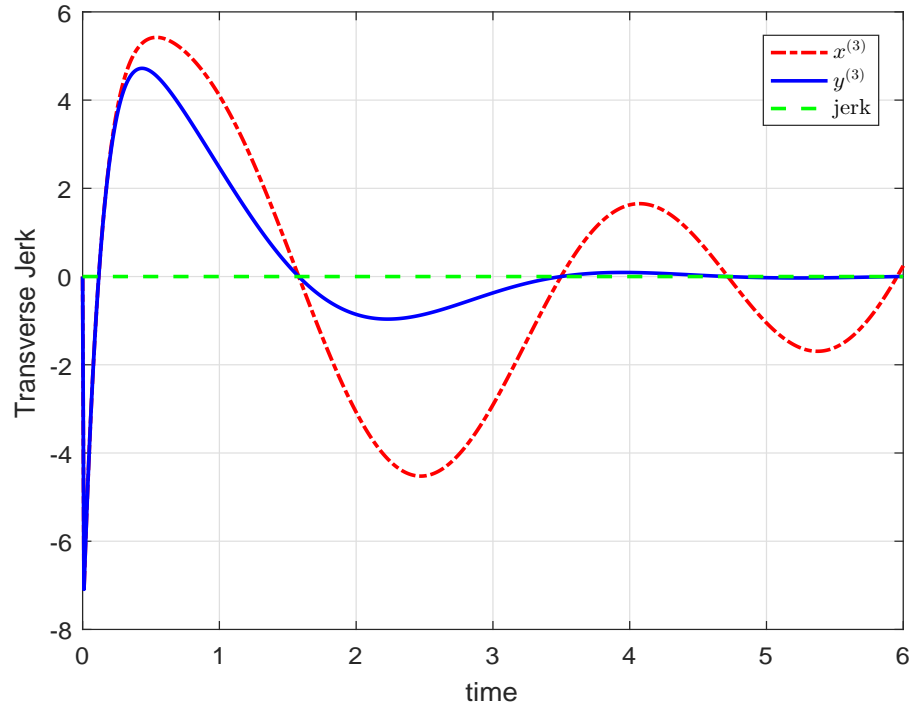
FIGURE 6.7: Third-Order NHS (a) States $(q(t), \dot{q}(t))$ corresponding to $(1, \pi/4, -1, 0, 0, 0, 0, 0, 0))$ (b) Control effort (f_x, f_y)

6.3   Summary

Adaptive integral sliding mode based stabilizing control algorithms for higher-order nonholonomic are proposed in this chapter. The proposed methods are applied to a planar PPR manipulator model with a jerk constraint. The model belongs to the third-order nonholonomic family. The effectiveness of the proposed methods is verified through simulations. The aim was to steer the systems from any initial configuration state to a desired one. Robustness of the proposed methodology is verified by introducing perturbation in a control input. Simulation results validate that the control objective has been achieved.

Chapter 7

Conclusion and Future Work

The control design of dynamical systems in the presence of disturbances and uncertainties pose a special question while considering real-world systems. The effect of these disturbances on the dynamics of each system should be cautiously studied during the design phase as these perturbations can aggravate the system performance and/or even cause instability in the system. For these reasons, the problem of designing control for dynamical systems in the presence of input and modelling uncertainties has become a principal area of research. As a consequence, considerable progress has been made in robust methodologies, such as model predictive control, nonlinear adaptive control, SMC, backstepping and others. These methods are capable of assuring that the control objectives are achieved in spite of parameter uncertainties and/or modelling errors affecting the nonlinear dynamical system.

Stabilization of a class of nonholonomic systems having matched uncertainties has been addressed in this dissertation using novel adaptive integral SMC techniques. The class consists of first-, second- and higher-order nonholonomic systems that can be modified into the canonical chained forms. The control of these systems has proved to be challenging since, generally, these systems cannot be stabilized by any continuous, static state-feedback. Additionally, the inclusion of a drift term in the system dynamics of second- and higher-order NHS makes the stabilization of these systems much more difficult. The proposed approaches are general and can

be applied to systems with higher-order nonholonomic constraints. The applicability of the theoretical development has been illustrated by introducing matched perturbations in system models and the inputs.

The main result of the dissertation also includes construction of discontinuous nonlinear feedback controller for higher-order nonholonomic systems and the closed loop equilibrium point at the origin is made globally attractive. Adaptive integral SMC based solution is provided for the stabilization of a planar PPR robot manipulator subjected to a jerk constraint. The research provides control laws that are insensitive to system/control parameter variation, achieve robustness and offer improved disturbance rejection.

7.1   Conclusions

1. Feedback stabilization of nonholonomic drift-free systems is presented using adaptive ISMC. Novel stabilizing control algorithm for first-order drift-free nonholonomic systems is proposed. The control algorithm is general and can easily be extended to higher-order NHS. Extended Lie bracket system is used as a nominal system which can easily be asymptotically stabilized. The proposed method is applied to two different nonholonomic drift-free systems. Another approach based on function approximation technique is also proposed for the first-order NHS in chained form.

2. Robust stabilizing control algorithm based on AISMC is provided for the first-order perturbed nonholonomic system in chained form. The algorithm is applied to an underwater vehicle example and perturbations in matched form are added to the original underwater vehicle system. The importance of this research is further highlighted by the fact that the proposed methodology is general and can be applied to other nonholonomic mechanical systems such as wheeled mobile robots (WMRs), helicopters, Vertical Take Off and Landing (VTOL) aircrafts, robotic manipulators and surface vehicles. At

the same time, the proposed methodology provides robustness for the whole state space as the reaching phase is eliminated because of integral SMC.

3. A novel stabilizing algorithm for second-order mechanical nonholonomic systems in chained form is provided. The proposed method is tested on two different second-order nonholonomic systems; a three DOF manipulator with a passive joint model and a planar PPR manipulator model. Both models belong to the second-order nonholonomic family that are transferable into second-order chained form. The robustness of the proposed methods is verified by applying algorithms to perturbed second-order nonholonomic systems.

4. Stabilizing control algorithms are proposed for a higher-order perturbed nonholonomic system in chained form. The proposed method is applied on a planar PPR manipulator model with a jerk constraint. The model belongs to the third-order nonholonomic family. The effectiveness of the proposed method is verified through simulations.

7.2   Future Directions

Real-life second- and higher-order nonholonomic systems are special systems and these systems are opening new research avenues in nonlinear control theory. Few possible directions for future research are as follows:

1. Application of other soft computing methods in conjunction with SMC may be explored for possible advantages.

2. Future work may concern the development of robust algorithms for general nonholonomic mechanical systems that are affected with unmatched uncertainties.

3. Formation/consensus control of AUVs or UAVs may be studied, as cooperative control of these vehicles and its real-world implementation are active areas of research. Cooperative control of multi-agent systems is relatively a new subject with general design framework based on graph theory and matrix theory.

4. Collision avoidance mechanisms with actuator limitations for the complex dynamic environment may be studied. For aerial vehicles, the collision avoidance tasks represent a new direction. A practical solution to communication imperfections, parameter variations, sensor noise and neglected dynamics may be investigated in detail.

5. Problems concerning link and joint flexibilities, multiple end-effectors and three-dimensional manoeuvers in planar PPR robot manipulator under jerk constraint may represent new research directions.

6. Implementing proposed algorithms on new higher-order nonholonomic platforms for the verification purpose.

In this section, few areas of possible future research directions are highlighted. With the passage of time, new applications of NHS will emerge and, in reality, the true potential of nonholonomic systems/applications is yet to be explored.

Appendix A

Some Basic Definitions of Differential Geometry

Manifold:

An n-dimensional *manifold* is a set M which is locally homeomorphic to $\mathbb{R}^n$.

Tangent Space:

The *tangent space* of manifold M at a point p is a set of all derivations $X_p : C^\infty(p) \to \mathbb{R}$. It is denoted as $T_p M$. The individual elements of the tangent space are known as *tangent vectors*. Let (ϕ, U) be a coordinate chart on manifold M with local coordinates $(x_1, \cdots, x_n)$, then the set of derivations $\{\frac{\partial}{\partial x}\}$ forms a basis for $T_p M$ and is written as:

$$X_p = X_1 \frac{\partial}{\partial x_1} + \cdots + X_n \frac{\partial}{\partial x_n}$$

The vector $(X_1, \cdots, X_n) \in \mathbb{R}^n$ is a local coordinate representation of $X_p \in T_p M$.

Vector Field:

A *vector field* on $\mathbb{R}^n$ is a smooth map that allocates a tangent vector $f(x) \in T_x \mathbb{R}^n$ to every point x. The vector field $f(x)$ is represented by a column vector whose elements depend on x in local coordinates, i.e. $f(x = \begin{bmatrix} f_1(x) & \cdots & f_n(x) \end{bmatrix}^T$.

When all the elements $f_i(x)$ are *smooth* the vector field is known as *smooth vector field*.

Remark A.1. A set of vector fields $\{f_1, \cdots, f_m\} \in \mathbb{R}^n$ is called *linearly independent* when $\alpha_1 f_1 + \cdots + \alpha_m f_m = 0$ means $\alpha_1 = \cdots = \alpha_m = 0$, otherwise it is linearly dependent.

Remark A.2. Linearly independent vector fields $\{g_1, \cdots, g_m\} \in \mathbb{R}^n$ are *involutive* if $\{g_1, \cdots, g_m, [g_i, g_j]\}$ is linearly dependent for any possible choice of g_i and g_j with $i \neq j$.

Flow of a Vector Field:

If f is a vector field, the parametrized maximal integral curve of the differential equation $\dot{x} = f(x)$ passing through $x \in \mathbb{R}^n$ at starting zero time is denoted as $\phi_t^f(x)$ and the mapping is called the *flow* generated by f.

Lie Derivative:

Lie Derivative of V along f is defined as:

$$L_f V = \frac{\partial V}{\partial x} f(x)$$

It is simply the time derivative of V along the flow of vector field $f(x)$.

Motivation for the use of Lie Brackets:

The operation of Lie Bracket on two vector fields can be better understood by the visualization shown in figure A.1.

Starting at any initial position, the Lie Bracket operation consists of a flow along q_1 for ϵ seconds, followed by flows along q_2, -q_1 and -q_2 for ϵ seconds each. For small ϵ, taylor series in ϵ can be used to determine the value of the differential equation $\dot{x} = f(x)$.

Lie Bracket:
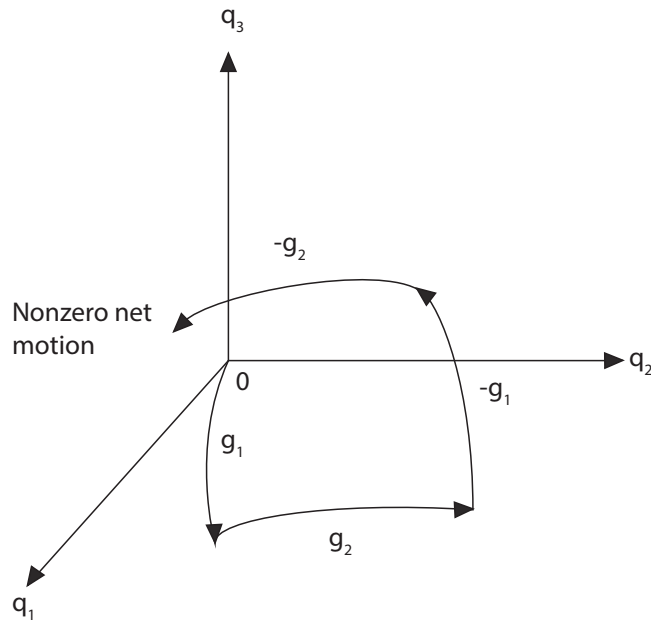
FIGURE A.1: The Lie Bracket Motion Effect.

For $f(x)$ and $g(x)$ vector fields, the operation of Lie Bracket in local coordinates is defined as:

$$[f,g](x) = \frac{\partial g}{\partial q}f(x) - \frac{\partial f}{\partial q}g(x)$$

Properties of Lie Bracket:

Given any vector fields $f(x)$, $g(x)$, $h(x)$ on $\mathbb{R}^n$, the Lie bracket satisfies the properties of skew-symmetry and Jacobi identity:

$$[f,g] = -[g,f],$$

$$[f,[g,h]] + [h,[f,g]] + [g,[h,f]] = 0,$$

Lie Algebra:

If there exists a bilinear operator $V \times V \to V$ denoted as $[.,.]$, the vector space V (over $\mathbb{R}$) is called *Lie algebra*. It satisfies:

1. Skew-symmetry:

$$[w, y] = -[y, w], \quad \text{for all} \quad w, y \in V$$

2. Jacobi identity:

$$[v, [w, y]] + [y, [v, w]] + [w, [y, v]] = 0, \quad \text{for all} \quad v, w, y \in V$$

The vector space of all smooth vector fields on a manifold M is an infinite-dimensional Lie algebra under Lie bracket operation on vector fields.

Distribution:

For a set of vector fields $\{g_j(x), j = 1, \cdots, m\}$, and for any fixed $x \in \mathbb{R}^n$, $\Delta = span\{g_1(x), \cdots, g_m(x)\}$ is called the *distribution* of the set of vector fields.

If the spanning vector fields g_i's are smooth then the distribution is called a smooth distribution. The *dimension* of a distribution at a point $x \in \mathbb{R}^n$ is the dimension of the vector space $\Delta(x)$.

Regular Distribution:

For a set of vector fields $\{g_j(x), j = 1, \cdots, m\}$, its distribution is *regular* if Δ does not change with x i.e. $dim(\Delta(x)) =$constant.

Involutive Distribution:

A distribution $\bar{\Delta}$ is *involutive* if it is closed under the Lie bracket operation, i.e. it implies that:

1. $\bar{\Delta}$ is a Lie algebra.

2. $\bar{\Delta}$ contains all linear combinations of g_1 upto g_m, their Lie brackets and all combinations of these as well.

Bibliography

[1] H. Hertz, *Gesammelte Werke: Band III.: Die Prinzipien der Mechanik.* Hansebooks, 2016.

[2] J. Baillieul, A. Bloch, P. Crouch, J. Marsden, D. Zenkov, P. Krishnaprasad, and R. Murray, *Nonholonomic Mechanics and Control*, ser. Interdisciplinary Applied Mathematics. Springer New York, 2015.

[3] I. Kolmanovsky and N. H. McClamroch, "Developments in nonholonomic control problems," *IEEE Control Systems*, vol. 15, no. 6, pp. 20–36, Dec 1995.

[4] Y. Liu and H. Yu, "A survey of underactuated mechanical systems," *IET Control Theory Applications*, vol. 7, no. 7, pp. 921–935, May 2013.

[5] J. Huang, J. Chen, H. Fang, and L. Dou, "An overview of recent progress in high-order nonholonomic chained system control and distributed coordination," *Journal of Control and Decision*, vol. 2, no. 1, pp. 64–85, 2015.

[6] C. Yang, Y. Qiu, F. Chen, and L. Xiang, "Distributed control for coupled nonholonomic mobile robots under the event-triggered and self-triggered frameworks," *Asian Journal of Control*, vol. 19, no. 3, pp. 900–917, 2017.

[7] R. W. Brockett, "Asymptotic stability and feedback stabilization," in *Differential Geometric Control Theory*. Birkhauser, 1983, pp. 181–191.

[8] N. P. I. Aneke, H. Nijmeijer, and A. G. de Jager, "Tracking control of second-order chained form systems by cascaded backstepping," *International Journal of Robust and Nonlinear Control*, vol. 13, no. 2, pp. 95–115, 2003.

[9] J. R. Hervas, "Dynamics and control of higher-order nonholonomic systems," Ph.D. dissertation, Embry-Riddle Aeronautical University, Daytona Beach, FL., USA, 2013.

[10] R. M. Murray and S. S. Sastry, "Steering nonholonomic systems in chained form," in *[1991] Proceedings of the 30th IEEE Conference on Decision and Control*, vol. 2, Dec 1991, pp. 1121–1126.

[11] W. Xu and B. Ma, "Stabilization of second-order nonholonomic systems in canonical chained form," *Robotics and Autonomous Systems*, vol. 34, no. 4, pp. 223 – 233, 2001.

[12] R. M. Murray and S. S. Sastry, "Nonholonomic motion planning: steering using sinusoids," *IEEE Transactions on Automatic Control*, vol. 38, no. 5, pp. 700–716, May 1993.

[13] G. Jacob, "Motion planning by piecewise constant or polynomial inputs," in *Nonlinear Control Systems Design 1992*, ser. IFAC Symposia Series, M. Fliess, Ed. Oxford: Pergamon, 1993, pp. 239 – 244.

[14] R. T. M'Closkey and R. M. Murray, "Exponential stabilization of driftless nonlinear control systems using homogeneous feedback," *IEEE Transactions on Automatic Control*, vol. 42, no. 5, pp. 614–628, May 1997.

[15] J. Guldner and V. I. Utkin, "Stabilization of non-holonomic mobile robots using Lyapunov functions for navigation and sliding mode control," in *[1994] Proceedings of the 33rd IEEE Conference on Decision and Control*, vol. 3, Dec 1994, pp. 2967–2972.

[16] A. M. Bloch and S. Drakunov, "Stabilization of a nonholonomic system via sliding modes," in *[1994] Proceedings of the 33rd IEEE Conference on Decision and Control*, vol. 3, Dec 1994, pp. 2961–2963.

[17] J. P. Laumond, "Feasible trajectories for mobile robots with kinematic and environment constraints," in *Intelligent Autonomous Systems, An International Conference*. Amsterdam, The Netherlands, The Netherlands: North-Holland Publishing Co., 1987, pp. 346–354.

[18] A. M. Bloch, M. Reyhanoglu, and N. H. McClamroch, "Control and stabilization of nonholonomic dynamic systems," *IEEE Transactions on Automatic Control*, vol. 37, no. 11, pp. 1746–1757, Nov 1992.

[19] J. P. Laumond, "Controllability of a multibody mobile robot," *IEEE Transactions on Robotics and Automation*, vol. 9, no. 6, pp. 755–763, Dec 1993.

[20] M. Reyhanoglu and E. Al-Regib, "Nonholonomic motion planning for wheeled mobile systems using geometric phases," in *[1994] Proceedings of the 9th IEEE International Symposium on Intelligent Control*, Aug 1994, pp. 135–140.

[21] G. Walsh, W. Tilbury, S. Sastry, R. Murray, and J. P. Laumond, "Stabilization of trajectories for systems with nonholonomic constraints," *IEEE Transactions on Automatic Control*, vol. 39, pp. 216–222, 1994.

[22] O. J. Sordalen and O. Egeland, "Exponential stabilization of nonholonomic chained systems," *IEEE Transactions on Automatic Control*, vol. 40, no. 1, pp. 35–49, Jan 1995.

[23] M. Reyhanoglu and N. H. McClamroch, "Controllability and stabilizability of planar multibody systems with angular momentum preserving control torques," in *1991 American Control Conference*, June 1991, pp. 1102–1107.

[24] Y. Nakamura and R. Mukherjee, "Nonholonomic path planning of space robots via a bidirectional approach," *IEEE Transactions on Robotics and Automation*, vol. 7, no. 4, pp. 500–514, Aug 1991.

[25] Z. Jiang, E. Lefeber, and H. Nijmeijer, "Saturated stabilization and tracking of a nonholonomic mobile robot," *Systems and Control Letters*, vol. 42, no. 5, pp. 327–332, 2001.

[26] J. M. Godhavn and O. Egeland, "A Lyapunov approach to exponential stabilization of nonholonomic systems in power form," *IEEE Transactions on Automatic Control*, vol. 42, no. 7, pp. 1028–1032, Jul 1997.

[27] A. Astolfi, "Discontinuous control of nonholonomic systems," *Systems & Control Letters*, vol. 27, no. 1, pp. 37 – 45, 1996.

[28] I. Kolmanovsky, M. Reyhanoglu, and N. McClamroch, "Switched mode feedback control laws for nonholonomic systems in extended power form," *Systems & Control Letters*, vol. 27, no. 1, pp. 29–36, 1996.

[29] Z. P. Jiang and H. Nijmeijer, "A recursive technique for tracking control of nonholonomic systems in chained form," *IEEE Transactions on Automatic Control*, vol. 44, no. 2, pp. 265–279, Feb 1999.

[30] A. A. J. Lefeber, "Tracking control of nonlinear mechanical systems," Ph.D. dissertation, Enschede, The Netherlands, 2000.

[31] M. Reyhanoglu, A. van der Schaft, N. H. McClamroch, and I. Kolmanovsky, "Dynamics and control of a class of underactuated mechanical systems," *IEEE Transactions on Automatic Control*, vol. 44, no. 9, pp. 1663–1671, Sep 1999.

[32] A. D. Mahindrakar, R. N. Banavar, and M. Reyhanoglu, "Controllability and point-to-point control of 3-DOF planar horizontal underactuated manipulators," *International Journal of Control*, vol. 78, no. 1, pp. 1–13, 2005.

[33] M. Reyhanoglu and J. R. Hervas, "Nonlinear dynamics and control of space vehicles with multiple fuel slosh modes," *Control Engineering Practice*, vol. 20, no. 9, pp. 912 – 918, 2012.

[34] J. R. Hervas and M. Reyhanoglu, "Control of a spacecraft with time-varying propellant slosh parameters," in *[2012] 12th International Conference on Control, Automation and Systems*, Oct 2012, pp. 1621–1626.

[35] Y. P. Tian and K. C. Cao, "Time-varying linear controllers for exponential tracking of non-holonomic systems in chained form," *International Journal of Robust and Nonlinear Control*, vol. 17, no. 7, pp. 631–647, 2007.

[36] H. Yuan and Z. Qu, "Smooth time-varying pure feedback control for chained non-holonomic systems with exponential convergent rate," *IET Control Theory Applications*, vol. 4, no. 7, pp. 1235–1244, July 2010.

[37] W. Lin, R. Pongvuthithum, and C. Qian, "Control of high-order nonholonomic systems in power chained form using discontinuous feedback," *IEEE Transactions on Automatic Control*, vol. 47, no. 1, pp. 108–115, Jan 2002.

[38] N. Marchand and M. Alamir, "Discontinuous exponential stabilization of chained form systems," *Automatica*, vol. 39, no. 2, pp. 343 – 348, 2003.

[39] F. Rehman, "Feedback stabilization of nonholonomic control systems with drift," *Asian Journal of Control*, vol. 6, no. 1, pp. 97–103, 2004.

[40] C. Jammazi, "Continuous and discontinuous homogeneous feedbacks finite-time partially stabilizing controllable multichained systems," *SIAM Journal on Control and Optimization*, vol. 52, no. 1, pp. 520–544, 2014.

[41] E. Jarzebowska, "Control oriented dynamic formulation for robotic systems with program constraints," *Robotica*, vol. 24, no. 1, pp. 61–73, 2006.

[42] J. R. Hervas and M. Reyhanoglu, "Control and stabilization of a third-order nonholonomic system," in *[2013] 13th International Conference on Control, Automation and Systems (ICCAS 2013)*, Oct 2013, pp. 17–22.

[43] P. Freeman, "Minimum jerk trajectory planning for trajectory constrained redundant robots," Ph.D. dissertation, Washington University, St. Louis, Missouri, 2012.

[44] H. Khalil, *Nonlinear Systems*, ser. Pearson Education. Prentice Hall, 2002.

[45] Z. Qu, *Robust Control of Nonlinear Uncertain Systems*, ser. A Wiley-Interscience publication. Wiley, 1998.

[46] Z. P. Jiang, "Robust exponential regulation of nonholonomic systems with uncertainties," *Automatica*, vol. 36, no. 2, pp. 189 – 209, 2000.

[47] J. B. Pomet, "Explicit design of time-varying stabilizing control laws for a class of controllable systems without drift," *Systems & Control Letters*, vol. 18, no. 2, pp. 147 – 158, 1992.

[48] C. Samson, "Control of chained systems application to path following and time-varying point-stabilization of mobile robots," *IEEE Transactions on Automatic Control*, vol. 40, no. 1, pp. 64–77, Jan 1995.

[49] J. P. Laumond, M. Taix, and P. Jacobs, "A motion planner for car-like robots based on a mixed global/local approach," in *IEEE International Workshop on Intelligent Robots and Systems, Towards a New Frontier of Applications*, vol. 2, Jul 1990, pp. 765–773.

[50] G. Lafferriere, "A general strategy for computing steering controls of systems without drift," in *[1991] Proceedings of the 30th IEEE Conference on Decision and Control*, vol. 2, Dec 1991, pp. 1115–1120.

[51] A. R. Teel, R. M. Murray, and G. Walsh, "Nonholonomic control systems: from steering to stabilization with sinusoids," in *[1992] Proceedings of the 31st IEEE Conference on Decision and Control*, vol. 2, 1992, pp. 1603–1609.

[52] V. Jurdjevic and J. Quinn, "Controllability and stability," *Journal of Differential Equations*, vol. 28, no. 3, pp. 381 – 389, 1978.

[53] J. M. Coron, "Global asymptotic stabilization for controllable systems without drift," *Mathematics of Control, Signals and Systems*, vol. 5, no. 3, pp. 295–312, Sep 1992.

[54] G. Walsh and L. Bushnell, "Stabilization of multiple input chained form control systems," *Systems & Control Letters*, vol. 25, no. 3, pp. 227 – 234, 1995.

[55] M. C. Laiou and A. Astolfi, "Quasi-smooth control of chained systems," in *Proceedings of the 1999 American Control Conference*, vol. 6, 1999, pp. 3940–3944.

[56] E. D. Sontag, "Universal nonsingular controls," *Systems & Control Letters*, vol. 19, no. 3, pp. 221 – 224, 1992.

[57] T. Sun, H. Pei, Y. Pan, H. Zhou, and C. Zhang, "Neural network-based sliding mode adaptive control for robot manipulators," *Neurocomputing*, vol. 74, no. 14, pp. 2377 – 2384, 2011.

[58] D. E. Chaouch, Z. A. Foitih, and M. F. Khelfi, "A self-tuning fuzzy inference sliding mode control scheme for a class of nonlinear systems," *Journal of Vibration and Control*, vol. 18, no. 10, pp. 1494–1505, 2012.

[59] E. Jarzebowska, "On derivation of motion equations for systems with non-holonomic high-order program constraints," *Multibody System Dynamics*, vol. 7, no. 3, pp. 307–329, 2002.

[60] I. Kovacic, "On the field method in nonholonomic mechanics," *Acta Mechanica Sinica*, vol. 21, pp. 192–196, Mar. 2005.

[61] S. Emelyanov, *Variable Structure Control Systems*. Nauka(in Russian), Moscow, 1967.

[62] S. Korovin and V. Utkin, "Using sliding modes in static optimization and nonlinear programming," *Automatica*, vol. 10, no. 5, pp. 525 – 532, 1974.

[63] V. Utkin and J. Shi, "Integral sliding mode in systems operating under uncertainty conditions," in *Proceedings of 35th IEEE Conference on Decision and Control*, vol. 4, Dec 1996, pp. 4591–4596 vol.4.

[64] V. Utkin, "Variable structure systems with sliding modes," *IEEE Transactions on Automatic Control*, vol. 22, no. 2, pp. 212–222, Apr 1977.

[65] C. Edwards and S. Spurgeon, *Sliding Mode Control: Theory And Applications*, ser. Series in Systems and Control. Taylor & Francis, 1998.

[66] V. Utkin, J. Guldner, and J. Shi, *Sliding mode control in electro-mechanical systems and optimization.* CRC Press, 2009.

[67] W. Perruquetti and J. Barbot, *Sliding Mode Control In Engineering*, ser. Automation and Control Engineering. CRC Press, 2002.

[68] L. M. Fridman, "Chattering analysis in sliding mode systems with inertial sensors," *International Journal of Control*, vol. 76, no. 9-10, pp. 906–912, 2003.

[69] A. Levant, "Principles of 2-sliding mode design," *Automatica*, vol. 43, no. 4, pp. 576 – 586, 2007.

[70] J. Slotine and W. Li, *Applied Nonlinear Control.* Prentice Hall, 1991.

[71] K. D. Young, V. I. Utkin, and U. Ozguner, "A control engineer's guide to sliding mode control," *IEEE Transactions on Control Systems Technology*, vol. 7, no. 3, pp. 328–342, May 1999.

[72] Y. Pan, C. Yang, L. Pan, and H. Yu, "Integral sliding mode control: Performance, modification, and improvement," *IEEE Transactions on Industrial Informatics*, vol. 14, no. 7, pp. 3087–3096, July 2018.

[73] J. Lee, P. H. Chang, and M. Jin, "Adaptive integral sliding mode control with time-delay estimation for robot manipulators," *IEEE Transactions on Industrial Electronics*, vol. 64, no. 8, pp. 6796–6804, Aug 2017.

[74] J. Lian, J. Zhao, and G. M. Dimirovski, "Integral sliding mode control for a class of uncertain switched nonlinear systems," *European Journal of Control*, vol. 16, no. 1, pp. 16 – 22, 2010. [Online]. Available: http://www.sciencedirect.com/science/article/pii/S0947358010706142

[75] Y.-X. Li, "Adaptive integral sliding mode control fault tolerant control for a class of uncertain nonlinear systems," *IET Control Theory Applications*, vol. 12, pp. 1864–1872(8), September 2018.

[76] H. Tirandaz and H. Sabzevari, "Adaptive integral sliding mode control method for synchronization of supply chain system," 2018.

[77] S. Vaidyanathan, *Adaptive Integral Sliding Mode Controller Design for the Control and Synchronization of a Novel Jerk Chaotic System.* Cham: Springer International Publishing, 2017, pp. 393–417.

[78] A. D. Luca and G. Oriolo, *Modelling and Control of Nonholonomic Mechanical Systems.* Vienna: Springer Vienna, 1995, pp. 277–342.

[79] Z. Li and R. Montgomery, "Dynamics and optimal control of a legged robot in flight phase," in *Proceedings of IEEE International Conference on Robotics and Automation*, vol. 3, May 1990, pp. 1816–1821.

[80] L. Bushnell, D. Tilbury, and S. Sastry, "Steering three-input nonholonomic systems: The fire truck example," *The International Journal of Robotics Research*, vol. 14, no. 4, pp. 366–381, 1995.

[81] K. Watanabe, Y. Ueda, I. Nagai, and S. Maeyama, "Stabilization of a fire truck robot by an invariant manifold theory," *Procedia Engineering*, vol. 41, no. Supplement C, pp. 1095 – 1104, 2012.

[82] J. Yuh, "Design and control of autonomous underwater robots: A survey," *Autonomous Robots*, vol. 8, no. 1, pp. 7–24, Jan 2000.

[83] R. B. Wynn, V. A. Huvenne, T. P. L. Bas, B. J. Murton, D. P. Connelly, B. J. Bett, H. A. Ruhl, K. J. Morris, J. Peakall, D. R. Parsons, E. J. Sumner, S. E. Darby, R. M. Dorrell, and J. E. Hunt, "Autonomous underwater vehicles (AUVs): Their past, present and future contributions to the advancement of marine geoscience," *Marine Geology*, vol. 352, no. Supplement C, pp. 451 – 468, 2014.

[84] F. Y. Bi, Y. J. Wei, J. Z. Zhang, and W. Cao, "Position-tracking control of underactuated autonomous underwater vehicles in the presence of unknown ocean currents," *IET Control Theory Applications*, vol. 4, no. 11, pp. 2369–2380, November 2010.

[85] Y. Kim, S. Mohan, and J. Kim, "Task space-based control of an underwater robotic system for position keeping in ocean currents," *Advanced Robotics*, vol. 28, no. 16, pp. 1109–1119, 2014.

[86] D. Panagou and K. J. Kyriakopoulos, "Dynamic positioning for an underactuated marine vehicle using hybrid control," *International Journal of Control*, vol. 87, no. 2, pp. 264–280, 2014.

[87] H. Joe, M. Kim, and S. C. Yu, "Second-order sliding-mode controller for autonomous underwater vehicle in the presence of unknown disturbances," *Nonlinear Dynamics*, vol. 78, no. 1, pp. 183–196, Oct 2014.

[88] I. Eski and S. Yildirim, "Design of neural network control system for controlling trajectory of autonomous underwater vehicles," *International Journal of Advanced Robotic Systems*, vol. 11, no. 1, p. 7, 2014.

[89] J. Ghommam and M. Saad, "Backstepping-based cooperative and adaptive tracking control design for a group of underactuated AUVs in horizontal plan," *International Journal of Control*, vol. 87, no. 5, pp. 1076–1093, 2014.

[90] H. Akakaya and L. G. Smer, "Robust control of variable speed autonomous underwater vehicle," *Advanced Robotics*, vol. 28, no. 9, pp. 601–611, 2014.

[91] Z. Dong, L. Wan, Y. Li, T. Liu, J. Zhuang, and G. Zhang, "Point stabilization for an underactuated AUV in the presence of ocean currents," *International Journal of Advanced Robotic Systems*, vol. 12, no. 7, p. 100, 2015.

[92] D. C. Rucker, J. Das, H. B. Gilbert, P. J. Swaney, M. I. Miga, N. Sarkar, and R. J. Webster, "Sliding mode control of steerable needles," *IEEE Transactions on Robotics*, vol. 29, no. 5, pp. 1289–1299, Oct 2013.

[93] A. S. Matveev, M. Hoy, J. Katupitiya, and A. V. Savkin, "Nonlinear sliding mode control of an unmanned agricultural tractor in the presence of sliding and control saturation," *Robotics and Autonomous Systems*, vol. 61, no. 9, pp. 973 – 987, 2013.

[94] Q. Xu, "Adaptive discrete-time sliding mode impedance control of a piezo-electric microgripper," *IEEE Transactions on Robotics*, vol. 29, no. 3, pp. 663–673, June 2013.

[95] S. Wadoo, "Feedback control and nonlinear controllability of nonholonomic systems," Master's thesis, Virginia Polytechnic Institute, Virginia,, 2013.

[96] L. Yang and J. Yang, "Stabilization for a class of nonholonomic perturbed systems via robust adaptive sliding mode control," in *Proceedings of the 2010 American Control Conference*, June 2010, pp. 1178–1183.

[97] M. Reyhanoglu, A. van der Schaft, N. H. McClamroch, and I. Kolmanovsky, "Nonlinear control of a class of underactuated systems," in *Proceedings of 35th IEEE Conference on Decision and Control*, vol. 2, Dec 1996, pp. 1682–1687.

[98] G. He, C. Zhang, W. Sun, and Z. Geng, "Stabilizing the second-order non-holonomic systems with chained form by finite-time stabilizing controllers," *Robotica*, vol. 34, no. 10, pp. 2344–2367, 2016.

[99] M. Asif, M. J. Khan, and N. Cai, "Adaptive sliding mode dynamic controller with integrator in the loop for nonholonomic wheeled mobile robot trajectory tracking," *International Journal of Control*, vol. 87, no. 5, pp. 964–975, 2014.

[100] N. Adhikary and C. Mahanta, "Integral backstepping sliding mode control for underactuated systems: Swing-up and stabilization of the cartpendulum system," *ISA Transactions*, vol. 52, no. 6, pp. 870 – 880, 2013.

[101] H. Lee and V. I. Utkin, "Chattering suppression methods in sliding mode control systems," *Annual Reviews in Control*, vol. 31, no. 2, pp. 179 – 188, 2007.

[102] A. C. Huang, Y. F. Chen, and C. Y. Kai, *Adaptive Control Of Underactuated Mechanical Systems*.   World Scientific Publishing Company, 2015.

[103] A. D. Luca and G. Oriolo, "Trajectory planning and control for planar robots with passive last joint," *The International Journal of Robotics Research*, vol. 21, no. 5-6, pp. 575–590, 2002.

[104] S. S. Ge, Z. Sun, T. H. Lee, and M. W. Spong, "Feedback linearization and discontinuous control of second-order nonholonomic chained systems," in *Proceedings of the 2001 IEEE International Conference on Control Applications (CCA'01) (Cat. No.01CH37204)*, Sept 2001, pp. 990–995.

[105] E. Jarzebowska, *Model-based tracking control of nonlinear systems.* Taylor & Francis Group, Boca Raton, 2012.

[106] S. Macfarlane and E. A. Croft, "Jerk-bounded manipulator trajectory planning: design for real-time applications," *IEEE Transactions on Robotics and Automation*, vol. 19, no. 1, pp. 42–52, Feb 2003.

[107] D. Mellinger and V. Kumar, "Minimum snap trajectory generation and control for quadrotors," in *2011 IEEE International Conference on Robotics and Automation*, May 2011, pp. 2520–2525.

[108] J. R. Hervas and M. Reyhanoglu, "Controllability and stabilizability of a class of systems with higher-order nonholonomic constraints," *Automatica*, vol. 54, no. Supplement C, pp. 229 – 234, 2015.